Marine Technology Society JOURNAL

Diving Deeper: Expanded Papers from Recent MTS Conferences

THE INTERNATIONAL, INTERDISCIPLINARY SOCIETY DEVOTED TO OCEAN AND MARINE ENGINEERING, SCIENCE, AND POLICY
VOLUME 43, NUMBER 2, SPRING 2009

Marine Technology Society Officers

BOARD OF DIRECTORS

President
Elizabeth Corbin
Hawaii, Department of Business, Economic Development and Tourism

President-elect
Jerry Boatman
Planning Systems, Inc.

Immediate Past President
Bruce C. Gilman, P.E.
Consultant

VP—Section Affairs
Kevin Hardy
DeepSea Power and Light

VP—Education and Research
Jill Zande
MATE Center

VP—Industry and Technology
Jerry C. Wilson
Fugro Pelagos, Inc.

VP—Publications
Karin Lynn

Treasurer and VP—Budget and Finance
Debra Kill
Consultant

VP—Government and Public Affairs
Karen Kohanowich
NURP

SECTIONS

Canadian Maritime
Vacant

Florida
Prof. Mark Luther
University of South Florida

Gulf Coast
Ted Bennett
Naval Oceanographic Office

Hampton Roads
Raymond Toll
SAIC

Hawaii
Philomene Verlaan, Ph.D., J.D.

Houston
Evalyn Shea
Shea Writing and Training Solutions

Japan
Prof. Toshitsugu Sakou
Tokai University

Monterey
Jill Zande
MATE

New England
Chris Jakubiak
UMASS Dartmouth-SMAST

Puget Sound
Fritz Stahr
University of Washington

San Diego
Barbara Fletcher
SSC-San Diego

South Korea
Dr. Seok Won Hong
Maritime & Ocean Engineering Research Inst. (MOERI/KORDI)

Washington, D.C.
Barry Stamey
Noblis

PROFESSIONAL COMMITTEES

Industry and Technology

Buoy Technology
Dr. Walter Paul
Woods Hole Oceanographic Institution

Cables & Connectors
Vacant

Deepwater Field Development Technology
Dr. Benton Baugh
Radoil, Inc.

Diving
Vacant

Dynamic Positioning
Howard Shatto
Shatto Engineering

Manned Underwater Vehicles
William Kohnen
SEAmagine Hydrospace Corporation

Moorings
Vacant

Oceanographic Instrumentation
Dr. Jim Irish
University of New Hampshire

Offshore Structures
Dr. Peter W. Marshall
MHP Systems Engineering

Remotely Operated Vehicles
Drew Michel
ROV Technologies, Inc.

Renewable Energy
Vacant

Ropes and Tension Members
Evan Zimmerman
Delmar Systems

Seafloor Engineering
Vacant

Underwater Imaging
Dr. Fraser Dalgleish
Harbor Branch Oceanographic Institute

Unmanned Maritime Vehicles
Justin Manley
Battelle

Education and Research

Marine Archaeology
Brett Phaneuf
ProMare, Inc.

Marine Education
Dr. Susan B. Cook
Consortium for Ocean Leadership

Marine Geodetic Information Systems
Dave Zilkoski
NOAA

Marine Materials
Vacant

Ocean Exploration
Vacant

Physical Oceanography/Meteorology
Dr. Richard L. Crout
National Data Buoy Center

Remote Sensing
Herb Ripley
Hyperspectral Imaging Limited

Government and Public Affairs

Marine Law and Policy
Capt. Craig McLean
NOAA

Marine Mineral Resources
Dr. John C. Wiltshire
University of Hawaii

Marine Security
Dallas Meggitt
Sound & Sea Technology

Ocean Economic Potential
James Marsh
University of Hawaii

Ocean Observing Systems
Donna Kocak
Maritime Communication Systems, HARRIS Corporation

Ocean Pollution
Vacant

STUDENT SECTIONS

Duke University
Counselor: Douglas Nowacek, Ph.D.

Florida Atlantic University
Counselor: Douglas A. Briggs, Ph.D.

Florida Institute of Technology
Counselor: Stephen Wood, Ph.D., P.E.

Long Beach City College
Counselor: Scott Fraser

Massachusetts Institute of Technology
Counselor: Alexandra Techet, Ph.D.

Monterey Peninsula College
Counselor: Jeremy R. Hertzberg

Texas A&M University—College Station
Counselor: Patrick Lynett

Texas A&M University—Galveston
Counselor: Victoria Jones, Ph.D.

University of Hawaii
Counselor: Reza Ghorbani

University of Southern Mississippi
Counselor: Stephen Howden, Ph.D.

HONORARY MEMBERS

†Robert B. Abel
†Charles H. Bussmann
John C. Calhoun, Jr.
John P. Craven
†Paul M. Fye
David S. Potter
†Athelstan Spilhaus
†E. C. Stephan
†Allyn C. Vine
†James H. Wakelin, Jr.
†deceased

Front Cover: NOAA Ship *Okeanos Explorer*. Photo courtesy of NOAA (see Keener-Chavis et al., p. 73).

Back Cover: Clockwise from left: *Theseus* hybrid vehicle (see McFarlane, p. 9); PRMS sub hybrid, created by OceanWorks and ISE (see McFarlane, p. 9); graphic of telepresence technology from the Keener-Chavis et al. paper, p. 73; image courtesy of Paul Oberlander, WHOI.

Text: SPi
Cover and Graphics:
Michele A. Danoff, Graphics By Design

The Marine Technology Society Journal
(ISSN 0025-3324) is published by the Marine Technology Society, Inc., 5565 Sterrett Place, Suite 108, Columbia, MD 21044.

MTS members can purchase the printed Journal for $27 domestic and $50 (plus $50 S&H) international. Non-members and library subscriptions are $420 online only, $124 print—domestic, $140 (plus $50 S&H) print—international, $435 print and online (worldwide); Single-issue (hardcopy) is $20 plus $5.00 S&H (domestic), $10 S&H (international); Pay-per-view (worldwide): $15/article. Postage for periodicals is paid at Columbia, MD, and additional mailing offices.

POSTMASTER:
Please send address changes to:

Marine Technology Society Journal
5565 Sterrett Place
Suite 108
Columbia, Maryland 21044

Marine Technology Society JOURNAL

Volume 43, Number 2, Spring 2009

Diving Deeper: Expanded Papers from Recent MTS Conferences

In This Issue

The Marine Technology Society is a not-for-profit, international professional society. Established in 1963, the Society's mission is to promote the exchange of information in ocean and marine engineering, technology, science, and policy.

Please send all correspondence to:
The Marine Technology Society
5565 Sterrett Place, Suite 108
Columbia, MD 21044
(410) 884-5330 Tel.
(410) 884-9060 FAX

MTS Journal:	morganteeditorial@verizon.net
Publications:	publications@mtsociety.org
Membership:	Jeanne.Glover@mtsociety.org
Programs:	Michael.Hall@mtsociety.org
Director:	Rich.Lawson@mtsociety.org
Online:	www.mtsociety.org

MEMBERSHIP INFORMATION

may be obtained by contacting the Marine Technology Society. Benefits include:

- Free subscription to the online Marine *Technology Society Journal*, with highly reduced rates for the paper version
- Free subscription to the bimonthly newsletter, *Currents,* covering events, business news, science and technology, and people in marine technology
- Member discounts on all MTS publications
- Reduced registration rates to all MTS and MTS-sponsored conferences and workshops
- Member-only access to an expansive Job Bank and Member Directory
- Reduced advertising rates in MTS publications
- National recognition through our Awards Program

Individual dues are $75 per year. Life membership is available for a one-time fee of $1,000. Patron, Student, Emeritus, Institutional, Business, and Corporate memberships are also available.

ADVERTISING

Advertising is accepted by the *Marine Technology Society Journal.* For more information on MTS advertising and policy, please contact the managing editor at: morganteeditorial@verizon.net.

ABSTRACTS

MTS Journal article abstracts, if available, can be accessed for free at http://www.ingentaconnect.com/content/mts/mtsj.

Print and electronic abstracts of *MTS Journal* articles are also available through *GeoRef* <http://www.agiweb.org/georef/>, *Aquatic Sciences and Fisheries Abstracts,* published by Cambridge Scientific Abstracts <http://www.csa.com/factsheets/aquclust-set-c.php>, and *Geobase's Oceanbase* published by Elsevier Science.

CONTRIBUTORS

Contributors can obtain an information and style sheet by contacting the managing editor. Submissions that are relevant to the concerns of the Society are welcome. All papers are subjected to a stringent review procedure directed by the editor and the editorial board. The *Journal* focuses on technical material that may not otherwise be available, and thus technical papers and notes that have not been published previously are given priority. General commentaries are also accepted and are subject to review and approval by the editorial board.

FOREWORD

Message from the Editor...

Justin Manley
MTS Journal Editor

An unexpected benefit, or perhaps cost, of the increased frequency of *MTS Journal* publication is the opportunity to provide more of these "Words from the Editor." I am not convinced that my opening remarks bring you, the reader, to the *Journal*. But with increased issues comes the need for more innovative themes for those issues. I do hope you come back for those.

This month we present another new concept. The *MTS Journal* is the flagship publication of our Society. Likewise, the MTS/IEEE OCEANS conference is our premier annual event. In this issue we combine the two. While the OCEANS conference publishes proceedings, those papers are page limited and their oral presentations are usually kept to twenty minutes. As a regular attendee at OCEANS, I often feel that there is rich additional content to be shared. In this issue we test that hypothesis.

The following papers are all derived from papers presented at the OCEANS'08 MTS/IEEE Quebec City conference in Canada. A variety of authors were approached to expand their original papers into longer, more detailed pieces. Despite their base in previously reviewed material, all papers were carefully peer-reviewed. Some authors chose to take more time to address the review comments, and we will bring you their final papers in future issues.

This issue covers a variety of subjects, but it is not hard to see the theme of unmanned maritime vehicles (UMVs) running through several of the submissions. As the Chair of the UMV Committee, I attend many of these sessions at OCEANS. I saw many interesting papers and reached out to those authors. I encourage all readers to forward recommendations for papers worthy of expansion based on their own experience at OCEANS events.

In addition to more pages to expand their ideas, we also offer authors the chance to share more figures and data with us. Dick Crout's technical note presents a wealth of oceanographic data and thus highlights the value of expanding conference papers into more detailed discussions. Dr. McFarlane's commentary is derived from a retrospective paper he presented in Quebec City, where he was recognized by MTS with the Compass Distinguished Achievement Award. We appreciate his developing that summary work for our readers and further sharing many of his "lessons learned."

While this issue recognizes some of the exceptional papers presented at our MTS/IEEE OCEANS conference, I also want to highlight the volunteer team that helps bring you the *MTS Journal*. The Editorial Board helps me conceive issue themes and review the many proposals we receive for special issues. They also provide reviews of commentaries and an occasional full review of technical papers—and step up to the plate themselves to guest-edit special themed issues of the *Journal*.

Take a moment to review the biographies of the Editorial Board and get to know the individuals behind the publication. These individuals are leaders in their own fields who bring many valuable perspectives, and we appreciate their contributions. We have included as many photos as we could get. If you see them at an MTS event, perhaps OCEANS, take a moment to say hello and thank them for their service to the Society.

As always, your feedback is welcome. If you want to propose a special issue, volunteer to join the Editorial Board, or otherwise comment on the *MTS Journal*, you may reach me at Justin.manley@mtsjournal.org.

MTS Journal Editorial Board Biographies

Current Editorial Board Members

Justin Manley, Editor
Battelle

Justin Manley has been working with marine technology since 1990. Working with his family's business, Chicago Marine Towing, he helped expand company towing and salvage operations, developing a fleet of commercial vessels that serves the southern quarter of Lake Michigan.

Mr. Manley holds three degrees, B.S. Ocean Engineering, B.S. History and M.S. Ocean Engineering, from the Massachusetts Institute of Technology. Between 1994 and 2002 he was a principal in the development of autonomous marine robots at the MIT Sea Grant College Program. Mr. Manley concluded his career at MIT Sea Grant leading the Autonomous Underwater Vehicles (AUV) Lab.

In addition to at-sea experience in marine towing and salvage, Mr. Manley has participated in many ocean science and engineering field expeditions including: under-ice AUV operations, multi-static acoustic mine hunting using AUVs and deep-sea marine archaeology. In 2003 Mr. Manley supported the use of AUVs in the search for submerged debris from the Space Shuttle Columbia. In 2004 he served as a navigator for ROVs used to explore and create high-resolution photo mosaics of the RMS Titanic.

Since 2002 Mr. Manley has provided consulting services to the U.S. government. As Lead Ocean Engineer at Mitretek Systems and subsequently Senior Research Scientist and Research Leader at Battelle, he has supported clients developing and applying advanced undersea technology. He has worked extensively for the National Oceanic and Atmospheric Administration (NOAA), particularly its Office of Ocean Exploration and Research (OER). He was the founding Chair of the NOAA-wide AUV Working Group and led that team in its early efforts to increase awareness and application of AUVs in the agency.

Currently Mr. Manley's research interests include the application of "telepresence" to ocean exploration; technical standards, policies and concepts of operation for the use of unmanned maritime vehicles; "dual use" applications for military technologies in ocean science and the development of new *in situ* sensors for biological and chemical oceanography.

Mr. Manley is the Chair of the Unmanned Maritime Vehicles (UMV) Committee of the Marine Technology Society. He is a Senior Member of IEEE and co-chairs the UMV Committee of the IEEE Oceanic Engineering Society. He serves as membership secretary of ASTM Committee F41 developing technical standards for UMVs.

Corey Jaskolski
Hydro Technologies

Corey Jaskolski, president of Hydro Technologies, graduated from MIT with a Master's Degree in Electrical Engineering and Computer Science. While at MIT he also worked at unmanned underwater vehicle (UUV) developer Bluefin Robotics, where he led the early development of the first pressure-tolerant Lithium Polymer battery packs. In 2001, Jaskolski spent several weeks aboard the Russian science vessel, the Academic Keldysh, in support of James Cameron's documentary filming of the Titanic. During this expedition, Jaskolski got the opportunity to descend 12,500 feet to the wreck of the Titanic to support robotic operations. Jaskolski is featured in the film "Ghosts of the Abyss," a Walt Disney picture that covers this expedition.

More recently, Corey served as Director of Technology for a group at National Geographic involved in developing marine imaging systems, deploying live web cams in challenging environments, such as on the Belizian barrier reef, and capturing gigapixel spherical panoramic images of some of the world's cultural icons. Currently, Corey spends his time leading the development of Hydro Technologies' Hull Penetrator Replacement System

(HPRS), a magnetically coupled through metal power and data transmission system. In his free time Corey enjoys hiking Colorado's mountains with his wife Ann and trying to see the world in a different light through his photography.

Donna Kocak

Maritime Communication Services/ HARRIS Corporation

Donna Kocak has over 19 years experience in the ocean engineering field supporting design, development and testing of various scientific and engineering projects involving computer vision, instrumentation, and real-time systems. In her present position as Systems Engineer at Maritime Communication Services (MCS), HARRIS Corporation, she is leading the seafloor development of an ocean observing system for commercial and scientific use. Prior research and development activities included a patented, high-speed underwater 3-D laser mapping system; automated tracking and identification of bioluminescent plankton from sequential video images; control and identification algorithms for a manatee protection system currently being used throughout Florida; an optical mass gauge sensor for measuring hydrogen and oxygen in zero-g for NASA; and a fluorescent imaging system for detecting contamination on beef carcasses being used in commercial packing plants. In addition, Ms. Kocak founded her own firm, Green Sky Imaging LLC, specializing in software and processing services for undersea video photogrammetry and mensuration. She earned an MBA from the University of Florida and both an MS and BS in computer science from the University of Central Florida. From 2004 – 2008 she served as Chair of the Underwater Imaging Committee of the Marine Technology Society, and in 2008 she founded and now serves as Chair of the Society's new Committee on Ocean Observing Systems. She joined the *MTS Journal*'s Editorial Board after serving as Guest Editor of the special issue on "The State of Technology in 2008."

Scott Kraus, Ph.D.

New England Aquarium

Scott Kraus is the Vice President for Research at the New England Aquarium in Boston, Massachusetts. He has been a research scientist in the Aquarium's Edgerton Research Laboratory since 1980. He received his B.A. from College of the Atlantic, his M.S. in biology from the University of Massachusetts, and a Ph.D. from the University of New Hampshire.

Dr. Kraus has studied the biology of North Atlantic right whales since 1980, publishing numerous papers on many aspects of right whale biology and conservation. He is co-editor of *The Urban Whale*, a 2007 Harvard University Press book on right whales in the north Atlantic. He was a member of the original U.S. right whale recovery team, and currently serves on the U.S. harbor porpoise take reduction team and the U.S. large whale take reduction team. He is adjunct faculty at the University of Massachusetts at Boston and the University of Southern Maine. Kraus produced both the first North Atlantic humpback whale catalog and the first North Atlantic right whale catalog, research publications that utilize individually distinctive markings on animals to track life history. His early research focused on expanding the application of individual photo-identification studies into population biology.

Dr. Kraus' recent studies are looking at methods for reducing bycatch of small cetaceans in fishing gear using acoustic "pingers" and innovative fishing gear. His research is increasingly focused on conservation issues faced by endangered species and habitats, and the difficulties of identifying features that animals need to survive in an increasingly urban ocean.

Dhugal John Lindsay, Ph.D.

JAMSTEC

Dhugal John Lindsay received his Ph.D. in aquatic biology from the University of Tokyo in 1998. He is a Research Scientist with the Japan Agency for Marine-Earth Science & Technology (JAMSTEC) and holds adjunct professorships at Yokohama Municipal University and Kitazato University. Dr. Lindsay's research focuses on mid-water ecology, particularly concentrating on gelatinous organisms that are too fragile to be sampled by conventional methods and their associated fauna. Dr. Lindsay has extensive experience with the Japanese research vessel and submersible fleet, both as Chief Scientist and as a member of multidisciplinary teams. His sailing experience includes over 46 cruises aboard various Japanese research vessels and 21 dives in crewed submersibles. He has used conventional sampling techniques such as nets and sediment traps (e.g., IKMT, MTD, ORI, Norpac, IONESS, MOCNESS, R/V Tanseimaru, University of Tokyo; R/V Ronald H. Brown, NOAA) and towed camera arrays (e.g., 4000m and 6000m Deep-Tow Cameras, R/V Kaiyo,) and has also used both manned submersibles (e.g. Shinkai

2000, R/V Natsushima; Shinkai 6500, R/V Yokosuka) and remotely-operated vehicles (e.g. ROV Dolphin 3K, R/V Natsushima; ROV Ventana, R/V Point Lobos; ROV HyperDolphin, R/V Kaiyo; ROV Kaiko, R/V Kairei; uROV PICASSO; mROV) to investigate fauna from depths as shallow as the euphotic layer to as deep as the Challenger Deep, Mariana Trench. He is Project Leader of JAMSTEC's PICASSO Project. Dr. Lindsay is a member of the Japanese Society of Biologging Science, Plankton Society of Japan, and the Oceanographic Society of Japan; is on the editorial board of the journals "Scientia Marina", "Plankton and Benthos Research" and "The Marine Technology Society Journal"; and served on the National Academies of Science (U.S.) Ocean Studies Board, Committee on Future Needs in Deep Submergence Science. He serves on the Steering Committee of the Census of Marine Zooplankton (Census of Marine Life: CoML), and also on the Japanese National Regional Implementation Committee of CoML. Dr. Lindsay is also a reknowned and prolific haiku poet, working in the Japanese language.

Stephanie Showalter
University of Mississippi

Stephanie Showalter is the Director of the National Sea Grant Law Center at the University of Mississippi, and has served in this position for over three years. Stephanie received a B.A. in History from Penn State University and a joint J.D./Master's of Studies in Environmental Law degree from Vermont Law School. Ms. Showalter oversees a variety of legal education, research, and outreach activities, including providing legal research services to Sea Grant constituents on ocean and coastal law issues. Ms. Showalter holds adjunct positions at the University of Mississippi School of Law and the University of Southern Mississippi, teaching such courses as Ocean and Coastal Law and Wetlands Law and Regulation. Ms. Showalter's research on natural resources, marine, and environmental law issues has been published in a variety of publications. Recent works include "The United States and Rising Shrimp Imports from Southeast Asia and Central America: An Economic or Environmental Issue" in the Vermont Law Journal and "The Legal Status of Underwater Vehicles" in the Marine Technology Society Journal. Ms. Showalter's duties also include the supervision of law student research and writing projects and providing assistance to organizations and governmental agencies with interpretation of statutes, regulations, and case law. Ms. Showalter is licensed to practice law in Pennsylvania and Mississippi.

Jason Stanley
Schilling Robotics

Jason Stanley joined Schilling Robotics in 2001 as a systems integration engineer. He was quickly promoted to director of remote systems application in 2002, assuming responsibility for investigating new opportunities for the company's Remote Systems Engine and remotely operated vehicle (ROV) product lines. In 2003, he was promoted to vice president of sales and marketing for remote systems. In his current capacity, he is responsible for sales activities for standard and engineered-to-order systems, including ROVs, manipulators, and subsea control system applications. He develops strategic sales initiatives for the company worldwide.

Mr. Stanley brought to Schilling over 19 years of subsea-related experience, with emphasis on offshore operational engineering and management. He has served as a project manager, project engineer, and ROV fleet operations support at companies such as Perry Slingsby Systems, Ceanic Corporation (now part of the Acergy Group), and Sonsub. With both Sonsub and Ceanic, Stanley gained expertise as a field engineer, ROV supervisor, ROV pilot, and ROV pilot/technician, making him a valuable resource on product usability to Schilling customers.

Mr. Stanley earned a B.S. in Ocean Engineering from Texas A&M University in College Station, and has completed coursework in computer information systems at the University of St. Thomas in Houston, Texas. He is active in the professional community through the Marine Technology Society (MTS), the Society of Underwater Technology (SUT), the International Marine Contractors Association (IMCA), the Society of Petroleum Engineers (SPE), the Association for Unmanned Vehicle Systems International (AUVSI) and the Project Management Institute (PMI).

Edith Widder, Ph.D.

Ocean Research & Conservation Association

Dr. Edith "Edie" Widder is a biologist and deep-sea explorer who is applying her expertise in oceanographic research and technological innovation to reversing the worldwide trend of marine ecosystem degradation. She graduated Magna cum laude from Tufts University where she received her B.S. Degree in Biology. She then went on to earn a Master's Degree in Biochemistry and a Ph.D. in Neurobiology awarded by the University of California in Santa Barbara.

Two years after completing her Ph.D., Dr. Widder became certified as a Scientific Research Pilot for Atmospheric Diving Systems. She is certified to dive the deep diving suit WASP, as well as the single-person untethered submersibles Deep Rover and Deep Worker and she has made over 250 dives in the Johnson Sea-Link submersibles. Her research involving submersibles has been featured in BBC, PBS, Discovery Channel and National Geographic television productions.

A specialist in bioluminescence (the light chemically produced by many ocean organisms), Dr. Widder has been a leader in helping to design and invent new submersible instrumentation, and equipment to enable unobtrusive deep-sea observations. Working with engineers, she has conceived of and built several unique devices that enable humans to see beneath the waves in new ways, including HIDEX, a bathyphotometer that is the U.S. Navy standard for measuring bioluminescence in the ocean. Dr. Widder also developed LoLAR, an ultra-sensitive deep-sea light meter that measures light in the deep ocean, both dim down-welling sunlight and bioluminescence. Most recently, Widder created a remotely operated deep-sea camera system, known as ORCA's Eye-in-the-Sea (EITS), an unobtrusive deep-sea observatory and the world's first deep-sea web cam. EITS has produced footage of rare sharks, fish, and never seen before animal behaviors as well as discovered a new species of large squid. This work was recently featured on the Discovery Channel series *Midwater Mysteries* and PBS's *NOVA ScienceNOW*.

In 2005, Dr. Widder resigned from her 16-year post at Harbor Branch Oceanographic Institution to co-found the Ocean Research & Conservation Association (ORCA), a non-profit organization dedicated to the protection of marine ecosystems and the species they sustain through development of innovative technologies and science-based conservation action. While translating complex scientific issues into technological solutions, Dr. Widder is fostering greater understanding of ocean life as a means to better, more informed stewardship. In September of 2006, based on her work with ORCA, Dr. Widder was awarded a prestigious MacArthur Fellowship from the John D. and Catherine T. MacArthur Foundation.

Jill Zande

MATE Center

Jill Zande is the Associate Director of the Marine Advanced Technology Education (MATE) Center and Competition Coordinator for the MATE Student ROV Competition. Ms. Zande holds an M.S. in Oceanography & Coastal Studies from the Louisiana State University and a B.S. in Biology from Penn State University.

As the Associate Director, Co-PI, and Competition Coordinator for the MATE Center, Ms. Zande's role is to work closely with industry to ensure that educational programs are aligned with workforce needs and to facilitate partnerships among educators, students, employers, and working professionals. Jill maintains relationships with well over 100 businesses, research institutions, government agencies, and professional societies and nearly 200 middle schools, high schools, colleges, and universities that participate in MATE ROV competitions each year.

Ms. Zande is an active member of the Marine Technology Society (MTS). She served on the MTS Education Task Force, the MTS Journal editorial board, as chair of the Monterey Bay section, and is currently VP of Education and Research. She is also a member of the MTS ROV and Education Committees.

Prior to marine technical education, her focus was on marine research. During her Master's degree program at LSU, she participated in research cruises that investigated hydrocarbon seep communities in the Gulf of Mexico using the Johnson Sea-Link and Alvin submersibles. As a research technician at the Dauphin Island Sea Lab (DISL),

Ms. Zande's focus shifted from the deep ocean to the coastal environments where she studied seagrass communities.

MTSJ Editorial Board members who rotated off the board between 2006 and 2008

James Lindholm, Ph.D.

Cal State University Monterey Bay

Dr. James Lindholm (B.A. California Polytechnic State University; M.A. and Ph.D. Boston University) is currently James W. Rote Distinguished Professor of Marine Science and Policy at California State University Monterey Bay. He is an ecologist and conservation biologist with interests across a wide range of taxa and geographic regions. His research interests include the landscape ecology of fishes, the recovery of seafloor habitats and associated taxa following the cessation of fishing activity, and the design and efficacy of marine protected areas. Current research activities include projects along the central coast of California, the Florida Keys, and the Gulf of Maine.

Dr. Lindholm is also the founder and Director of the Institute for Applied Marine Ecology (IfAME) at CSU Monterey Bay. The mission of the IfAME is to develop clear linkages between ecological phenomena and potential and realized management regimes along the California coast, across the U.S., and throughout the world. To accomplish this mission, Dr. Lindholm, colleagues and students work closely with the state and federal government agencies, non-governmental organizations, and other academic institutions.

Phil Nuytten, Ph.D

Nuytco Research, Ltd.

Dr. Phil Nuytten has spent his life in subsea exploration. In the 1960s and 70s, Nuytten was heavily involved in experimental deep-diving and the development of mixed gas decompression tables; during this period, he co-founded Oceaneering International Inc., a company that pioneered many early subsea development projects, and has gone on to become one of the largest underwater skills companies in the world.

In 1997, Nuytten and his design team produced the 2,000-foot-rated micro-submersible 'DeepWorker 2000', a revolutionary deep-diving system that has been called an "underwater sports car". Nuytten and Nuytco Research Ltd. received a five-year contract from the National Geographic Society to provide DeepWorker 2000 submersibles and crews on Dr. Sylvia Earle's 'Sustainable Seas Expeditions', an initiative to study deep ocean environmental impact. In 1999, NASA contracted a pair of DeepWorkers to study their possible use in the recovery of the Space Shuttle booster rockets, and in 2000 DeepWorkers successfully recovered the Space Shuttle booster rockets from the May flight to the U.S. Space Station. In 2003, Nuytten and his design team completed the first side-by-side Dual DeepWorker, designed for a pilot and one observer. Designed with the use of deep-depth underwater tourism in mind, this 2000-foot-rated submersible has commercial and scientific applications as well.

Dr. Phil Nuytten has earned many international honors and awards. These include commercial diving's highest award from the Association of Diving Contractors International, the Academy of Underwater Art and Sciences 'Nogi' award, induction into the 'Diving Hall of Fame', and the Explorer's Club's prestigious 'Lowell Thomas' Award.

Terrence Schaff

Woods Hole Oceanographic Institution

Since July 2003, **Terry Schaff** has served as the Director of Government Relations for the Woods Hole Oceanographic Institution where he is responsible for interactions with Congress and the major ocean science agencies. Prior to that, Terry was the Associate Director for Investment and Implementation for the U.S. Commission on Ocean Policy. There he helped develop the Commission's recommendations for government structure and investment requirements and the strategy for implementing the Commission's recommendations. Terry has also served as Senior Advisor for Legislative Affairs to the Director of the National Science Foundation, was the Director of Federal Relations for the Consortium for Oceanographic Research and Education and spent three years working on ocean issues for the House of Representatives. Terry has a Master's degree in Oceanography from North Carolina State University and a Bachelor's degree in Marine Biology from the University of North Carolina at Wilmington.

COMMENTARY

Tethered and Untethered Vehicles: The Future Is in the Past

AUTHOR

James R. McFarlane[1]
International Submarine Engineering Ltd.

Abstract

Underwater vehicle development in Canada has been active for more than 40 years. Most of this work has been carried out in British Columbia. The developments include manned submersibles (subs), remotely operated vehicles (ROVs), autonomous underwater vehicles (AUVs), and unmanned underwater vehicles. The users of these vehicles include offshore petroleum, telephone cable maintenance, science, surveying, salvage, and military. The enabling technologies for these integrations are mature.

Today, some services may not be provided by relevant agencies with marine missions worldwide because they are short of the funding needed to discharge duties. There is the constant lament that there are not enough ships, people, or hardware. Perhaps if we are smart enough, we can accomplish a portion of these tasks using advanced technology, which is sometimes considered to be unconventional wisdom—namely robotics.

Some may observe that many types of underwater vehicles already exist, or at least subsets exist. Therefore, some might wonder if they are any good and why are not more people using them. The reasons are that there is confusion regarding where to establish the boundary conditions for proper comparisons of performance. Another issue is the lack of appreciation of the state of technological evolution. Also, all potential vehicle integrations have not been fielded.

Another important aspect concerning acceptance that limits the use of vehicles is the changes required in the personnel establishment and the training of people who will use them. We are in a period of transition, and in these transitional periods, false starts can be expected as the vision of the customer and the supplier is sometimes not clear because of a lack of experience. We sometimes see this lack of experience manifested in specifications that describe impossible-to-build vehicles. In this situation, there are often enormously expensive development efforts attempting to meet impossible specifications.

This paper presents the use of existing integrations, which have contributed to the development of hybrid vehicles. This contributes to the capability to integrate systems to acquire the data to support the acquisition of data for the submission to the Internal Sea Bed Authority in accordance with Article 76 for those countries that have ratified the United Nations "Law of the Sea" Treaty.

Article 76 provides instructions regarding how coastal states exercise sovereign rights beyond the customary 200 nautical mile limit. The procedures for defining the outer limits of extended jurisdiction are based upon bathymetric and geological criteria. The procedures impose requirements to assemble, manipulate, visualize, and analyze a wide range of information in an accurate and well-documented fashion that is consistent with the reporting requirements of the International Seabed Authority. Underwater vehicles will be used to obtain some of the information required.

We need to look at the past and present to project the future.

> *"Time present and time past are both perhaps present in time future, and time future contained in time past."* T.S. Elliot, 1888-1995

Over the last four decades, there has been a series of revolutions in our ability to conduct underwater work.

To date, we appear to have moved through four revolutions. Each of these has adopted the use of their predecessor systems. These are manned subs, ROVs, AUVs, and hybrids.

Manned Submersibles (Subs)

The First Revolution: Diving and Manned Subs in the 1960s

- January 1960: Walsh and Piccard to the bottom of the Challenger Deep.
  - Remotely operated vehicles (ROVs) and autonomous

[1]Editor's Note: This submission was solicited from Dr. McFarlane in recognition of his long experience in this field, and based on a similar work presented at the OCEANS'08 MTS/IEEE Quebec City conference in Canada. This commentary is focused on technologies and products developed at International Submarine Engineering Ltd. (Port Coquitlam, BC Canada). The author's analysis is presented in the context of his own experience. The *MTS Journal* appreciates and welcomes Dr. McFarlane's experience and analysis, but does not promote or endorse specific products or companies.

underwater vehicles (AUVs): U.S. Navy CURV *ROV* was fielded; University of Washington fields AUV *SPURV*.

- Mixed Gas Diving:
  - Hannas Keller
  - Captain George Bond, United States Navy (USN)
  - Captain Cousteau
- Manned subs
- Star I, Deep Ocean Work Boat (DOWB), Beaver Mark IV (MKIV), Shelf Diver, Diver Lockout SDL-1

With the exception of Woods Hole, the University of Hawaii, the PP Shirov Institute of Oceanography, and JAMSTEC, all other science performers use ROVs and AUVs. In addition to manned subs, JAMSTEC has used ROVs, e.g., *HYPERDOLPHIN*.

ROVs

The Second Revolution: ROVs in the 1970s

- Manned subs are produced in numbers. By 1974, there are 30 manned subs in the North Sea.
- In the late 1970s, ROV use moves ahead rapidly and displaced manned subs. The driving force is the offshore petroleum industry (MONEY).
- The late Frank Busby referred to this as the "Thundering Herd Syndrome."
- ROVs today span the range from small shallow-diving hand-launched ROVs to 250-HP 10-ton ROVs. ROVs' diving depths reach as far as 6,000 m. They carry manipulators, TV, Sonar, and other tools. They are used for science, accident investigation, telephone cable maintenance, military, mineral exploration, and support for the offshore petroleum industry.

AUVs

The Third Revolution: AUVs, Autonomous Marine Vehicles

- The third revolution includes AUVs, autonomous and remotely supervised semi-submersibles, and autonomous boats.
- Autonomous Marine Vehicle development begins in earnest in the 1980s.
- Although the concept has been around for a while, the Personal Computer (PC) revolution contributes to the feasibility. By the mid 1980s, the following had been achieved:
  - Surveys with AUVs
  - Obstacle avoidance
  - Line following/way point processing
  - Fully autonomous operation

Nikola Tesla devised the first autonomous vehicle in 1898. At the time, Tesla wrote:

> *"They will be produced capable of acting as if possessed of their own intelligence and their advent will create a revolution."*

It has taken more than 100 years to implement his vision. Although there have been many examples of AUVs since Tesla, it has only been since the introduction of the microprocessor that the major advances have been made in the development of autonomous vehicles. Examples include *EXPLORER* and *THESEUS*.

We are interested in AUVs as a way to reduce the cost of a diverse set of missions, including defense. The capacity to wage political war, drug war, or fish war must be included in the industrial capacity.

Today AUVs have been built in sizes from the diminutive *GAVIA* to the 9-ton *THESEUS*, *Bluefin*, *Hydroid*, and *HUGIN*.

EXPLORER: The modular design and the use of inexpensive materials for the payload section of the vehicle create an open architecture that permits the easy reconfiguration of the vehicle for a variety of applications and missions. In the same context, an open approach to software design avoids legacy problems and allows the operator to adapt the behavior of the vehicle to meet new requirements. It is most often fitted with a 10.4-kW h rechargeable lithium battery that can be discharged to 100% of its capacity and which carries a guarantee of 2,000 cycles. Typical dimensions are length = 4.5-6 m and diameter = 0.69 m. However, in any case of sampling, is there enough data to characterize process? It depends on the process to be characterized. We have to satisfy Nyquist's Theorem; for example, Air drops and Gliders Gulf Stream.

Semi-Submersibles: *DOLPHIN/DORADO*

DOLPHIN and *DORADO* are autonomous semi-submersibles developed by ISE Research Ltd. to provide a stable sensor platform for operation in high sea states. They have proven to be viable and cost-effective vehicles for geophysical and hydrographic survey as well as minehunting missions. The vehicles' configuration allows for an easy integration of towed and hull-mounted sensor equipment. Sensor data links, which may require high-bandwidth microwave channels, can also be easily integrated into the vehicles with the antenna mounted on. *DOLPHIN* is fitted with a 150-HP engine and *DORADO* with a 450-HP engine. The low cost and autonomy make semi-submersibles ideal for hazardous missions. Because they are snorkling diesel semi-submersibles, they have significant advantages in com-

munication, range, and speed capabilities over fully submersible or surface vehicles with sea state capability comparative displacement. They can be teleoperated from a ship or a shore station via an ultra high frequency radio link or pre-programmed with a set of waypoints and run autonomously. When running autonomously, the control radio can allow the checking of vital signs and the monitoring of the mission progress. The existing software is capable of operating multiple vehicles using only one pair of radio channels. Launch-recovery and refueling systems have been developed for use underway in Sea States up to Beaufort 6. This type of vehicle has applications for surveying and rapid response to mine threats. For example, a *DORADO* was delivered from the west coast to the east coast in 6.5 h. Because they can be supervised from satellite, air, land, or sea, the supervision does not have to be in harms way.

Hybrid Vehicles

Hybrid integrations of manned subs, ROVs, and AUVs are robust because they are using parts that have been in use in other fields. They are composed of two or more of the exiting vehicle types (Figure 1). The potential was first noted in James McFarlane's 1986 Robert Bruce Wallace Lecture at Massachusetts Institute of Technology (MIT). Hybrids are now being produced. For example,

- A submersible that delivers and deploys an ROV
- An AUV carrying an ROV to a satellite field
- Vehicles for exploration and sampling, which can act like ROVs or AUVs
- The new USN Submarine Rescue Systems, which are a combination of an ROV and a manned sub.

FIGURE 1

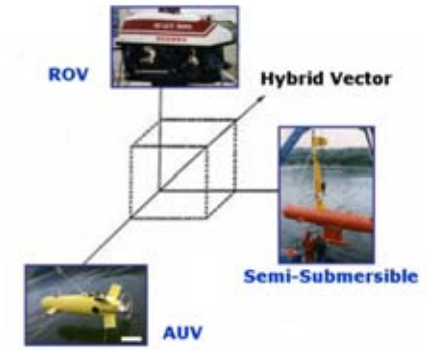

THESEUS Hybrid

FIGURE 2

Theseus in Indian Arm – 1995 at the start of acoustic telemetry trials in 200 m of water.

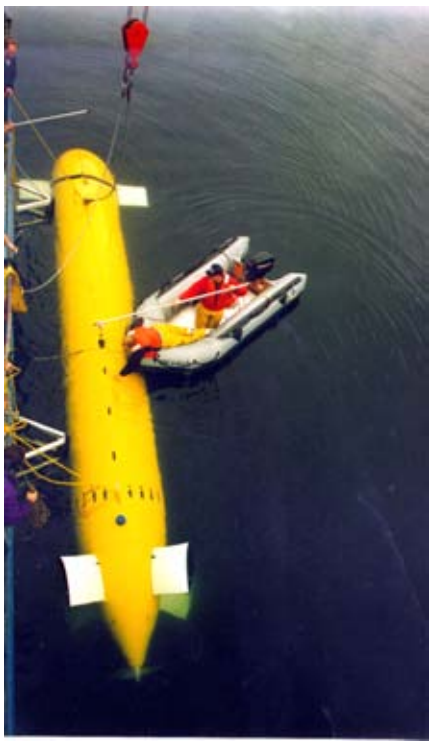

The Canadian *THESEUS* in the Arctic

THESEUS is an AUV that has operated in the Arctic out of Alert, Ellesmere Island 82°28' north. It can transverse under the ice to ranges of 850 km at 2.5 knots. It has a payload of 1 ton. It has been used to lay a continuous length of fiber optic cable 175 km long under the Arctic ice. The speed for cable laying was 4 knots. These three axes shows ROVs, AUVs, and semi-submersibles. They are bound to the space occupied by planer and spatial hybrids.

FIGURE 3

Theseus AUV under the Arctic ice cap at the start of a cable-laying mission – 1996.

Some have thought that *THESEUS* was an AUV. It is sometimes, but when it is laying fiber optics, there is real-time full duplex communications over 175 km of fiber. In this condition, it can be considered an ROV. It also shows that it would be relatively easy to communicate with a vehicle in the "Challenger Deep," which is only 11 km down.

THESEUS has the ability to plan and replan paths and to avoid obstacles. This vehicle is stationed at ISER on behalf of the Defense Research Establishment Atlantic (DREA). It is available for commercial projects, R&D, or the military. Other applications include covert operations, package delivery, survey, and reconnaissance.

SAILARS: A Semi-Submersible ROV Hybrid

FIGURE 4

SAILARS Conceptual Drawing.

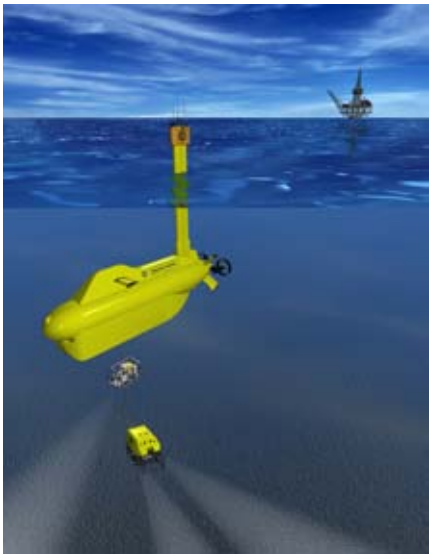

SAILARS is a hybrid AUV-ROV that can operate and provide power for 50-150-HP work class ROVs.

SAILARS is designed to accommodate a variety of existing ROVs without modification and operate in Sea State 6 at distances of up to approximately 15 mi from the controlling platform.

Compared to the fully submersible AUV in the hybrid role, the semi-submersible *SAILARS* can provide much higher levels of endurance and power to the ROV, has a continuous ability to transmit high bandwidth ROV data to the controlling platform, and can provide more accurate positioning, Additionally, *SAILARS* does not require any infrastructure support from oil and gas platforms. The work was funded by J. Ray McDermott.

SWIMMER AUV

FIGURE 5

Rover/Gofer hybrid AUV-ROV delivery system.

Since 2001, Cybernetix has been proving that the concept of using a hybrid AUV-ROV for inspection, maintenance, and repair tasks in deep-water oil fields and remote locations is both feasible and economic. This concept deploys a dedicated AUV, which is the shuttle and is only one subsystem of the overall *SWIMMER* concept. The other component is a lightweight work ROV system, which transports the ROV to a deep-water structure where it is fully capable of the tasks required of a traditional ROV. It can transit to a satellite field using the flow line as a guide. This vehicle system eliminates compounded costs involved with surface vessel transport and standby, as well as other costs that can be extensive such as deployment time, labor, and handling.

ROVER/GOFER is another example of a hybrid AUV-ROV delivery system.

REMORA and *PRMS*

FIGURE 6

Ocean Works International-Pressurized Rescue Module System (PRMS).

REMORA and *PRMS* are ROV and manned sub hybrids. They are remotely controlled vehicles with an ROV console. The ROV propulsion is used to maneuver the pressure hull to mate up with the submarine escape hatch. This enables the rescue of people trapped in submarines. More than 200 transfers have been made using this system. OceanWorks and ISE have created these systems.

Conclusion

Manned subs, ROVs, AUVs, and hybrids all have a place in contributing to the efficiency of our underwater work capability. Each year, there are new integrations that add to our capability. Additional vehicle designs, such as subs as beer can- or juice can-sized air droppable units and gliders, will be required in some cases to provide enough data to characterize processes. Thus, the subsea revolution that started 40 years ago is still ongoing. The difference is that many sub system components are now mature.

TECHNICAL NOTE

Oil and Gas Platform Ocean Current Profile Data from the Northern Gulf of Mexico

AUTHOR

Richard L. Crout
NOAA National Data Buoy Center

ABSTRACT

Approximately 40 deep water oil production platforms and drilling rigs continue to provide real-time current profile data to NOAA's National Data Buoy Center (NDBC). The NDBC receives and quality controls the data and transmits it over the Global Telecommunications System. The NDBC stores the raw binary current profile data where it can be extracted in order to forecast the Loop Current and Loop Eddies for oil and transportation concerns in the Gulf of Mexico and to investigate the oceanography of the northern Gulf of Mexico. After quality control, the NDBC also stores the processed data.

In addition to aiding the oil and gas industry to understand and design for the forces in the water column generated by strong currents in the Gulf of Mexico, the three years of ocean profile data show a number of oceanographic phenomena. This paper presents an examination of the Loop Current and associated eddies based on the oil and gas industry data. The high currents of the Loop Current that extend to several hundred meters depth are present and generally impact oil platforms as it moves into the northern Gulf of Mexico. Loop Eddies exhibit many of the same characteristics as the Loop Current, then move into the western Gulf of Mexico to impact oil platforms there before currents diminish. Cyclonic eddies formed from interactions between the Loop Current and topographic or land features are also present. Five-day plots of the current profiles show the passage of eddies. Wind-driven inertial currents propagate throughout the water column in all regions of the Gulf. The current profiles from delayed-mode, bottom-mounted profilers show that hurricane-generated near-inertial currents reach great depths.

Keywords: Loop Current, Loop Eddies, Oil and Gas Platforms, National Data Buoy Center, Northern Gulf of Mexico

Introduction

The Loop Current and associated Loop Eddies impact deep water oil platforms in the northern Gulf of Mexico in a number of adverse ways. The Minerals Management Service (MMS) therefore requires that deep water oil drilling and production platforms in the northern Gulf of Mexico collect and provide current profile data to the National Data Buoy Center (NDBC). The oil industry in the Northern Gulf of Mexico currently provides current profile data in response to Notice To Lessees (NTL) No. 2009-G02 (expires 27 January 2014), which replaces previous NTLs, the first was released in April 2005. The NTL states that the current profile data are required to

- provide the necessary ocean current data needed for planning, designing, and operating mobile offshore drilling units, floating production platforms, and their ancillary equipment (i.e., drilling risers, production risers, flowline and pipeline risers, tension leg platform (TLP) tendons, and mooring systems);
- provide the necessary ocean current data to evaluate drilling risers, production risers, TLP tendons, and mooring systems for fatigue;
- ensure the sharing of ocean current data to develop a better understanding of ocean currents and bathymetry; and
- allow for the tracking of loop currents and eddy currents.

Oil companies or their operators collect current profile data using Teledyne RD Instruments Inc. Acoustic Doppler Current Profilers (ADCPs) when drilling wells or operating production platforms in water greater than 400 m deep. They are required to collect the data at 20 min intervals and transmit the data via FTP to the NDBC. The NDBC processes and quality controls the current data, then displays the resulting currents on the NDBC Web site. A committee of oil company, industry, and government representatives determined the data collection, processing, and quality assurance methods to be used for all program data. The NDBC implemented quality control algorithms. In addition to the resulting imagery and data, including quality control flags available on the public NDBC Web site, the raw binary, non-quality controlled data are also available.

Environment

The Loop Current is part of the Gulf Stream Western Boundary Current system, linking the Caribbean Current from the Caribbean Sea through the Yucatan Straits to the Florida Current and the Gulf Stream in the Atlantic Ocean. The extent and complexity of the Loop Current have emerged during the past 40 years. Infrared and visible satellite imagery in the late 1960s and 1970s allowed scientists to see the extent of warm Loop waters far into the eastern Gulf of Mexico. During the late 1980s and 1990s, satellite altimetry provided the ability to determine the position and movement of the Loop Current and Loops eddies throughout the Gulf of Mexico. The assimilation of altimetry has allowed numerical models to accurately position these oceanographic features and forecast their movement.

The Loop Current does not often take the direct path from the Yucatan Straits through the Florida Straits. The historical record shows many examples of Loop penetration far into the Central Gulf of Mexico. Often these penetrations lead to the separation of a Loop Eddy, akin to the Warm Core Rings that form from the Gulf Stream and Kuroshio western boundary currents. The detachment and separation of a Loop Eddy are complex, involving westward propagation of the Loop Current and cyclones that wrap around the Loop Current (Schmitz et al., 2005) and possibly upstream impacts. Loop Eddies may be small, medium, large, or huge. Their fates include numerous reattachments to the Loop Current, absorption by the Loop Current, merging with other detached Loop Eddies, splitting into two eddies, or dissipation in the western Gulf of Mexico. During the two decades between 1973 and 1992, 22 Loop Eddy separations were detected. From 1993 to 2002, 17 Loop Eddies separated from the Loop Current. Leben (2005) indicated that the period for separation of a Loop Eddy varies from a few weeks to 18 months. The power spectrum shows peaks at periods of approximately 6, 12, and 18 months.

An example of the structure of the Loop Current and associated Loop and cyclonic eddies is presented in Figure 1. The Loop current enters the Gulf of Mexico through the Yucatan Straits, turns back toward the south at approximately 25°N, and exits through the Florida Straits to form the core of the Gulf Stream. Inoue et al. (2008) showed data from a mooring in this region with currents at 60 m depth that exceed 170 cm/s. Currents in the lower layer, below 1550 m, exceed 50 cm/s. A strong Loop Current Eddy, Eddy Cameron, recently detached from the Loop Current, is centered at 26.5°N, 89.5°W. An older detached Loop Current Eddy, Eddy Brazos, is centered in the western Gulf of Mexico (Horizon Marine Name Indices, 2009). The shedding process is related to cyclonic eddies that rotate clockwise around the Loop Current. Cyclonic eddies are found throughout the Gulf of Mexico. Oil and gas platforms have begun drilling in deeper waters of the Gulf of Mexico (Figure 2) and have moved into a region of high currents associated with the Loop Current and its associated eddies. Exploration, installation, and production activities are impacted by the currents. The location of drilling rigs and platforms may move, structural bending and stress on platform components may occur, excessive riser angles may result, and costly damage can be inflicted. Diving and remotely operated vehicle operations, pipe laying, and anchoring operations are more difficult as a result of the high currents (Coholan et al., 2008).

Approximately 70 production platforms and drilling rigs in the northern Gulf of Mexico have provided data to the NDBC since the beginning of this program. The distribution of participating oil and gas platforms on 27 April 2009 is shown in Figure 2. Yellow diamonds indicate platforms transmitting data, and red diamonds indicate platforms that are presently inactive. Most of the sites are located on the outer continental shelf and slope of the northern Gulf of Mexico,

FIGURE 1

20 July 2008 Gulf of Mexico Naval Research Laboratory Navy Layered Ocean Model surface current output showing the Loop Current and Eddies Cameron in the east and Brazos in the west.

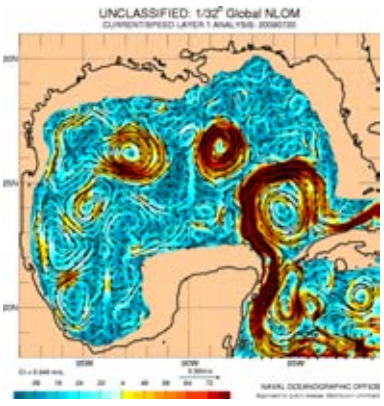

FIGURE 2

Distribution of oil and gas platforms and drilling rigs registered with NDBC 27 April 2009. Yellow stations are currently providing data to NDBC. (Color versions of figures available online at: http://www.ingentaconnect.com/content/mts/mtsj/2009/00000043/00000002.)

stretching from Texas to south of Alabama. As many as 48 stations have simultaneously provided data to the NDBC.

Access to all of the data transmitted to the NDBC is unlimited. The raw, binary data may be transmitted via FTP from the NDBC, and quality control algorithms may be applied as desired. The quality-controlled data may also be extracted from the NDBC. Alternatively, hourly data are transmitted to the world via the Global Telecommunications System. These *in-situ* current profiles may be assimilated into numerical models, used to develop nowcasts, or used to verify model runs.

Loop Current

The location of the Loop Current within the Gulf of Mexico is shown in a composite sea surface temperature image (Figure 3) from early May 2005. The letters on the figure indicate the location of four platforms (B, Brutus; N, Nautilus; J, Jim Thompson; U, Ursa) discussed in the following paragraphs. At this time, the Loop Current had progressed far into the Gulf of Mexico and into an area offshore of Louisiana, where the oil and gas industry has a number of production platform and drilling rigs. The complex structure during this time is due to the fact that the Eddy Vortex was undergoing one of its four reattachments to the Loop Current. ADCP current profile data from four platforms show the ocean dynamics associated with the Loop Current and Eddy Vortex at this time (Figures 4, 5, 6, 7). Stick plots show one, three, or five days of data collected at each site. The current vectors begin at each measurement depth. North is toward the top of the plot and east is toward the right. The scale is provided on the right side of the plot and "scale doubled due to high current speeds" indicates that the scale is 0-100 cm/s instead of 0-50 cm/s.

The first plot (Figure 4) shows 36 h of current vectors for the Brutus platform (denoted B in Figure 3) west of the Loop Current. The plot indicates current velocities generally less than 20 cm/s. Some currents between 20 and 40 cm/s are present during the middle portion of the period in the upper 150 m of the water column. Currents are toward the north-northwest (Figure 5) at the drilling rig Nautilus

FIGURE 3

2 May 2005 Gulf of Mexico composite sea surface temperature image from the Naval Oceanographic Office. The letters signify the positions of the Brutus (B), Nautilus (N), Jim Thompson (J), and Ursa (U) platforms and ADCP data.

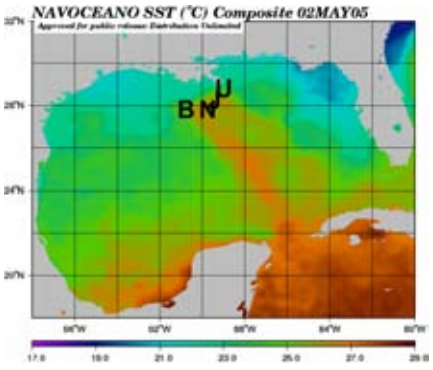

FIGURE 4

Thirty-six hours of current profile data as a current stick plot for 2 May 2005 from the Brutus production platform.

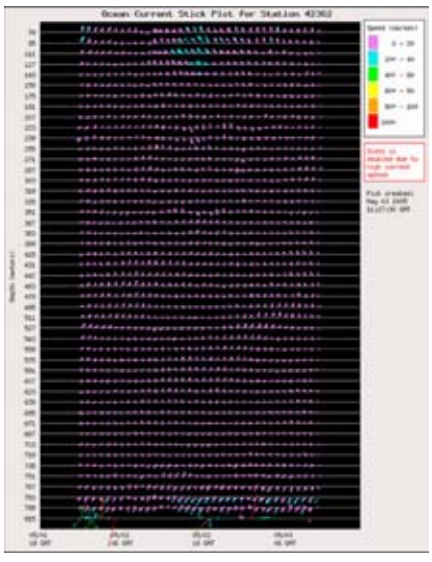

FIGURE 5

Thirty-six hours of current profile data as a current stick plot for 2 May 2005 from the Nautilus drilling rig.

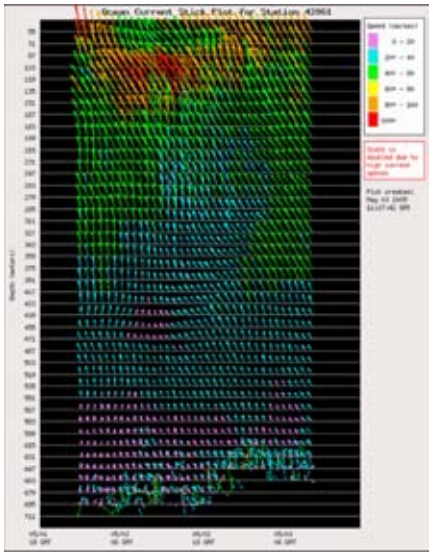

FIGURE 6

Thirty-six hours of current profile data as a current stick plot for 2 May 2005 for drilling platform Jim Thompson.

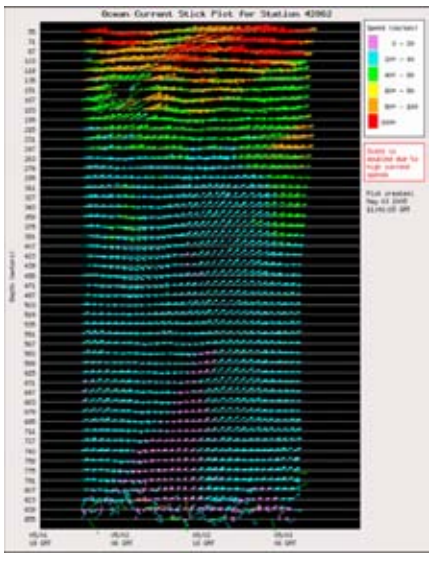

FIGURE 7

Thirty-six hours of current profile data as a current stick plot for 2 May 2005 at the Ursa production platform.

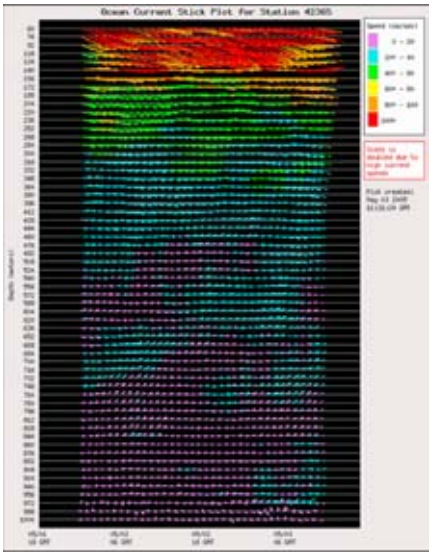

(denoted N in Figure 3), indicating that this platform is on the western side of the Eddy Vortex.

The drilling rig Jim Thompson (denoted J in Figure 3) is north-northeast of Nautilus, and the eastward currents in the upper 200 m of the water column in excess of 50 cm/s, with some currents exceeding 100 cm/s, indicate flow in the northern margin of the Eddy Vortex (Figure 6).

Strong currents toward the east-southeast (Figure 7) at the production platform Ursa (denoted U in Figure 3) indicate that it is located on the northeastern edge of the Loop Current.

Loop Current and Cyclonic Eddies

Two figures from the Colorado Center for Astrodynamics Research of surface currents in the Gulf of Mexico (Figure 8) show the detachment of Eddy Cameron during a three-week period in July 2008. An older Loop Eddy, Eddy Brazos, has translated farther westward, and two paired eddies north of Eddy Cameron have been generated in response to the event. The action of two cyclonic eddies, one on the west and one on the east, of the Loop Current appear to have played a role in the detachment of the eddy.

FIGURE 8

Dynamics in the Gulf of Mexico during July 2008 shown in the Colorado Center for Astrodynamics Research (CCAR) Gulf of Mexico Near-Real-Time Altimeter Data Viewer, sponsored by the University of Colorado, Boulder. The detachment of Loop Eddy Cameron (C) from the Loop Current (L); Loop Eddy Brazos (B) located in the western Gulf of Mexico; and cyclonic eddies (E) are shown.

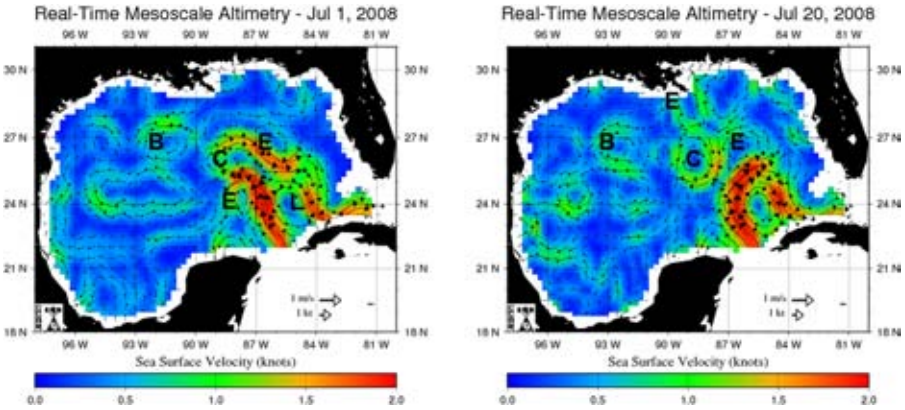

The positions of nine platforms providing data 20 July 2009 are presented in Figure 9. The positions are relevant to the discussions regarding current profiles collected at these platforms and their relationship to the dynamics of the ocean discussed in the paragraphs that follow.

Three oil and gas platforms that provide ADCP data to the NDBC are located in or adjacent to the older detached Loop Eddy Brazos, centered at approximately 26.8°N, 91.5°W in the Western Gulf of Mexico. The drilling rig Lorris Bouzigard is on the northwest edge of Eddy Brazos and exhibits currents toward the northwest (Figure 10). To the southeast is the Magnolia production platform, where currents on the northeast edge of Eddy Brazos flow south-southeastward (Figure 11). To the southwest of Magnolia is the drilling rig Discoverer Spirit, where the currents on the southeastern edge of Eddy Brazos flow southward (Figure 12). The drilling rig Ocean America is southwest of Lorris Bouzigard and shows evidence of an eddy passing the rig at depths of 200 to 700 m (Figure 13).

FIGURE 9

The approximate locations of various production platforms and drilling rigs discussed in the text in relation to the oceanographic features previously described. The positions are for 20 July 2008. L–Louis Bouzigard, M–Magnolia, S–Discoverer Spirit, O–Ocean America, D–Development Driller 2, N–Neptune, G–Genesis, H–Horn Mountain, and C–Cajun Express.

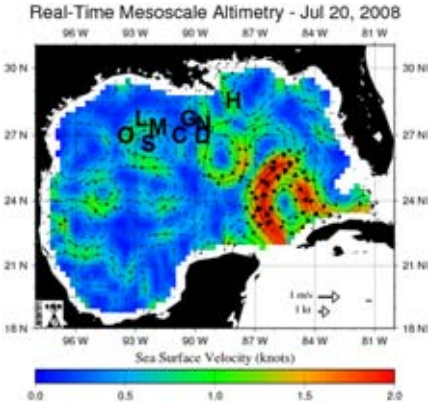

FIGURE 10

Forty-eight hours of stick plots from 20–21 July 2008 for the drilling platform Lorris Bouzigard showing flow around the northeast margin of detached Eddy Brazos in the Western Gulf of Mexico.

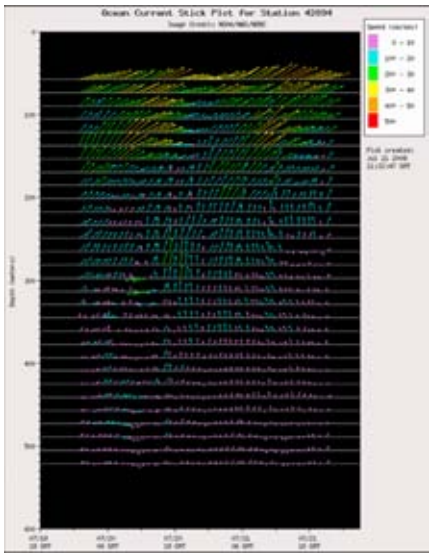

FIGURE 11

Forty-eight hours of current profile data shown as stick plots at the Magnolia platform showing flow around the northeast edge of Eddy Brazos in the Western Gulf of Mexico.

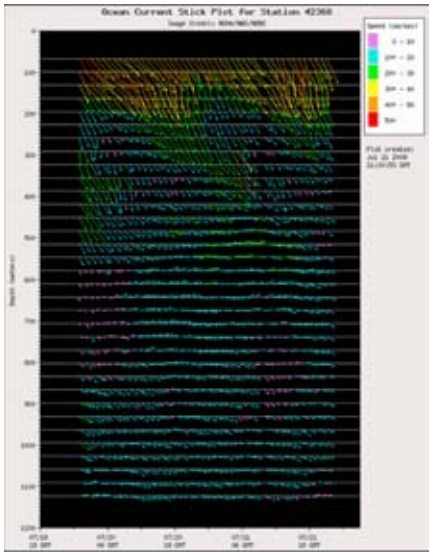

FIGURE 12

Stick plots of current profile data showing flow around the southeast edge of Eddy Brazos from the MODU Discoverer Spirit.

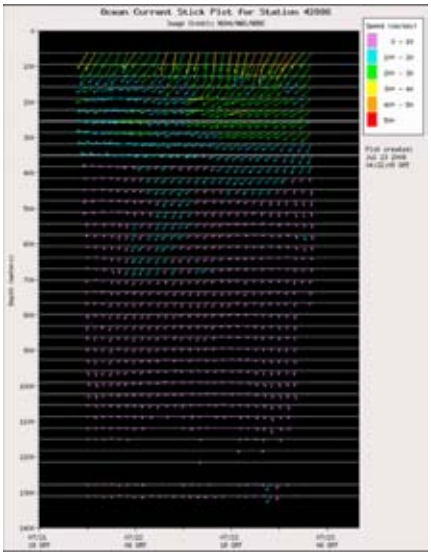

FIGURE 13

Five days of stick plots showing current direction and speed at the Drilling Rig Ocean America on the northern edge of Eddy Brazos.

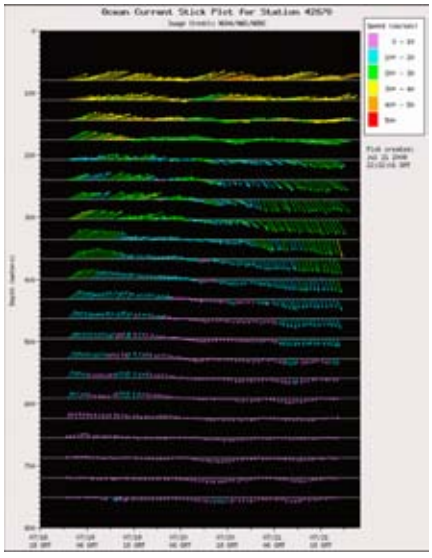

FIGURE 14

Stick plots for the Development Driller II drilling rig showing flow to the north-northeast along the eastern edge of Eddy Cameron.

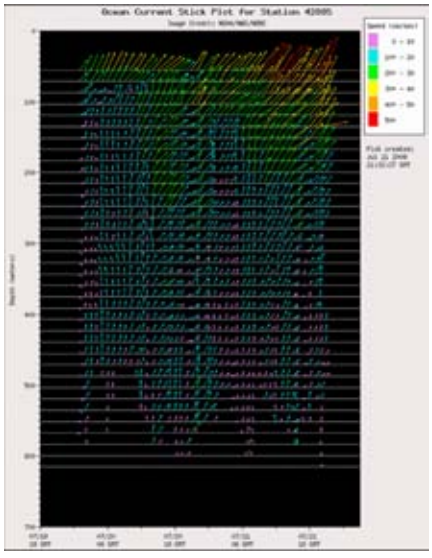

FIGURE 15

Stick plots showing forty-eight hours of current profiles for the Neptune drilling rig showing flow to the north-northeast along the eastern edge of Eddy Cameron.

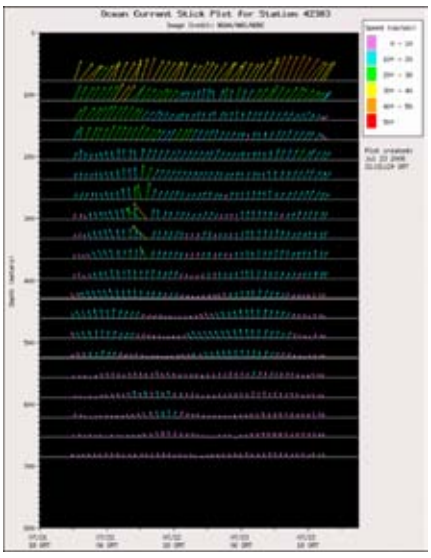

FIGURE 16

Stick plots showing a pulse of 40–60 cm/s water at 300 meter depth at the Genesis platform.

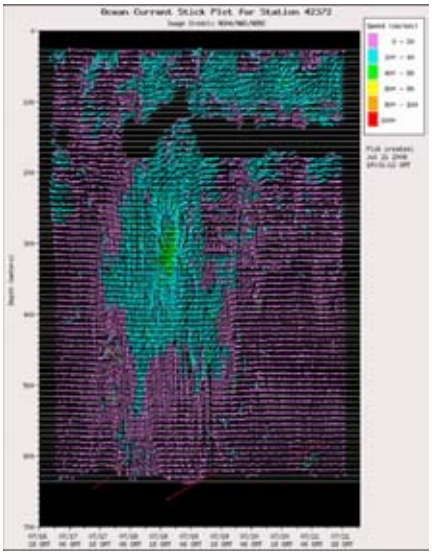

FIGURE 17

Stick plots showing inertial flow superimposed on flow around a cyclonic eddy at the Horn Mountain Platform.

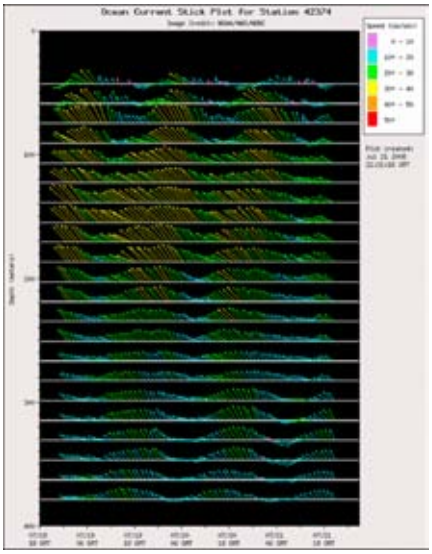

FIGURE 18

Stick plot showing forty-eight hours of currents at the Cajun Express drilling rig in July 2008.

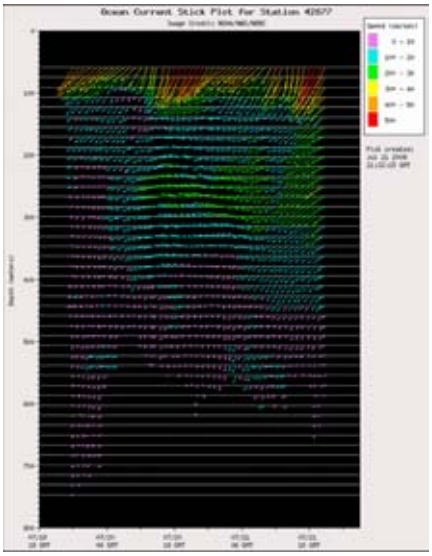

Two platforms that transmitted data to the NDBC during this period show evidence of being in the newly detached Loop Eddy Cameron. The ADCP data from the drillship *Development Driller II* (Figure 14) suggest that the northwest edge of the Loop Eddy is encroaching on the location. Currents are to the north-northeast and gaining strength as the Loop Eddy nears. Currents at the nearby Neptune production platform (Figure 15) are similar to those at *Development Driller II*.

A cyclonic eddy appears between the Loop Eddy and the Mississippi Delta region. Figures 16 and 17 clearly show currents generated by this feature, an example of cyclones that may block further the northward expansion of the Loop Eddies and the Loop Current (Schmitz et al., 2005). Two production platforms, Genesis and Horn Mountain, provide data that support the flow around the cyclonic eddy. The Genesis platform on the western margin supports the idea of a southward flow along the western side of the cyclonic eddy (Figure 16). North-northwestward currents at Horn Mountain of 40 cm/s suggest the northward flow along the eastern side of the cyclone (Figure 17). The northward flowing currents at Horn Mountain are modified by inertial currents that are generated at the ocean surface by winds. They travel down through the water column and then back up again. Figure 17 shows the inertial currents returning to the surface.

The drilling rig, Cajun Express (Figure 18), shows flow to the south-southwest on the western side of a cyclonic eddy apparently trapped between two Loop Current eddies.

Bottom Currents

The Na Kika platform southeast of the Mississippi Delta was less than 100 km to the right of the track of Hurricane Katrina as it approached Louisiana on 28 August 2005. A bottom-mounted ADCP had been deployed near Na Kika to collect bottom current profile data since 18 June 2005. The data were processed and quality controlled at the NDBC following the recovery of the sensor. Analysis of the data (Coholan et al., 2008) shows that the bottom currents at Na Kika, which normally range from 0 to 5 cm/s, were impacted by Hurricane Katrina. The currents at 1900 m depth responded within 12 h to the passage of the storm. Maximum currents recorded at the site exceeded 30 cm/s (Figure 19). Currents remained above the background 5 cm/s for approximately 12 days. Analysis of the Na Kika bottom current data set also revealed responses of the data to Hurricanes Rita (maximum speeds greater than 20 cm/s and impact for 21 days) and Wilma (maximum speeds greater than 20 cm/s and impact for 13 days) during 2005 (Crout, 2007), indicating that the periodicity of the near-inertial oscillations shown in Figure 19 is related to the dimensions of the Gulf of Mexico at depth (C. Li, 2009, personal communication).

FIGURE 19

Bottom currents from the Na Kika platform following the passage of Hurricane Katrina, August-September 2005.

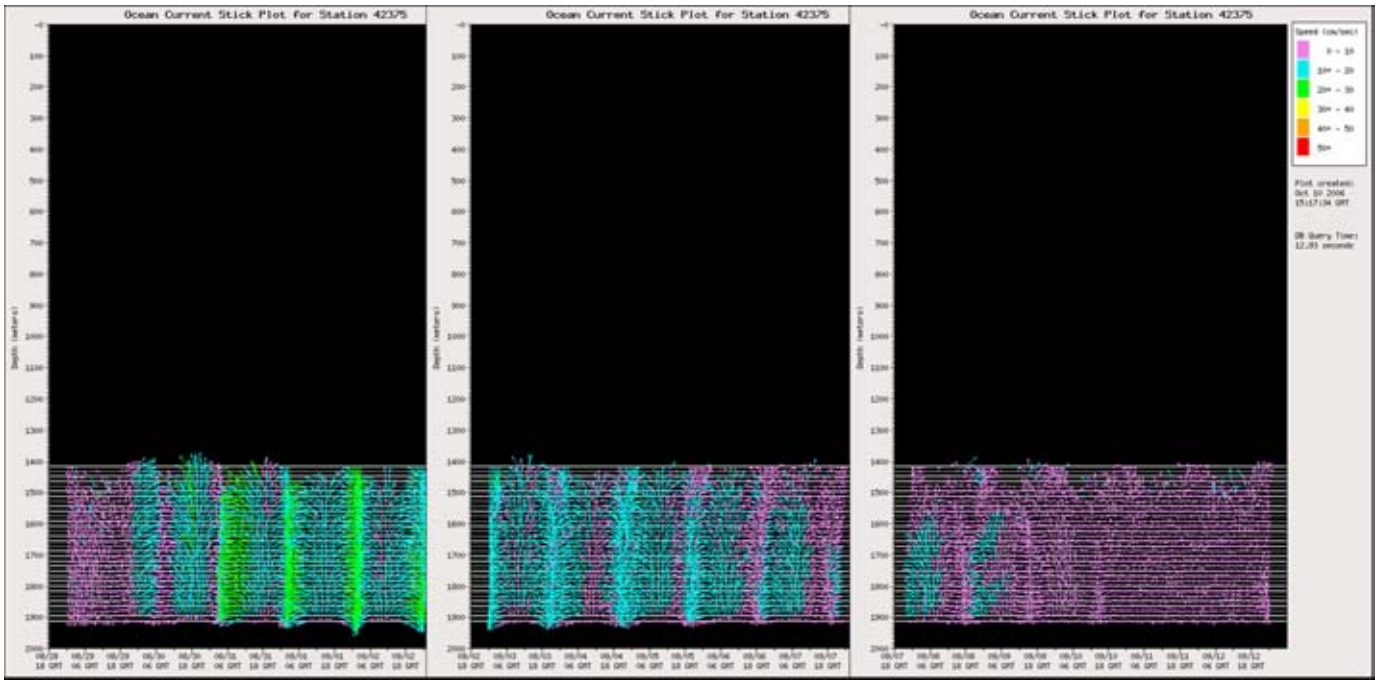

Conclusions

High current areas in the northern Gulf of Mexico associated with the Loop Current and associated Loop and cyclonic eddies can affect oil exploration and production operations. High currents cause shifts in locations of platforms, structural bending of platform components, stress, and excessive riser angles and may inflict costly damage (Coholan et al., 2008). Additionally, diving, remotely operated vehicles operations, pipe laying, and anchoring operations are more difficult and often impossible in high current areas.

Current profile data collected by oil and gas companies at drilling rigs and production platforms in the northern Gulf of Mexico in response to the MMS NTL of 2005 were intended to address these issues. Additionally, the data have been used by commercial and academic entities to generate nowcasts to initialize models, update models though assimilation, and verify and validate model output. In this paper, the current profiles reveal flow in the Loop Current, in newly detached and older Loop Current eddies, in cyclonic eddies that translate clockwise around the Loop Current, and in near-bottom near-inertial oscillations in response to catastrophic events such as hurricanes.

In a summary of model efforts in the Gulf of Mexico, Oey et al. (2005) noted that there are similarities in the model behavior for the Loop Current eddy shedding process, eddy propagation following detachment, and propagation of deep cyclones. Future work will include simulations of Topographic Rossby Waves, deep currents, eddy-shelf/slope interactions, frontal eddies, and eddy-shedding dynamics. The data collected by the drilling interests in the northern Gulf of Mexico since early 2005 are available from the NDBC for model validation and verification. The data are also available for other investigations at www.ndbc.noaa.gov. A new NTL has been published, extending the agreement until 2014.

Acknowledgments

The author would like to thank the efforts of individuals at the National Data Buoy Center, the Minerals Management Service, the Offshore Oceanography Committee, and Teledyne RDI who made this effort possible. Two anonymous reviewers provided useful comments that improved this technical note.

References

Coholan, P.D., Feeney, J.W., Anderson, S.P. 2008. Life and times of Eddy Zorro: A review of the 2007 Gulf of Mexico Loop Current Activity. In: Presented at the Offshore Technology Conference, Houston: TX, 508 May 2008, OTC Copyright 19413.

Crout, R.L., 2007. National Data Buoy Center (NDBC) processing, display, and observation of near-bottom currents acquired by oil companies in the northern Gulf of Mexico. In: OCEANS'07 MTS/IEEE Vancouver, Canada: Conference Proceedings CD. 5 pp.

Horizon Marine Name Indices, 2009. Available from http://horizonmarine.com/nameindices.html

Inoue, M., Welsh, S.E., Rouse, L.J., 2008, Deepwater currents in the eastern GOM. Deep Water Technol. 229(7):10 pp.

Leben, R.R. 2005. Altimeter-derived Loop Current metrics. In: Circulation in the Gulf of Mexico, Observations and Models, W. Sturges and A. Lugo-Fernandez (eds.), Geophysical Monograph Series. AGU, pp. 181-202.

Oey, L.-Y, Ezer, T., Lee, H.-C. 2005. Loop Current, rings, and related circulation in the Gulf of Mexico: A review of numerical models and future challenges. In: Geophysical Monograph Series. AGU, pp. 31-56.

Schmitz, W.J., Biggs, D.C., Lugo-Fernandez, A., Oey, L.-Y., Sturges, W. 2005, A synopsis of the circulation in the Gulf of Mexico and on its continental margins. In: Geophysical Monograph Series. AGU, pp. 11-30.

PAPER

HERMES—A High Bit-Rate Underwater Acoustic Modem Operating at High Frequencies for Ports and Shallow Water Applications

AUTHORS

Pierre-Philippe J. Beaujean
Edward A. Carlson
Department of Ocean Engineering, Florida Atlantic University

ABSTRACT

An underwater acoustic modem capable of point-to-point transmission of data at high bit rates is presented in this article. The high data-rate acoustic uplink operates between 262 kHz and 375 kHz in three sub-bands. The lower sub-band (262.5 kHz to 337.5 kHz) carries the binary information. The middle sub-band (347-373 kHz) is for detection purposes. The higher sub-band carries a narrow-band, 375-kHz tone designed to improve the Doppler-tracking capability of the high bit-rate acoustic uplink. The acoustic uplink uses phase-modulated symbols of adjustable bandwidth (25 kHz, 50 kHz or 75 kHz). The peak data rate is 87,768 bits-per-second at a maximum range of 180 m using an omni-directional source and an omni-directional receiver. The source level required to achieve this range is 185.8 dB re 1 µPa at 1 m. This modem is also equipped with an acoustic downlink designed for command-and-control in a lower frequency band (62-76 kHz) and at a lower data rate. The focus of this paper is on the high bit-rate uplink. A series of experimental results demonstrate that this underwater acoustic modem can operate reliably in difficult environments such as ports and very shallow waters. High-resolution sonar images are transmitted in real-time from various types of autonomous underwater vehicles during the inspection of ship hulls, walls and sea bottom.

Introduction

Acoustic channels, although noisy, can be a reliable means for live communication and the transmission of various data forms, including images and video. The three major concerns associated with broadband acoustic communication at high frequencies in harbors are reverberation, Doppler shift and, to a lesser extent, noise. Sound reverberation, originating from the scattering of acoustic waves off the surface, bottom, walls and obstacles, causes inter-symbol interference (ISI) (Beaujean and Strutt, 2005; Beaujean and Proteau, 2006). In the frequency domain, reverberation is equivalent to frequency-selective fading. Frequency-selective fading also includes the effect of sound refraction caused by sound velocity gradient. Doppler shift is caused by the relative motion of the communication platforms and boundaries, especially the water surface, ship hulls and some biological life. The combined effect of various Doppler shifts is known as Doppler spread, which is equivalent to time-selective fading in the frequency domain.

During the past two decades, a series of technological breakthroughs have allowed surface operators to communicate with underwater equipment and divers using underwater acoustic modems developed by the academia (LeBlanc and Beaujean, 2000; Beaujean and LeBlanc, 2004; Kilfoyle et al., 2005; Stojanovic, 2005), governmental laboratories (Yang, 2004; Gendron, 2007) and private industries (Green and Rice, 2000; Kebkal and Bannasch, 2002). Note that this list of reference is by no means exhaustive. Historically, the bulk of the effort in underwater acoustic communications has been contained within the frequency band from a few hundred Hertz, with a very low bit rate and a range of hundreds of kilometers, to approximately 30 kHz. At this higher frequency, digital voice communication, transmission of small images and command-and-control of autonomous underwater vehicles (AUV) become practical given an appropriate use of the acoustic modems. The range of operation varies from a few hundred meters to a few kilometers depending on the information bandwidth, the environment and the type of operations. In particular, vertical

communication in deep waters leads to better performance than horizontal communication in shallow waters. The latter case is usually much more challenging because of strong signal fading and translates to lower information rates. Unsurprisingly, the need for higher data rates has led to an observable increase in the operating frequency and bandwidth of the most modern underwater acoustic modems (Kojima et al., 2002; Pelekanakis et al., 2003; Roy et al., 2007; Zhu et al., 2007; Han et al., 2008; Ochi et al., 2008).

In the case where acoustic communication must be achieved over a limited range (less than 200 m), operating at comparatively low frequencies (30 kHz or less) makes little sense: the background acoustic noise level is high and the bandwidth is small. On the other hand, the background acoustic noise caused by boat traffic is relatively benign near 100 kHz (between 20 and 30 dB re 1 μPa/√Hz), whereas thermal noise only increases by 6 dB per octave above 100 kHz (Urick, 1983). To make matters worse, the low absorption coefficient at low frequencies becomes a disadvantage because the superior range of low-frequency acoustic devices can cause a significant increase in reverberation time, especially in the presence of walls.

AUV technology has found new applications in the field of hull survey and port security and remains a key feature of mine counter-measure operations. Some of the most advanced AUVs are now capable of hovering around a target or the hull of a ship and recording high-definition images with advanced sonar such as the Sound Metrics DIDSON or BlueView blazed array (Beaujean and Proteau, 2006; Beaujean, 2007a, b; Beaujean et al., 2008). The quality of the image created by this type of forward-look sonar is sufficient to visually identify potential threats such as divers and explosives. The AUV can complete its mission while keeping key personnel at a safe distance. In practice, such hovering AUVs are operated no more than a few hundred meters from the point of deployment. Having human-in-the-loop capability is essential during this type of operation and requires the transmission of images to a remote user. Present solutions are to transmit the data by copper or fiber-optic cable directly to the user or to equip the AUV with a tow-float and transmit the images through wide-band wireless Ethernet. In both cases, the cable connected to the AUV limits its maneuverability, causes drag, drastically increases the chances of entanglement and prevents the AUV from operating in confined areas.

Under these conditions, the use of high frequencies to achieve high data-rate acoustic communications makes perfect sense: the background acoustic noise is significantly lower and the bandwidth is significantly larger. Above 100 kHz, transducers are typically small and very power efficient, which simplifies the issues associated with power amplifier design and mounting on underwater vehicles. However, large amounts of Doppler shift and Doppler spread are expected in the high-frequency range and must be compensated by using phase-lock loops or re-sampling algorithms.

A large frequency bandwidth allows for a high data rate and an excellent time resolution. Therefore, decision feedback equalizing (DFE) processes can better compensate for the significant multipath, which is the main cause of limitation of this type of communication devices. There are also subtle advantages when using several high-frequency units at once: the limited range of such units limits the message latency, which means that clusters or closely located vehicles can interact more efficiently and sophisticated routing techniques for mobile ad-hoc networks can be applied (Carlson et al., 2006).

An underwater acoustic modem capable of point-to-point transmission of data at a high bit rate is presented in this article. The HERMES acoustic modem operates at high frequencies with concomitant benefits and achieves underwater acoustic communications at high data rate while remaining power efficient, thanks to a carefully designed signal equalizer. This technology has been successfully field tested and operated from various types of AUVs in challenging acoustic environments. Following an overview of the communication system and platforms in Chapter 2, the signal processing techniques used in HERMES are covered in detail in Chapter 3. Chapter 4 covers a series of experimental results obtained over the past 2 years.

Communication System

Overview

HERMES is an asymmetrical underwater acoustic modem operating in two separate frequency bands (Figure 1). The high data-rate uplink operates between 262 kHz and 375 kHz in three sub-bands (Figure 2). The lower sub-band (262.5 kHz to 337.5 kHz) carries the binary information. The middle sub-band (347-373 kHz) is for detection purposes. The higher sub-band carries a narrow-band, 375-kHz tone designed to improve the Doppler-tracking capability of the high bit-rate acoustic uplink. This acoustic uplink can operate at a maximum range of 180 m using an omni-directional source and an omni-directional receiver. The source level required to achieve this range is 185.8 dB re 1 μPa at 1 m,

FIGURE 1

System diagram of the HERMES acoustic communication system.

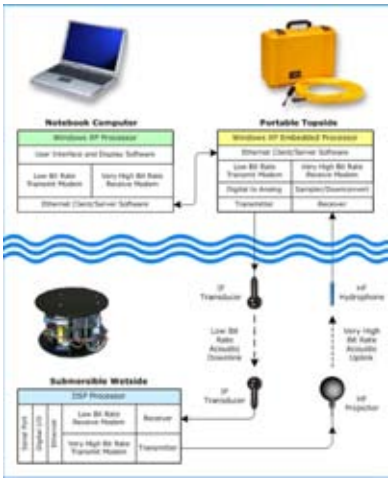

FIGURE 2

Individual message format for the high-rate acoustic uplink.

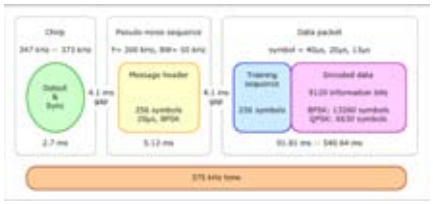

which corresponds to an acoustic power of 32 W. The downlink is designed for command-and-control and uses a lower frequency band (62-76 kHz) operated at the same source level but at a lower data rate.

The focus of this paper is on the high bit-rate uplink because it achieves exceptional data rates in acoustically challenging environments. The acoustic uplink uses either binary phase-shift keying (BPSK) or quaternary phase-shift keying (QPSK) modulation applied to symbols of adjustable bandwidth (25 kHz, 50 kHz or 75 kHz). The units presented in this document also use Bose-Chaudhuri-Hocquenghem (BCH) block error coding (Lin and Costello, 1983). The overall communication characteristics of the acoustic uplink are given in Table 1. The peak data rate is 87,768 bits-per-second.

The acoustic uplink is designed to move multiplexed data from the wetside component to the topside component. The data typically originate from the various subsystems of the underwater platform (typically an AUV), such as high-resolution sonar, cameras, motion and pressure sensors. In addition, the wetside modem can relay its own status and performance metrics. The multiplexed information is encoded into modem symbols and then modulated into digital modem samples. These digital modem samples are converted into analog modem signals and transmitted acoustically to the uplink receiver.

On the topside, the analog acoustic signals are filtered, sampled and down-converted into base-band (complex) digital modem samples. These samples are demodulated and decoded into digital data samples. The digital data samples are de-multiplexed and displayed to the operator or distributed to other topside destinations. The topside unit comes in the form of a single topside case equipped with a receiver hydrophone, equipped with analog-to-digital conversion electronics and a PC-type processor. In addition, a set of high-rate acoustic gateway (HAG) buoys equipped with the same acquisition system and wireless Ethernet can be used to extend the range coverage of the acoustic uplink. Figure 3 shows the topside case and a HAG buoy side-by-side.

Wetside input data are received through serial ports, Internet Protocol (IP) sockets (Transmission Control Protocol (TCP), User Datagram Protocol (UDP)) and digital input-output lines. A multiplexer is responsible for collecting data from all these input pipes and

TABLE 1

Data packet specifications.

Modulation Type	BPSK	BPSK	BPSK	QPSK	QPSK	QPSK
Symbol duration (μs)	40	20	13	40	20	13
Symbol bandwidth (kHz)	25	50	75	25	50	75
Information bits/frame	9120	9120	9120	9120	9120	9120
Packet duration (ms)	0.5491	0.2745	0.1830	0.2745	0.1373	0.0915
Message duration (s)	0.5615	0.2869	0.1954	0.2869	0.1497	0.1039
Information rate (bps)	16,243	31,784	46,668	31,784	60,935	87,768
Packet coded rate (bps)	25,000	50,000	75,000	50,000	100,000	150,000
Bits-per-Joule (bit/J)	2461.1	4815.8	7070.9	4815.8	9232.6	13298.2

BPSK, binary phase-shift keying; quaternary phase-shift keying, QPSK.

FIGURE 3

High-rate acoustic gateway buoy and topside HERMES unit (left); HERMES wetside unit (top center); Jetasonic H320 transducer (top right); Bluefin Robotics HAUV-1A (bottom left); LM Cetus-II hull inspection vehicle (SPAWAR San Diego) (bottom center); HERMES wetside module for Hydroid REMUS-100 (bottom right).

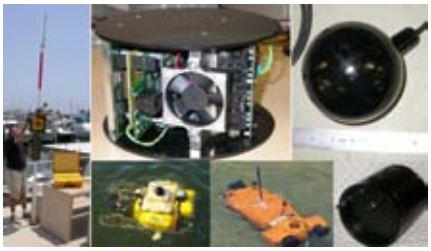

for merging the data into individual packets suitable for transmission by the acoustic uplink. The multiplexer reads the input pipes using a weighted fair queue, taking data from each pipe's queue according to its priority. This allows the blocks from some pipes to be sent at a higher rate than others while ensuring that all pipes get to send. After topside reception and decoding, each packet is sent to a de-multiplexer, which is responsible for splitting the merged data and routing it to the correct output pipes. Data are handled in discrete, stand-alone blocks. Any packet that is received successfully contains all of the necessary information for each of the blocks it contains. A lost packet loses only those blocks it contains. The multiplexer treats each input block as a black-box and only knows the pipe identity, the path priority, the block type and the size of each individual data block (which may vary from block to block). The multiplexer packet header describes the path identity and offset of each block contained within the packet, allowing the topside de-multiplexer to extract each block and route it to the correct output pipe.

Two input pipes are used in this paper: one for Sound Metrics DIDSON sonar images and the other for vehicle status. The DIDSON pipe can include wavelet difference reduction (WDR) compression and decompression if required. This third-party WDR compression technique is capable of a 64-to-1 compression ratio (Walker and Nguyen, 2000).

Wetside Unit and Vehicle Platforms

The wetside unit is 150 mm in diameter and 76 mm tall. It fits inside the main pressure vessel of a Bluefin Robotics Hovering Autonomous Underwater Vehicle-version 1A (HAUV-1A) or a Hydroid Remus-100 pressure vessel. The wetside unit can use a low-power, small source transducer (ITC-1089D) or a higher-power, larger transducer (Jetasonic H320). The receiver unit of the acoustic uplink and the HAG buoys use a single ITC-1089D. Figure 3 shows the wetside electronic module and the high-power Jetasonic H320 source transducer. The input voltage of the unit is 18-36V and can be operated from the power bus of most AUVs. The unit accepts data via the Ethernet, serial port and digital lines.

HERMES has been installed on various AUV platforms, including a Lockheed-Martin (LM) Cetus-II operated at SPAWAR San Diego and the BlueFin Robotics HAUV-1. A module has been designed and built for the Hydroid Remus-100 and will be operated in the course of 2009, in collaboration with the Woods Hole Oceanographic Institute. The various platforms are shown in Figure 3. All three vehicles are equipped with an extensive suite of sensors operating simultaneously. For example, the active sensors installed on the LM Cetus-II included a Desert Star Aqua Map operating at 50 kHz, three Tritech altimeters operating at 500 kHz, one RD Instruments (RDI) Doppler Velocity Log (DVL) operating at 1.2 MHz and a Sound Metrics DIDSON operating at 1.8 MHz. With its carefully selected frequency range, the acoustic uplink is capable of operating without interfering with any of these sensors.

Signal Processing

Preliminary Steps

A detailed description of the signal processing algorithm used to detect, authenticate, demodulate, equalize and error-check the incoming acoustic signals is available in the literature (Beaujean, 2007a, b; Beaujean et al., 2008). Figure 4 shows a flowchart of the algorithm used to process an incoming acoustic message (shown in Figure 2), using a single receiver hydrophone, and to produce an output binary sequence.

The first issue to be addressed is the proper detection and authentication of an incoming message. A challenging aspect of the acoustic uplink is that each message can be transmitted immediately after the previous one. As a result, the transmission duty cycle can exceed 80%, which leaves very little time to estimate the background noise floor within the frequency band monitored by the receiver unit. In addition, the incoming message can use various types of modulation and frequency band, depending on the active configuration. Finally, the retrieval of the binary information contained in the packet is sensitive to time synchronization and frequency shifts. Given these constraints, the uplink receiver process follows a series of initial steps, labeled (a) to (c) below, to accurately detect an incoming message and to identify the location and type of data packet present.

(a) The message trigger is a linear frequency-modulated chirp signal centered at 345 kHz with 26 kHz of bandwidth. A Blackman-Harris window is used to shape this chirp signal. The peak value of the cross-correlation between transmitted chirp and received signal is continuously monitored. The received signal contains only noise, unless a message is present. A trigger is deemed present if the signal-to-noise ratio (SNR) exceeds a detection threshold that can be dynamically adjusted based on the number of false alarms and slow changes of the noise power. The peak value of the cross-correlation corresponds to the beginning of the 2.7-ms

FIGURE 4

Signal processing flowchart of the HERMES high-rate uplink receiver (single unit).

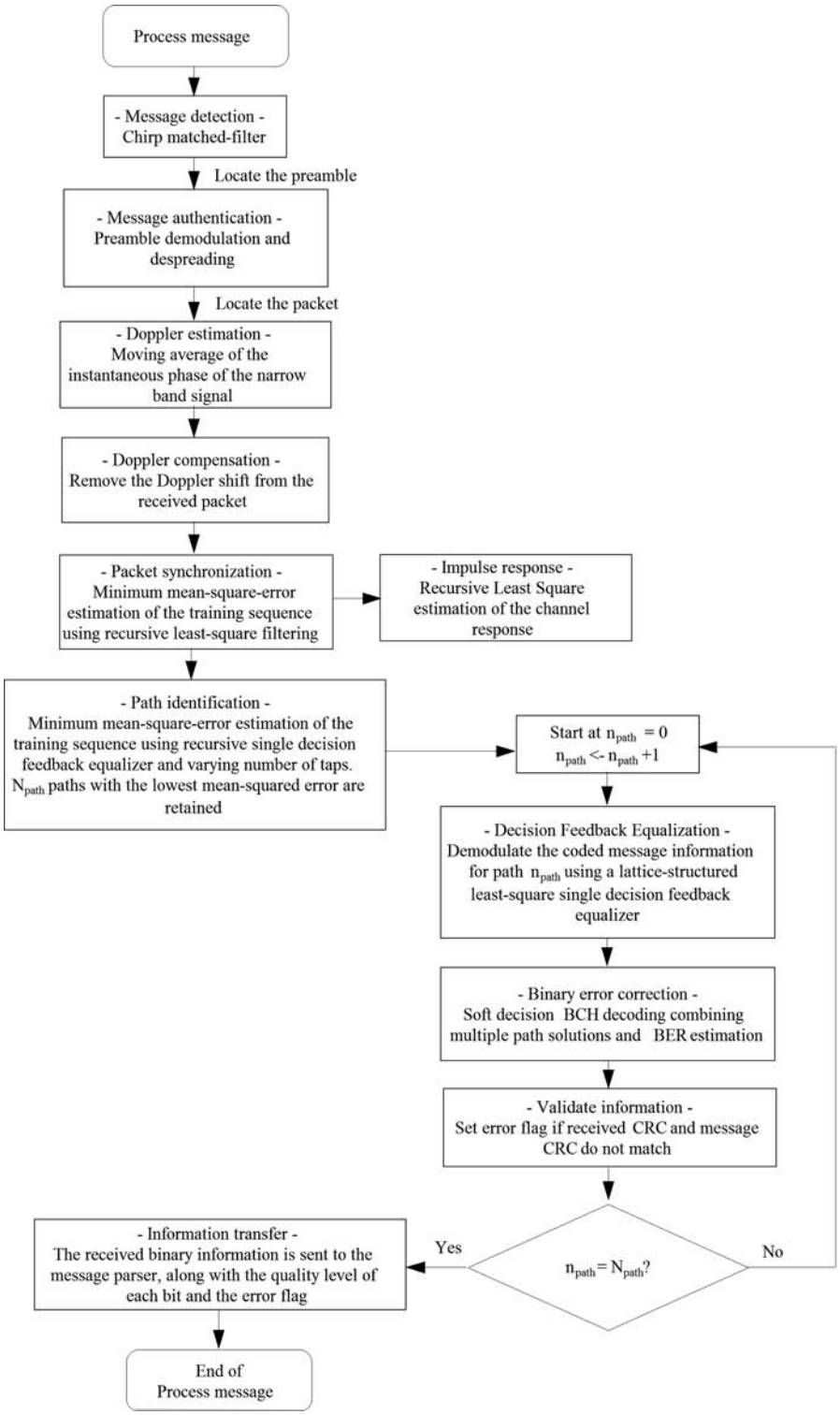

message trigger within the correlation's accuracy.

(b) The 5.12-ms preamble follows 4.1 ms later. This preamble contains the type of modulation (BPSK or QPSK) and symbol duration (40 μs, 20 μs or 13.3 μs) used in the data frame. The preamble uses direct-sequence spread spectrum to reduce the negative impact of fading. Three bits, which are used to code this information, are spread over 256 gold-coded bits (Lin and Costello, 1983). As a result, the preamble can only contain one of eight pre-defined, 256 bits sequences. This pseudo-noise (PN) sequence is gray-coded and BPSK-modulated at a carrier frequency of 300 kHz and using 50 kHz of bandwidth. Each symbol contains one bit (out of 256) and is shaped using a raised-cosine time window. As mentioned earlier, a 375-kHz tone is transmitted simultaneously so that the average Doppler shift within the preamble can be estimated and compensated. The phase of each BPSK-modulated, Doppler-compensated symbol is estimated, and the corresponding bit is retrieved. The identification process consists of matching the received binary PN sequence with up to 1,024 pre-defined binary sequences, with the understanding that only eight of these are valid. If the best match is one of these eight sequences, the detected signal is identified as a valid message, thus authenticated. The preamble correlation is also a mean to refine the estimated location of the packet following the preamble after a 4.1-ms dead time.

(c) Once the incoming message has been authenticated, the actual data packet is processed. A packet contains 9,120 data bits plus 32 redundancy bits Cyclic Redundancy Check (CRC-32). The combined 9,152 bits are block-

coded so that four parity bits are added to 11 data bits using a BCH (15,11,1) block code (Lin and Costello, 1983). A packet starts with a known 256-bit training sequence. The same modulation and symbol bandwidth is applied across the entire packet, which lasts between 103.9 ms and 561.5 ms depending on the modulation. Consequently, the data rate varies from 16,243 bps to 87,768 bps. In addition, a 375-kHz tone is transmitted simultaneously. The first processing step is the average Doppler shift compensation using the 375-kHz tonal component. The second step consists of accurately estimating the starting location of the packet and demodulating the symbols. This is achieved using minimum mean-square error estimation of the incoming sequence. This operation relies on a recursive least-square algorithm described by Beaujean and LeBlanc (2004).

At this stage of the process, an accurate estimate of the starting location of the packet has been found. The next step consists of demodulating the packet symbols. These symbols are distorted by noise, fading and ISI so that equalization is required to estimate the information content of the frame.

Decision Feedback Equalization

The focus of this section is on the novel aspects of the decision feedback equalizer itself. The high-rate uplink receiver uses a set of parallel Doppler-compensated Decision Feedback Equalizers combined with soft-decision error correction routines. The current routines are either BCH soft-decision decoding or Turbo decoding. The results shown in this publication cover solely the case of BCH. The routine combines the original work of the author in array processing (Beaujean and LeBlanc, 2004; Beaujean and Proteau, 2006), with the robustness of the lattice DFE introduced by Ling and Proakis (1985). DFE techniques have been covered extensively and applied in the field of underwater acoustic communications for over two decades (Linde, 1988). In a traditional approach, the DFE input is data vector $\mathbf{Z_{eq}}$, which comprises symbol vector $\mathbf{Z_{fr}}$ and decision vector $\mathbf{d_{fr}}$

$$\mathbf{Z_{eq,n}} = \left[z_{fr,n}, \ldots, z_{fr,n+1-N_{eq,f}}, \mathbf{d_{fr},}_{n-1}, \ldots, \mathbf{d_{fr},}_{n-N_{eq,b}}\right]^T \quad (1)$$

$N_{eq,f}$ represents the number of feed-forward taps, and $N_{eq,b}$ represents the number of feedback taps. The superscript ^{T} represents the vector transpose operator. Each filtered symbol at the output of the DFE is the product of $\mathbf{Z_{eq,n}}$ and the filter coefficient vector $\mathbf{C_{eq,n}}$ containing ($N_{eq,f}$ + $N_{eq,b}$) elements

$$r_{eq,n} = \mathbf{C}^H_{\mathbf{eq,n}}.\mathbf{Z_{eq,n}} \quad (2)$$

H is the Hermitian operator. The elements $z_{fr,n}$ and $d_{fr,n}$ represent input complex symbols and the symbols obtained following a prior DFE decision made on earlier symbols, respectively. The subscript *fr* simply indicate that the symbol belong to an information frame (or packet). $\mathbf{C_{eq,n}}$ minimizes the exponentially weighted cumulative squared error between the equalized output $r_{eq,n}$ and the desired response

$$\varepsilon^2_{eq} = \sum_{k=0}^{n} \lambda^{n-k} |r_{eq,k} - \mathbf{d_{fr},}_{k}|^2 \quad (3)$$

Parameter λ is known as the forgetting factor of the equalizer and controls the filter memory. This coefficient is positive and lower than 1. In the present case, λ varies between 0.990 and 0.999. The solution $\mathbf{C_{eq,n}}$ that minimizes the cumulative squared error in equation (3) is

$$\mathbf{C_{eq,n}} = \left(\sum_{k=0}^{n} \lambda^{n-k} \mathbf{Z_{eq,n}}.\mathbf{Z^H_{eq,n}}\right)^{-1} . \left(\sum_{k=0}^{n} \lambda^{n-k} \mathbf{Z_{eq,n}}.\mathbf{U^H_{fr}}\right) \quad (4)$$

This optimization problem is efficiently resolved using the least-squares lattice DFE algorithm covered in detail in the literature (Ling and Proakis, 1985). The usual approach consists of using $N_{eq,f}$ feed-forward filter coefficients and a lower number $N_{eq,b}$ of feedback coefficients. A well-known limitation of the traditional DFE approach resides in the number of taps caused by processing burden and stability issues (Ling and Proakis, 1985). A DFE is inherently an infinite impulse response filter with time-varying coefficients. The feedback filter coefficients are obtained following a nonlinear decision process and can cause severe instabilities, especially if the number of feedback filter coefficients is large. This issue has been at the root of some extensive research and publications aimed at making the DFE process more stable while remaining computationally efficient. The work presented in this section falls in this category.

The channel impulse response is estimated by minimizing the mean-square error between a measured sequence of symbols and a reference (equation (3)). If the symbol duration is too long and the channel characteristics change too rapidly, then the

minimization process does not necessarily produce an optimal estimate of the channel response. Instead, different impulse response estimates may lead to very comparable mean-square errors. If sufficiently different, each estimate constitutes a candidate model for the acoustic channel. Therefore, the quality of the received information should improve as we find more and more of these channel estimates, given that we know how to combine these appropriately. We can improve the system performance at the expense of processing power while keeping the source power, bandwidth and number of source and receivers the same.

At the frequency of operation of the acoustic uplink, the DFE process must compensate for closely packed echoes subject to significantly different Doppler shifts in the presence of fairly stationary noise. The uplink receiver of HERMES employs a phase-lock-looped DFE routine that leverages this complementary solution approach. The same equalizer routine is started at a different time interval of the received sequence, with a varying number of feed-forward taps and, optionally, a varying value for the forgetting factor λ. The governing equations of the DFE process become

$$\mathbf{Z_{eq,n,m}} = \left[z_{fr,n-m}, \ldots, z_{fr,n+1-N_{eq,f}-m}, \mathbf{d_{fr},}_{n-1}, \ldots, \mathbf{d_{fr},}_{n-N_{eq,b}}\right]^T \tag{5}$$

$$r_{eq,n,m} = \mathbf{C^H_{eq,n,m}}.\mathbf{Z_{eq,n,m}} \tag{6}$$

$$\varepsilon^2_{eq,m} = \sum_{k=0}^{n} \lambda^{n-k} |r_{eq,k,m} - \mathbf{d_{fr},}_{k,m}|^2 \tag{7}$$

$$\mathbf{C_{eq,n,m}} = \left(\sum_{k=0}^{n} \lambda^{n-k} \mathbf{Z_{eq,n,m}}.\mathbf{Z^H_{eq,n,m}}\right)^{-1}.\left(\sum_{k=0}^{n} \lambda^{n-k} \mathbf{Z_{eq,n,m}}.\mathbf{U^H_{fr}}\right) \tag{8}$$

Index m indicates a different configuration of the starting time interval and number of feed-forward taps. The minimum number of feed-forward coefficients is set to cover most or all of the multipath. The number of feedback coefficients is kept as low as possible for stability purposes: a single feedback tap has proved sufficient between 262.5 kHz and 337.5 kHz.

The equalizers producing the lowest mean-squared error estimation of the training sequence are retained (equation (7)), and the corresponding starting time, number of feed-forward coefficients and forgetting factor are stored. The entire message is equalized using each combination of starting time, number of coefficients and forgetting factor (Figure 5). For each candidate m, the k^{th} equalized symbol $r_{eq,k,m}$ is calculated and a decision $d_{eq,k,m}$ is made. Each set of estimates ($r_{eq,k,m}$, $d_{eq,k,m}$) is the input to a soft-decision BCH or Turbo decoder. In the unlikely case where error coding is not used, the symbol estimates ($r_{eq,k,m}$, $d_{eq,k,m}$) are combined using maximal ratio combining (Beaujean and LeBlanc, 2004).

Experimental Results

An Example of Mission, Boston Harbor

The benefits of the DFE technique presented in this article have been demonstrated in the field on various platforms. In December 2008, a series of eight missions was performed in Boston Harbor, in collaboration with Bluefin Robotics. The wetside unit was installed in the Bluefin Robotics HAUV-1A, and data were collected with a single hydrophone connected to the topside receiver unit located off the side of a boat at 2.1 m depth. The range of operation varied from 1 to 35 m. The SNR varied from 33 to 64 dB. The vehicle depth varied between 0 and 2.5 m, and the speed varied between 0 and 0.5 m/s. The overall water depth was 8 m. The bottom of the port was a combination of mud, sand and clutter. There was no control on the environment in terms of either boat traffic or biological activity. The purpose of the missions was the scanning of a boat hull 22 m in length by 6 m in width with a draft of 1.2 m (Figure 6).

Uncompressed, high-resolution DIDSON images and vehicle information were transmitted sequentially to the topside receiver for 2 h using a source level of 185 dB re 1 µPa at 1 m. The combination of a single image, vehicle information and additional acoustic modem data represented a combined 437,760 bits. Communication mode 4 was used so that the true data rate across an entire message, including the trigger and the preamble, was 46,668 bps. The coded data rate across an information packet was 75,000 bps. Symbols were BPSK-modulated and lasted 13.3 µs each. In this mode of communication, the 437,760 bits of information could

FIGURE 5

Decision feedback equalization of the data packet.

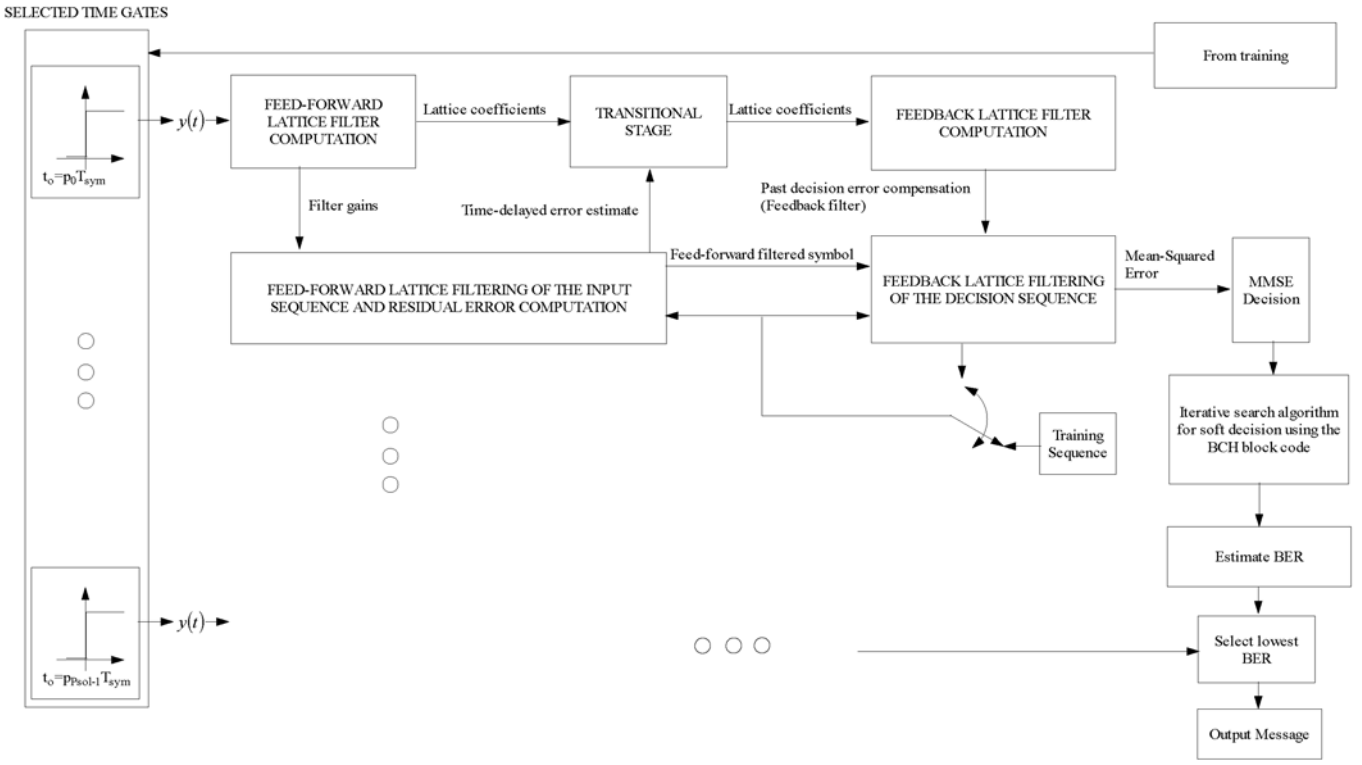

be transmitted in approximately 9.4 s using 48 sequential messages. Raw, digitally down-converted complex data were simultaneously stored and processed in real-time. The raw data storage allowed for the reprocessing of the same mission using an increasing number of DFE candidates (as described in the section entitled Decision Feedback Equalization), so that the benefits of the DFE technique could be demonstrated.

Because of the very large amount of information recorded, the following results focus on the transmission of a single DIDSON image in 48 messages. Figure 6 shows the trajectory followed by the vehicle. Figure 7 shows the bit error rate measured after BCH error correction using the candidate that best estimated the training sequence. This candidate was found using a single value of the forgetting factor (λ = 0.999) and a variable number of feed-forward taps and starting time locations. The number of feed-forward filter taps can be 15, 20, 25, 30, 35, or 40. The starting time fits within a time window equivalent to 40 symbols. Figure 8 shows the final Bit Error Rate (BER) obtained using the 60 candidates that best estimated the training sequence: in this case, the forgetting factor is

FIGURE 6

Bluefin Robotics HAUV-1A (top left) during a hull inspection in Boston Harbor (top right); trajectory of the Bluefin Robotics HAUV-1A during a hull inspection in Boston Harbor (bottom), December 2008.

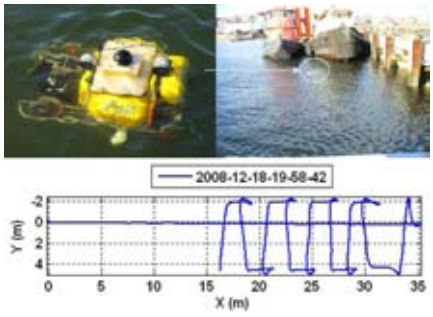

FIGURE 7

BER (%) measured for 48 consecutive messages (one complete DIDSON image with additional vehicle and modem information) during a hull inspection in Boston Harbor, December 2008. A single candidate was used and the forgetting factor was 0.999.

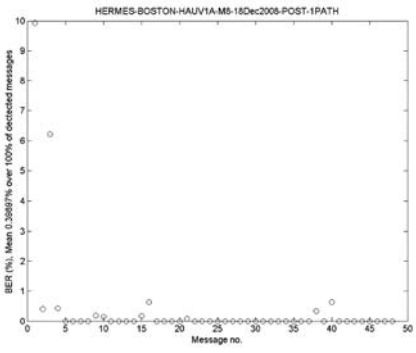

FIGURE 8

BER (%) measured for 48 consecutive messages (one complete DIDSON image with additional vehicle and modem information) during a hull inspection in Boston Harbor, December 2008. Sixty candidates were used, and the forgetting factor could be 0.996, 0.997, 0.998 or 0.999.

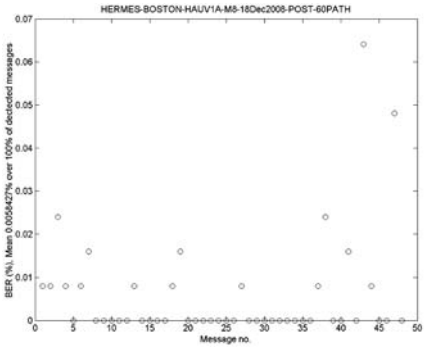

allowed to vary between 0.996 and 0.999. Figures 7 and 8 also show the average BER across the transmission of an entire image. Finally, Figure 9 summarizes the bit error rate measured across the entire image transmission with four DFE configurations: (a) using a single DFE candidate and a forgetting factor of 0.999 only, (b) using 20 DFE candidates and a forgetting factor of 0.999 only, (c) using 20 DFE candidates and a forgetting factor of 0.996 only, and (d) using 60 DFE candidates and a forgetting factor of

FIGURE 9

BER (%) measured for 48 consecutive messages (one complete DIDSON image with additional vehicle and modem information) using increasing numbers of candidates and configurations during a hull inspection in Boston Harbor, December 2008.

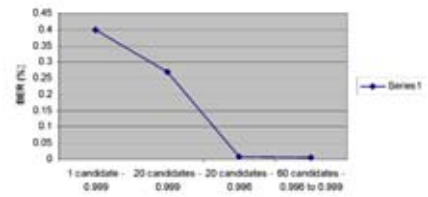

FIGURE 10

Complete DIDSON image received during a hull inspection in Boston Harbor, December 2008. A single candidate was used and the forgetting factor was 0.999. The BER was 0.39897%.

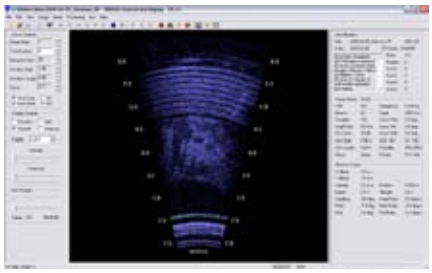

variable values (0.996, 0.997, 0.998 or 0.999). The drop in measured BER is significant as the number of candidates increases. In addition, a significant improvement in BER is observed when the forgetting factor is changed from 0.999 to 0.996 for the same number of candidates.

The impact of the BER on the quality of the received image is shown in Figures 10 and 11. In configuration (a), the BER is 0.39897%, which corresponds to 1,747 erroneous bits. In configuration (d), the BER is 0.0058427%, which corresponds to 26 erroneous bits. Although the received image is of sufficient quality for analysis in

FIGURE 11

Complete DIDSON image received during a hull inspection in Boston Harbor, December 2008. Sixty candidates were used, and the forgetting factor could be 0.996, 0.997, 0.998 or 0.999. The BER was 0.0058427%.

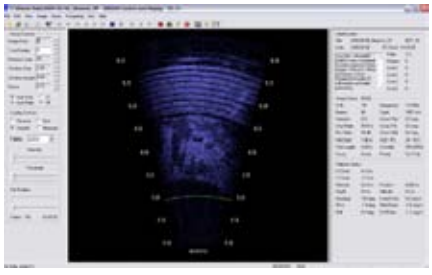

both cases, the quality of the received image is noticeably superior in case (d).

Port Everglades 2008

This section describes the experimental results obtained on July 25, 2008 at the Florida Atlantic University (FAU) SeaTech marina in Port Everglades, Florida. The source transducer was placed at 0.5 m below the surface at a distance of 25, 50, 95, 120, 140, 160 and 180 m. The sea bottom was composed of mud and fine sand. The relative speed between the source and the receiver did not exceed 1 m/s. The equalizer was configured so that only three candidates were used. The forgetting factor was 0.999, and the number of feed-forward taps could be 15, 20, 25, 30, 35 or 40. In addition, the received signal PSD and SNR were measured at 1 m, 200 m, 250 m and 300 m. Figure 12 shows the transducer location during the measurement and the bathymetry in the SeaTech marina at high-tide. Table 2 shows the measured SNR at each range in the data communication band and indicates that the SNR becomes marginally low beyond 200 m.

Figure 13 shows, as a function of range, the BER averaged across all

FIGURE 12

Aerial view of the location for experiments in SeaTech Marina, Port Everglades, Florida, indicating source and receiver positions (left) and bathymetry data (right).

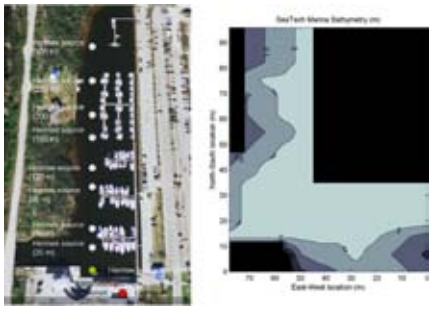

TABLE 2. Communication band SNR vs. range.

Range	1 m	25 m	50 m	95 m	160 m	200 m
Measured SNR, 280 kHz to 320 kHz (dB)	64	36	30	20	14	9

SNR, signal-to-noise ratio.

the messages that were properly detected, authenticated and recovered. The percentage of recoverable messages is shown in Figure 13 as a function of range and communication mode. In communication mode 4, each symbol is BPSK-modulated and uses 75 kHz of bandwidth. In communication mode 5, each symbol is QPSK-modulated and uses 75 kHz of bandwidth. An unrecoverable message is defined as a message that is so badly distorted that the estimated BER exceeds the error correction capability of the receiver. In the case of the soft-decision BCH, this BER threshold is approximately 10%.

The results clearly indicate that the high data-rate acoustic uplink can operate reliably in a difficult environment at a useful range: using 32 W of acoustic power, the system can be operated up to 180 m in very shallow waters. The maximum range can be further increased using a more powerful source if necessary. At 120-m range and using the fastest transmission mode (range-rate of 10,532 bps-km, SNR of 18 dB), 87.612% of the messages were properly detected, authenticated and recoverable. The average bit error rate across these messages was 0.36989%. At 160-m range and using the fastest transmission mode (range-rate of 14,043 bps-km, SNR of 14 dB), 70% of the messages were properly detected and authenticated. Of these, 75% were decoded with an average bit error rate of 0.36811%. These results indicate that the acoustic uplink of HERMES can relay information at a peak rate of 87,768 information bits-per-second and at a range of 180 m in very shallow waters, at a maximum relative speed of 1 m/s and in the presence of boat traffic, concrete walls and biological activity.

FIGURE 13

BER for modes 4 (75 kHz, BPSK) and 5 (75 kHz, QPSK) vs. range, excluding undetected and falsely authenticated messages (top); percentage of authenticated messages with a BER <10% in modes 4 and 5 (bottom).

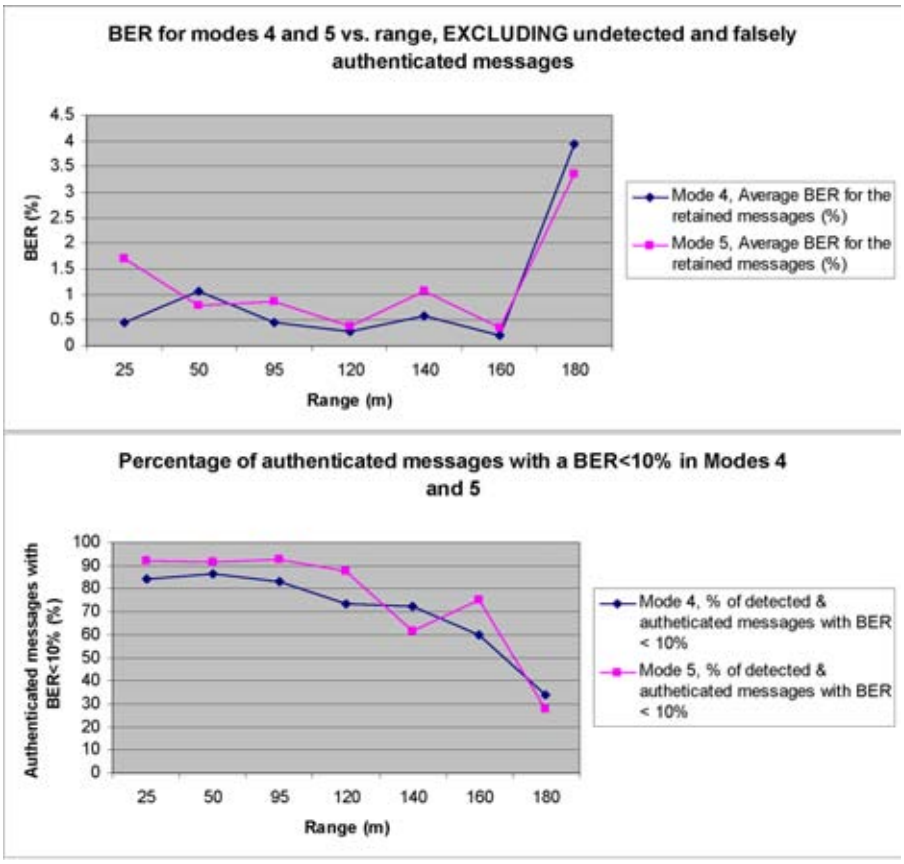

AUV Fest 2007 and AUV Fest 2008

Two generations of this high bit-rate, high-frequency uplink have been demonstrated in the field with the assistance of the Science and Technology program at the Office of Naval Research and the Explosive Ordnance Disposal program. The first and second generations of acoustic uplink perform the same functions and use the same signals and signal processing techniques. The first generation, used in 2007 and presented in detail in (Beaujean, 2007a, b), is limited to 6 W in peak acoustic power (equivalent to a source level of 178 dB re 1 µPa at 1 m) because of the use of a smaller acoustic source and relies on older, less compact electronics. The technical description of the second generation is presented earlier in this document.

During the AUV Fest 2007 event, a Lockheed-Martin Cetus-II vehicle, operated by SPAWAR San Diego, and the BlueFin HAUV-1 vehicle were equipped with the first-generation acoustic uplink and conducted multiple hull inspections successfully. The vehicles, equipped with a full suite of sensors, scanned the bottom of a large barge and relayed compressed acoustic images and vehicle status through the acoustic uplink in real-time at a preset rate of two updates per second. The active sensors installed on the vehicles included a Desert Star Aqua Map operating at 50 kHz, three Tritech altimeters operating at 500 kHz, an RDI DVL operating at 1.2 MHz, a Marine Sonics 1.8-MHz side-scan sonar and a Sound Metrics DIDSON operating at 1.8 MHz. With its carefully selected frequency range, the acoustic uplink was capable of operating without interfering with any of these sensors.

During AUV Fest 2008 (May 2008) at the Naval Undersea Warfare Center in Newport, Rhode Island, the hull of the USS Saratoga was inspected using the Bluefin Robotics HAUV-1A. The Bluefin Robotics HAUV-1A was equipped with the HERMES acoustic modem source (second generation). The HERMES source was operating at 4 W of output power (one-eighth of the maximum source power). Two receiver units were used: the HERMES topside unit and an ORE HAG buoy. The topside high-frequency hydrophone was placed 1.5 m below the surface, and the ORE buoy receiver hydrophone was placed 2 m below the surface. Both receivers were mostly static with minor current drift. The water depth was approximately constant (12 m), and the bottom of the basin was mud. BPSK-modulated, 195-ms messages using 13.3-µs symbols were transmitted at a rate of four messages per second. Figure 14 shows the experiment setup.

As an example, on June 9, 2007, the Cetus-II vehicle transmitted two compressed images per second for 46 min. Each update contained 9,120 bits of data so that 18,240 bits of information were transmitted every second. This preset configuration corresponds to one-fifth of the highest data rate. Overall, 50,223,840 information bits were received during the 46 min when images were transmitted. The acoustic uplink did not interfere with the other sensors. Each message contained a compressed DIDSON image (8,192 bits) and 928 bits of vehicle status, navigation information. The WDR compression routine was configured to achieve a compression ratio of 49-to-1. Figure 15 shows an example of a compressed image received using the acoustic uplink operated at 6 W of acoustic power. The top portion of Figure 15 is the uncompressed DIDSON image and data received using a fiber-optic tether. The bottom portion is the same data set transmitted in compressed format by the acoustic uplink. Both images were received almost simultaneously, in real-time and without any error.

FIGURE 14

AUV Fest 2008, Saratoga hull search experiment (Naval Undersea Warfare Center, Newport, 05/14/08, bottom right) using a high-rate acoustic gateway buoy.

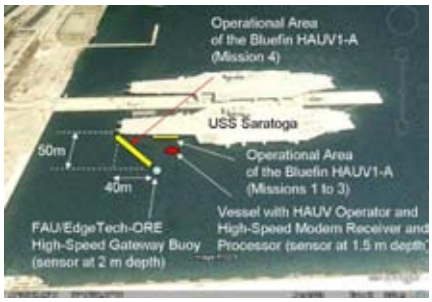

FIGURE 15

DIDSON image collected with the Lockheed-Martin Cetus-II hull inspection vehicle operated by SPAWAR San Diego on June 9, 2007 at AUV Fest 2007. The top image was received using a fiber-optics cable; the bottom compressed image was received using the high bit-rate acoustic uplink.

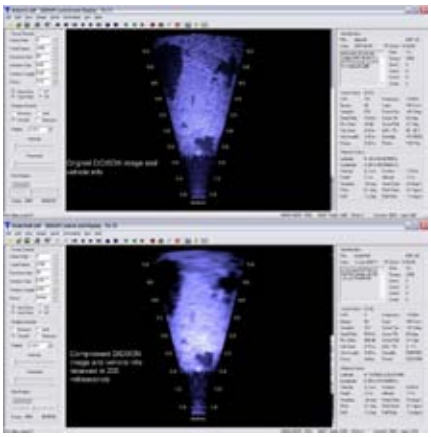

Conclusion

HERMES demonstrates that high-frequency, broadband underwater acoustic communications at high data rates are possible and practical. The high bit-rate uplink of this communication system achieves 87,768 bits-per-second at a maximum range of 180 m. This level of performance is sufficient to transmit high-resolution acoustic images from an AUV in a port during a ship hull inspection. The system is also small enough to fit in the main pressure vessel of a small underwater robot. Thanks to its ability to operate in the most challenging acoustic environments, this communication system can certainly be used for open ocean applications and can have useful applications in future underwater acoustic networks.

Acknowledgments

This work is supported by the Office of Naval Research Code 321OE and the Program Management Office for Explosive Ordnance Disposal. The author wishes to thank EdgeTech, EdgeTech-ORE and the FAU electronics laboratory for their technical support.

References

Beaujean, P.P.J., LeBlanc., L.R. 2004. Adaptive array processing for high-speed communication in shallow water. IEEE J. Oceanic Eng. 29:807-823.

Beaujean, P.P.J., Strutt., J.G. 2005. Measurement of the Doppler shift in forward-scattered waves caused by moderate sea surface motion in shallow waters. Acoust. Res. Lett. Online. 6:250-256.

Beaujean, P.-P. J., Proteau., J. 2006. Spatio-temporal processing technique for high-speed acoustic communications in shallow water at the South Florida Testing Facility: Theory and experiment. U.S. Navy J. Underw. Acoust. 56:317-347.

Beaujean, P.P.J. 2007a. High-speed high-frequency acoustic modem for image transmission in very shallow waters. Proc. of the OES/IEEE Oceans 2007 Europe. 1:1-6.

Beaujean, P.P.J. 2007b. Real-time image and status transmission from a UUV during a ship hull inspection in a port environment using a high-speed high-frequency acoustic modem. Proc. of the MTS/IEEE Oceans 2007. 1:1-9.

Beaujean, P.P.J., Carlson, E.A., Spruance, J., Kriel., D. 2008. A high-speed acoustic modem for real-time transmission of uncompressed image and status transmission in port environment and very shallow water. Proc. of the MTS/IEEE Oceans 2008. 1:1-9.

Carlson, E.A., Beaujean, P.P.J., An., E. 2006. An ad hoc wireless acoustic network simulator applied to multiple underwater vehicle operations in shallow waters using high-frequency acoustic modems. U.S. Navy J. Underw. Acoust. 56:113-139.

Gendron, P. 2007. High frequency coherent acoustic communications for the networked autonomous littoral surveillance system. Proc. of the OES/IEEE Oceans 2007 Europe. 1:1-6.

Green, M.D., Rice., J.A. 2000. Channel-tolerant FH-MFSK acoustic signaling for undersea communications and networks. IEEE J. Oceanic Eng. 25:28-39.

Han, J., Asada, A., Yagita., Y. 2008. Short range high speed PPP-based underwater acoustic network system. Proc. of the MTS/IEEE Kobe Techno-Ocean Conference. 1:1-4.

Kebkal, K.G., Bannasch., R. 2002. Sweep-spread carrier for underwater communication over acoustic channels with strong multipath propagation. J. Acoust. Soc. Am. 112:2043-2051.

Kilfoyle, D.B., Preisig, J.C., Baggeroer., A.B. 2005. Spatial modulation experiments in the underwater acoustic channel. IEEE J. Oceanic Eng. 30:406-415.

Kojima, J., Ura, T., Ando, H., Asakawa, K. 2002. High-speed acoustic data link transmitting moving pictures for autonomous underwater vehicles. Proc. IEEE Int. Symp. Underw. Technol. 1:278-283.

LeBlanc, L.R., Beaujean., P.P.J. 2000. Spatio-temporal processing of coherent acoustic communication data in shallow water. IEEE J. Oceanic Eng. 25:40-51.

Lin, S., Costello, D.J. 1983. Error Control Coding: Fundamentals and Applications. Englewood Cliffs: Prentice-Hall.

Linde, L.P. 1988. The performance of an adaptive least squares lattice decision-feedback equalizer on a fading multipath HF channel. Proc. of the IEEE COMSIG 1988. 1:86-92.

Ling, F., Proakis., J.G. 1985. Adaptive lattice decision feedback equalizers—Their performance and application to time-variant multipath channels. IEEE Trans. Commun. 33:348-356.

Ochi, H., Watanabe, Y., Shimura, T., Hattori., T. 2008. Experimental results of short range wideband acoustic communication using QPSK and 8PSK. Proc. of the MTS/IEEE Kobe Techno-Ocean Conference. 1:1-5.

Pelekanakis, C., Stojanovic, M., Freitag., L. 2003. High rate acoustic link for underwater video transmission. Proc. of the MTS-IEEE Oceans'03 Conference. 1:1091-1097.

Roy, S., Duman, T.M., McDonald, V., Proakis., J.G. 2007. High-rate communication for underwater acoustic channels using multiple transmitters and space-time coding: Receiver structures and experimental results. IEEE J. Oceanic Eng. 32:663-688.

Stojanovic, M. 2005. Retrofocusing techniques for high rate acoustic communications. J. Acoust. Soc. Am. 117:1173-1185.

Urick, R.J. 1983. Principles of Underwater Sound. Peninsula Publishing, Los Altos, California, 3rd ed. McGraw-Hill.

Walker, J.S., Nguyen., T.Q. 2000. Adaptive scanning methods for wavelet difference reduction in lossy image compression. Proc. of the IEEE 2000 Int. Conf. on Image Processing. 3:182-185.

Yang, T.C. 2004. Differences between passive-phase conjugation and decision-feedback equalizer for underwater acoustic communications. IEEE J. Oceanic. Eng. 29:472-487.

Zhu, W., Zhu, M., Wang, J., Huang, H., Yang, B., Xu, L., Zhao., L. 2007. Signal processing for high speed underwater acoustic transmission of image. Proc. of the OES/IEEE Oceans 2007-Europe Conference. 1:1-6.

PAPER

An Overview of Autonomous Underwater Vehicle Research and Testbed at PeRL

AUTHORS

Hunter C. Brown
Ayoung Kim
Ryan M. Eustice
University of Michigan

ABSTRACT

This article provides a general overview of the autonomous underwater vehicle (AUV) research thrusts being pursued within the Perceptual Robotics Laboratory (PeRL) at the University of Michigan. Founded in 2007, PeRL's research centers on improving AUV autonomy via algorithmic advancements in environmentally based perceptual feedback for real-time mapping, navigation, and control. Our three major research areas are (1) real-time visual simultaneous localization and mapping (SLAM), (2) cooperative multi-vehicle navigation, and (3) perception-driven control. Pursuant to these research objectives, PeRL has developed a new multi-AUV SLAM testbed based upon a modified Ocean-Server Iver2 AUV platform. PeRL upgraded the vehicles with additional navigation and perceptual sensors for underwater SLAM research. In this article, we detail our testbed development, provide an overview of our major research thrusts, and put into context how our modified AUV testbed enables experimental real-world validation of these algorithms.

Keywords: AUVs, SLAM, navigation, mapping, testbed

Introduction

The Perceptual Robotics Laboratory (PeRL) at the University of Michigan (UMich) is actively involved in three major research efforts: real-time vision-based simultaneous localization and mapping (SLAM), heterogeneous multi-vehicle cooperative navigation, and perception-driven control. To test and experimentally validate these algorithms, we have developed a new multi-autonomous underwater vehicle (AUV) testbed based upon a modified Ocean-Server Iver2 commercial AUV platform. This new AUV testbed provides a simple man-portable platform for real-world experimental validation and serves as a dedicated engineering testbed for proof-of-concept algorithmic implementations. In this article, we report on our developments in this area and provide an overview of this new experimental facility (Figure 1).

Overview of Underwater Navigation

One of the major limitations in the field of underwater robotics is the lack of radio-frequency transmission modes. The opacity of water to electromagnetic waves precludes the use of the global positioning system (GPS) as well as high-speed underwater radio communication (Stewart, 1991). Hence, communication and navigation underwater must rely upon other means. Kinsey et al. (2006) provided an overview of the current state-of-the-art in underwater vehicle navigation, of which we briefly summarize here.

Conventional Underwater Navigation Systems

Two broad categories of underwater navigation methods exist for localizing vehicles and instruments: absolute positioning and relative dead-reckoning. The traditional long-baseline (LBL) method of underwater

FIGURE 1

PeRL's multi-AUV testbed is based upon a modified Ocean-Server Iver2 AUV platform. Shown in the foreground is a modified vehicle displaying a new nose cone designed and fabricated by PeRL. For comparison, a stock vehicle displaying the original nose cone is shown in the background.

positioning estimates absolute position by measuring time-of-flight ranges to fixed beacons (Hunt et al., 1974; Milne, 1983). The precision of this estimate is bounded, and the accuracy is determined by system biases. The range of this solution is limited to a few kilometers in the best acoustic conditions, and the positioning resolution is on the order of 1 m. The slow update rate of LBL is constrained by the acoustic travel times—typically updating every few seconds. In contrast to slow, coarse, but absolute LBL positioning, a Doppler velocity log (DVL) or inertial navigation system (INS) instead estimates the distance traveled to infer position. Dead-reckoning is fast (~10 Hz) and delivers fine resolution (~1 cm), but the precision of this relative measurement is unbounded, growing monotonically with time. This makes it difficult to return to a known location or to relate measurements globally to one another.

Underwater SLAM

Over the past decade, a significant research effort within the terrestrial mobile robotics community has been to develop environmentally based navigation algorithms that eliminate the need for additional infrastructure and bound position error growth to the size of the environment—a key prerequisite for truly autonomous navigation. The goal of this work has been to exploit the perceptual sensing capabilities of robots to correct for accumulated odometric error by localizing the robot with respect to landmarks in the environment (Bailey and Durrant-Whyte, 2006; Durrant-Whyte and Bailey, 2006).

One of the major challenges of the SLAM problem is (1) defining fixed features from raw sensor data and (2) establishing measurement to feature correspondence [i.e., the problem of data association (Neira and Tardos, 2001)]. Both of these tasks can be nontrivial—especially in an unstructured underwater environment. In man-made environments, typically composed of planes, lines, and corners primitives, point features can be more easily defined; however, complex underwater environments pose a more challenging task for feature extraction and matching.

One approach to curbing the challenges of defining fixed features from raw sensor data is to seed the environment with artificial landmarks that are easily recognizable. For example, one practical application of a range-only underwater SLAM has been to localize an AUV in an acoustic-beacon network that has *a priori* unknown geometry (Newman and Leonard, 2003; Olson et al., 2006). In this scenario, the beacon geometry is learned online by the SLAM algorithm, eliminating the need to conduct an initial survey calibration of the acoustic-beacon network by a surface ship. Moreover, this paradigm can easily be extended to a scenario where the AUV self-deploys the acoustic beacons *in situ* over the survey site.

More recently, progress has been made in applying SLAM in an *a priori* unknown underwater environment without the aid of artificial landmarks. In particular, one SLAM methodology that has seen recent success in the benthic realm is to apply a pose-graph scan-matching approach (Fleischer, 2000; Eustice et al., 2006a). Pose-graph SLAM approaches do not require an explicit representation of features and instead use a data-driven approach based upon extracting relative-pose constraints from raw sensor data. The main idea behind this methodology is that registering overlapping perceptual data, for example, optical imagery as reported in by Eustice et al. (2006a, 2006b) or sonar bathymetry as reported by Roman and Singh (2005), introduces spatial drift-free edge constraints into the pose-graph. These spatial constraints effectively allow the robot to close-the-loop when revisiting a previously visited place, thereby resetting any accumulated dead-reckoning error.

Overview of PeRL's Research Thrusts

PeRL's three major research areas are (1) real-time visual SLAM, (2) cooperative multi-vehicle navigation, and (3) perception-driven control. In this section, we provide an overview of our laboratory's research thrusts as they pertain to AUV algorithms.

Real-Time Visual SLAM

The first of the three PeRL research domains, real-time vision-based SLAM algorithms, has direct application to areas such as autonomous underwater ship-hull inspection (Eustice, 2008; Kim and Eustice, 2009) and deep-sea archaeological missions (Ballard, 2008; Foley et al., 2009).

Present day means for ship-hull and port security inspection require either putting divers in the water or piloting a remotely operated vehicle (ROV) over the area of interest—both of these methods are manpower intensive and generally cannot quantitatively guarantee 100% survey coverage. Automating this task, however, is challenging and compounded by the fact that areas around ships in berth are severely confined, cluttered, and complex sensing environments (e.g., acoustically, optically, magnetically). Current tethered robotic inspection systems present issues of snagging, maneuver

degradation, and tether management, all of which make maneuvering around the ship at the pier difficult. Moreover, current robotic inspection methods require human in-the-loop intervention for both sensory interpretation and control (e.g., ROV piloting). Navigation feedback in these scenarios is typically performed using acoustic transponder time-of-flight ranging (Smith and Kronen, 1997). This necessitates the setup and calibration of the acoustic-beacon infrastructure, and therefore vitiates our ability to rapidly and repeatedly inspect multiple underwater structures.

Similarly, deep-sea archaeology also requires high-performance navigation (Ballard, 2008; Foley et al., 2009). Optical imagery, bathymetric sonar, and environmental measurements are all products of interest to the archeologist. The data may be collected over multiple missions or even multiple field seasons, and it is the precision of the navigation that makes it possible to transform these measurements into co-registered maps.

To combat the aforementioned navigation limitations (i.e., infrastructure-based and unbounded error growth), PeRL has been developing a camera-based navigation system that uses vehicle-collected imagery of the hull (port/hull inspection) or seafloor (underwater archeology) to extract measurements of vehicle motion. These camera-derived spatial measurements are fused with the onboard dead-reckoned data to produce a bounded-error navigation estimate (Figure 2).

In essence, the AUV builds a digital map of the seafloor or hull by registering overlapping digital-still images (both along-track and cross-track imagery). Images that are successfully registered produce a relative measurement of the vehicle's attitude (heading, pitch, and roll) and translational (x, y, z) displacement. When fused with the onboard navigation data from a bottom-lock DVL, the result is a navigation system whose error is commensurate or much better than LBL but which is infrastructure free. The significant advantage of this navigation paradigm is that it is *in situ*. For archeological surveys, this means that the AUV can be more easily deployed for exploratory surveys to investigate target shipwreck sites—without having to invest significant ship time in deploying a beacon network to obtain precision navigation; and for hull inspection surveys, no additional acoustic-beacon infrastructure is required for precise global localization along the hull. In layman's terms, these algorithms allow the AUV to navigate much like a human does by visually navigating with respect to the seafloor environment.

A useful and important by-product of this navigation methodology is that the overlapping registered imagery can be used to construct an optically derived bathymetry map (Figure 3). This map can be used to construct a quantitatively accurate three-dimensional (3-D) photomosaic by back-projecting the imagery over the optical bathymetry map. Figure 3 displays the result of applying this technology to the fourth-century B.C. Chios classical ancient shipwreck site (Foley et al., 2009). In particular, Figure 3a shows the optically derived bathymetry map for a 15 m by 45 m swath centered overtop

FIGURE 2

The foundation of visually augmented navigation (Eustice et al., 2008) is the fusion of "zero-drift" camera measurements with dead-reckoned vehicle navigation data to produce a bounded error position estimate. These constraints are fused with onboard navigation sensor data in a view-based stochastic map framework; the model is composed of a pose-graph where the nodes correspond to historical robot poses and the edges represent either navigation or camera constraints.

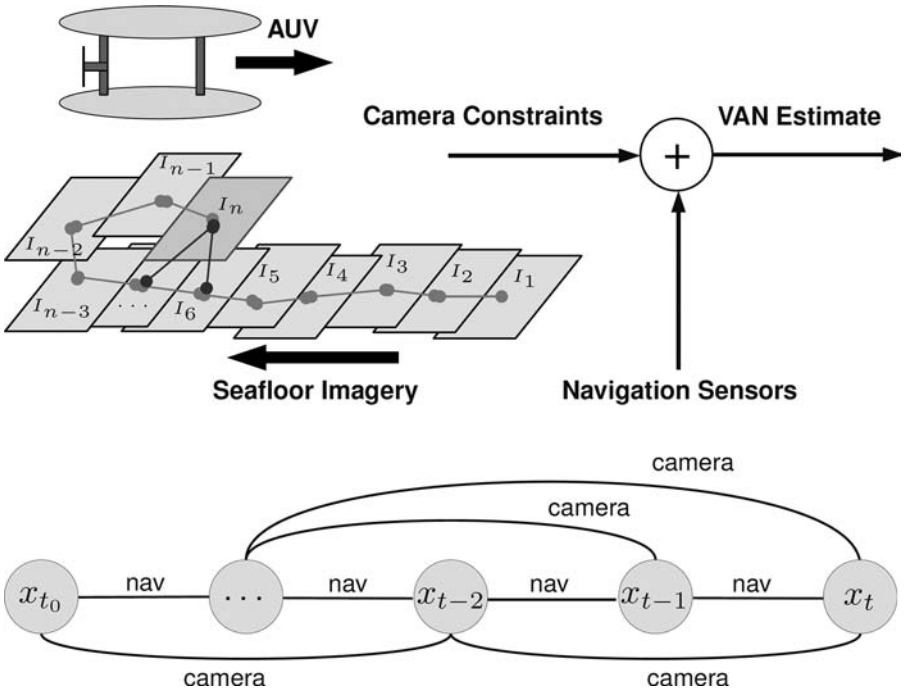

FIGURE 3

A by-product of camera-based AUV navigation is the ability to produce an optically derived bathymetry. VAN-derived bathymetric maps from the Chios 2005 shipwreck survey are depicted (Foley et al., 2009). (a) Triangulated 3-D point cloud from registered imagery. The point cloud is gridded to 5 cm to produce an optically derived bathymetry map. (b) A quantitatively correct 3-D mosaic is generated by back-projecting the imagery onto the optical bathymetry map. The gray areas correspond to regions of no image overlap. (c) A zoomed overhead view shows detail of the amphorae pile in the center mound of the 3-D photomosaic.

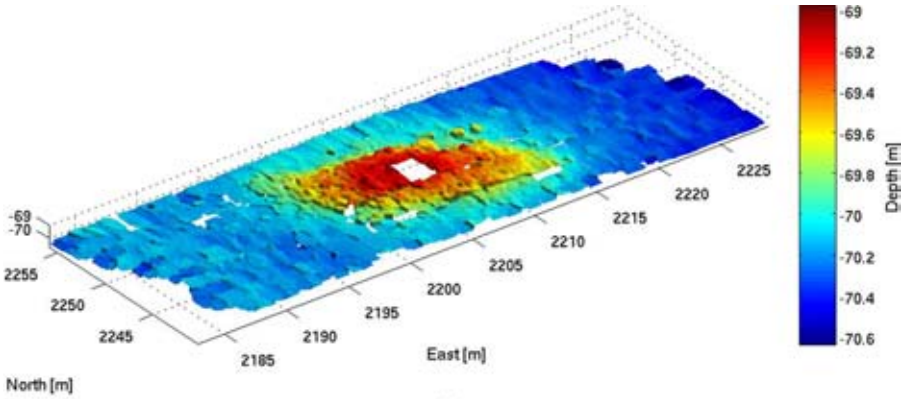

(a)

(b)

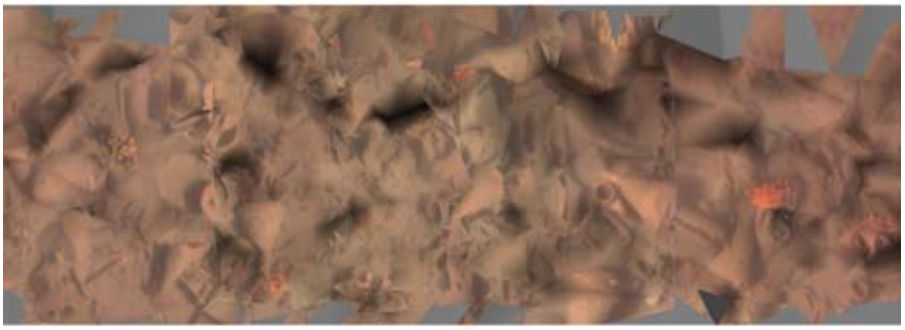

(c)

the wreck site. The optical bathymetry is generated from a 3-D triangulated point cloud derived from pixel correspondences. In Figure 3b, we display a quantitatively accurate 3-D photomosaic obtained by back-projecting the imagery onto the gridded surface. It should be emphasized that this result is fully automatic and metrically quantitative, in other words, measurements of object size and geometric relationships can be derived. Although this technology is still very much in the active research stage, its current and future value for *in situ*, rapid, quantitative documentation of marine archeological wreck sites or ship-hull inspection cannot be overstated.

Cooperative Navigation

In addition to real-time visual SLAM, PeRL is working toward cooperative multi-vehicle missions for large-area survey. Multi-vehicle cooperative navigation offers promise of efficient exploration by groups of mobile robots working together to pool their mapping capability. Most prior research in the SLAM community has focused on the case of single-agent mapping and exploration. Although these techniques can often be extended to a centralized multi-agent framework (Walter and Leonard, 2004) (provided that there are no communication bandwidth restrictions), the extension of single-agent techniques to a decentralized multi-vehicle SLAM framework is often neither obvious nor appropriate. Much of the previous research in the area of distributed multi-vehicle SLAM has focused primarily on terrestrial (i.e., land and aerial) applications (Williams et al., 2002; Ridley et al., 2002; Rekleitis et al., 2003; Bourgault et al., 2004; Ong et al., 2006; Partan et al., 2006). There, high-bandwidth radio commu-

nication is possible; however, underwater communication bandwidth is distinctly limited from that on land (Partan et al., 2006).

It requires on the order of 100 times more power to transmit than it does to receive underwater, which makes acoustic transmission and reception asymmetrical for medium access schemes (Partan et al., 2006). Half duplex time division multiple access networks are usual, with typical acoustic-modem data rates ranging from 5 kbits/s at a range of 2 km (considered a high rate) to as little as 80 bits/s (a low rate). The low acoustic data rates are not simply a limitation of current technology—the theoretical performance limit for underwater acoustic communications is 40 km kbps (e.g., a max theoretical data rate of 20 kbps at a range of 2 km) (Partan et al., 2006). Therefore, any type of multi-vehicle SLAM framework must adhere to the physical bandwidth limitations of the underwater domain.

In a previous work, Eustice et al. (2006c, 2007) developed a synchronous clock acoustic-modem-based navigation system capable of supporting multi-vehicle ranging. The system consisted of a Woods Hole Oceanographic Institution (WHOI) Micro-Modem (Freitag et al., 2005a, 2005b) (an underwater acoustic modem developed by WHOI) and a low-power stable clock board. This system can be used as a synchronous-transmission communication/navigation system wherein data packets encode time of origin information as well as local ephemeris data (e.g., x, y, z positional data and error metric). This allows for the direct measurement of inter-vehicle one-way travel time (OWTT) time-of-flight ranging. The advantage of a OWTT ranging methodology is that all passively receiving nodes within listening range are able to decode and measure the inter-vehicle range to the broadcasting node.

PeRL is currently investigating probabilistic fusion methods for a OWTT cooperative navigation multi-vehicle framework that scales across a distributed network of nodes in a non-fully connected network topology. The proposed acoustic-modem navigation framework will exploit inter-vehicle OWTT ranging to supplement perceptual SLAM localization thereby reducing the need for state communication. The goal is to distribute state estimation between the vehicles in a coordinated fashion, allowing navigation impoverished vehicles (e.g., no INS or DVL) to share from positional accuracies of better equipped vehicles (e.g., those with DVL bottom-lock, or VAN-navigated vehicles near the seafloor).

Figure 4 depicts preliminary results reported by Eustice et al. (2007), demonstrating the OWTT proof of concept. Here, a GPS-equipped surface ship navigationally aided a submerged AUV by broadcasting the ship GPS position to the network while the AUV measured its range to the ship via the OWTTs.

Perception-Driven Control

Another research focus is in the domain of perception-driven control. Algorithms are under development to enable a vehicle to respond to the environment by autonomously selecting alternative search patterns based upon perceived feature distributions in the environment. This creates improvements in survey efficiency by limiting the duration in benign feature-poor areas and instead spends more bottom-time over actual targets. A seafloor survey vehicle, for example, may drive into an area devoid of features during a mission. Instead of continuing to search the featureless space, where there is little return on investment from a visual navigation system, the vehicle would return to a previously known feature rich area and begin searching in another direction. PeRL is currently working on algorithms to

FIGURE 4

Preliminary OWTT results as reported by Eustice et al. (2007) for a two-node network consisting of an AUV and a surface ship. (left) The raw dead-reckoned AUV trajectory is shown in blue, GPS-derived ship position in cyan, OWTT fused AUV trajectory in red, and the LBL measured AUV position in green, which serves as an independent ground-truth. (right) Zoomed view of the AUV trajectory. (Color versions of figures available online at: http://www.ingentaconnect.com/content/mts/mtsj/2009/00000043/00000002.)

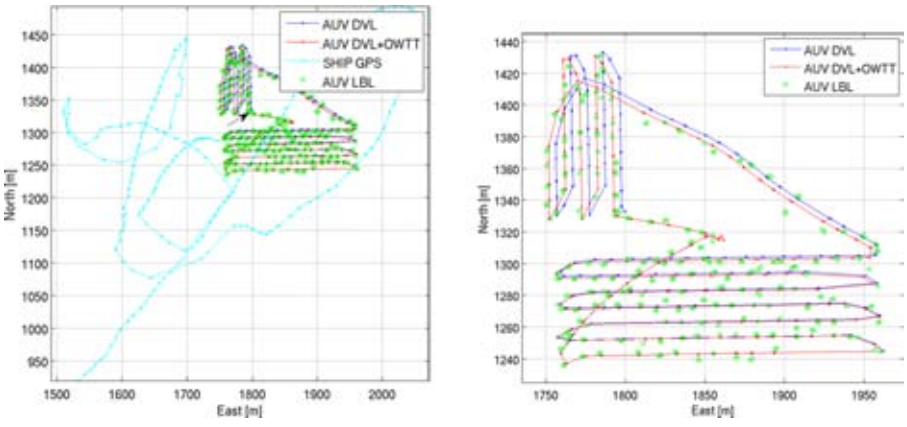

assist in the decision making process of when to revisit known landmarks versus continuing new exploration. For example, Figure 5 depicts imagery from a hull inspection survey of a decommissioned aircraft carrier (Kim and Eustice, 2009). At the one extreme, we see that some areas of the hull are very texture-rich (heavily biofouled), whereas other areas are nearly feature-less (no distinguishing features such as weld seams, rivets, port opening, etc). In this type of environment, it makes no sense to incorporate imagery from the featureless region into the visual SLAM map because the image registration algorithm will fail to localize the vehicle because of a lack of visual features. Instead, by coupling the visual navigation feedback into the trajectory planning and control, the AUV can more intelligently adapt its survey and map-building strategy so as to only return to feature-rich areas of the hull when it accrues too much pose uncertainty. By jointly considering along-hull pose uncertainty, map feature content, and energy expenditure accrued during AUV transit, we can frame the online path planning problem as a multi-objective optimization problem that seeks to find an optimal trajectory with respect to the possibly divergent criteria of exploration versus localization.

FIGURE 5

Depiction of the multi-objective constraints at play in perception-driven control.

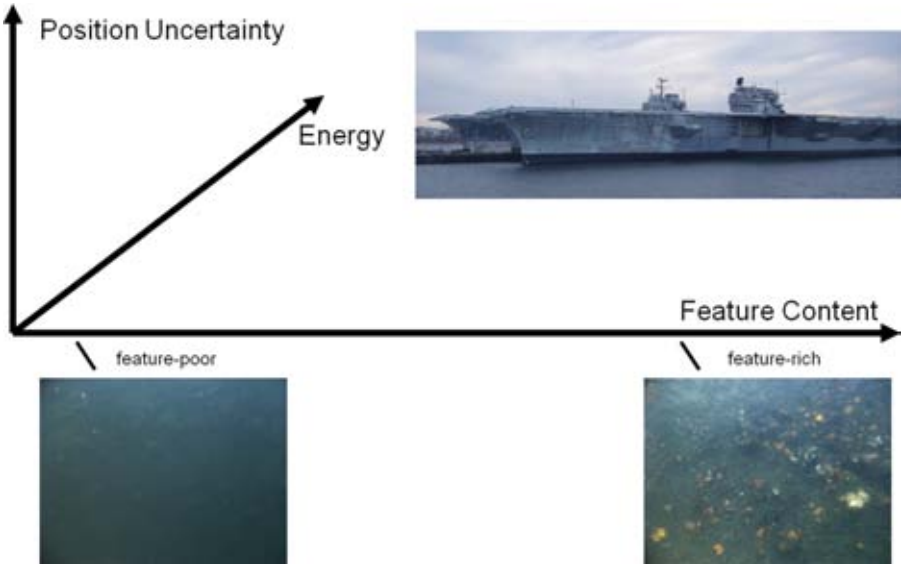

FIGURE 6

PeRL's modified Ocean-Server Iver2: external and internal view.

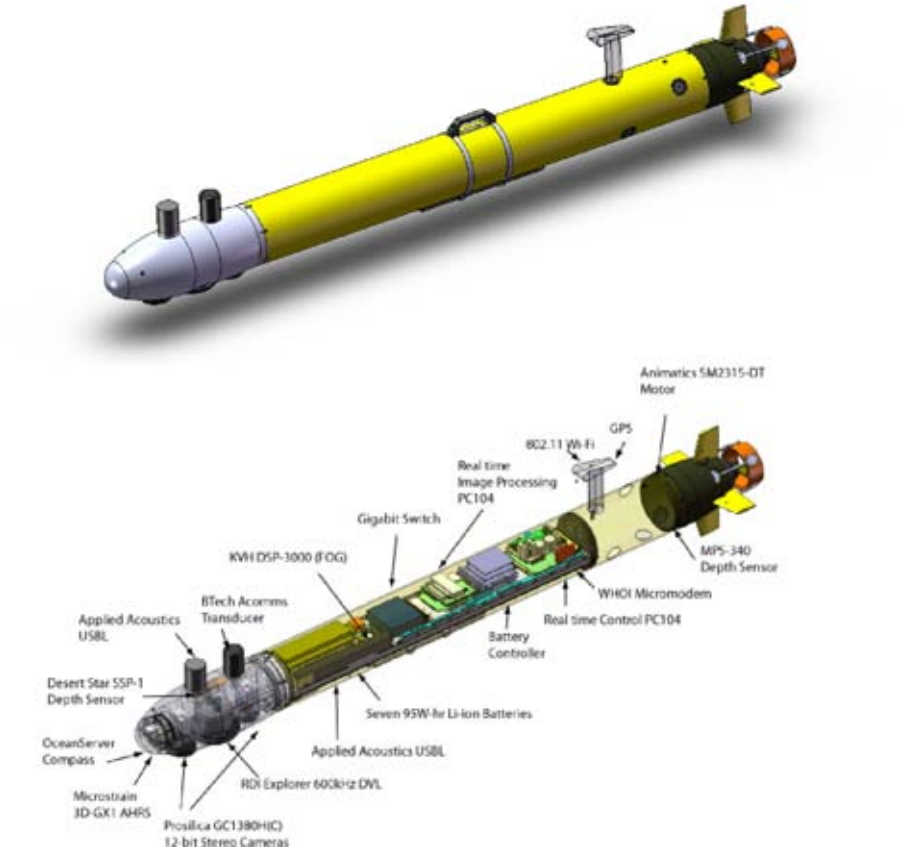

Overview of PeRL's AUV Testbed

To pursue PeRL's three research thrust areas, two commercial Ocean-Server Iver2 AUV systems were purchased and modified to serve as a real-world testbed platform for SLAM research at UMich. Although several other vehicle platforms currently include stereo-vision systems and DVL sensors, the Iver2 (Figure 6) was

selected as a testbed development platform because of its ability to be transported in a personal vehicle and launched by a single user. The vehicles, as shipped, are rated to a depth of 100 m, have a maximum survey speed of approximately 2 m/s (4 knots), and weigh approximately 30 kg allowing for transport by two people (Anderson and Crowell, 2005).

Because the commercial-off-the-shelf Iver2 vehicle does not come equipped with camera or DVL sensing, sensor upgrades were required to enable the stock vehicle to perform SLAM and coordinated multi-AUV missions. PeRL upgraded the vehicles with additional navigation and perception sensors (detailed in Figure 6b and Table 1), including 12-bit stereo down-looking Prosilica cameras, a Teledyne RD Instruments (RDI) 600 kHz Explorer DVL, a KVH Industries, Inc. (KVH) single-axis fiber-optic gyroscope (FOG), a Microstrain 3DM-GX1 attitude-heading-reference sensor, a Desert Star SSP-1 digital pressure sensor, and a WHOI Micro-modem for inter-vehicle communication. For illumination, we contracted the custom design and fabrication of a LED array by Farr and Hammar Engineering Services, LLC. To accommodate the additional sensor payload, a new Delrin nose cone was designed and fabricated. An additional 32-bit embedded PC104 CPU hardware was added for data-logging, real-time control, and *in situ* real-time SLAM algorithm testing and validation. Details of the design modification are discussed herein.

Mechanical/Electrical Design and Integration

The design goals during the integration phase of vehicle development consisted of minimizing the hydrodynamic drag, maintaining the neutral buoyancy, and maximizing the sensor payload capacity within the pressure hull. These requirements were achieved

TABLE 1

Integrated sensors on the PeRL vehicles.

Iver2 Instruments	Variable	Update Rate	Precision	Range	Drift
Ocean-Server OS5000 Compass	Attitude	0.01-40 Hz	1-3° (Hdg), 2° (Roll/Pitch)	360°	–
Measurement Specialties Pressure Sensor MSP-340	Depth	0.01-40 Hz	<1% of FS†	0-20.4 atm	–
Imagenex Sidescan Sonar (Dual Freq.)	Sonar image	330 or 800 kHz	–	15-120 m	–
USGlobalSat EM-406a GPS	XYZ position	1 Hz	5-10 m	–	–
New Instruments					
Prosilica GC1380H(C) Camera (down-looking stereo-pair)	Gray/color image	0.1-20 fps	1360 × 1024 pixels 12-bit depth	–	–
Strobed LED Array‡	Illumination	0.1-4 fps	–	2-4 m altitude	–
Teledyne RDI 600 kHz Explorer DVL	Body velocity	7 Hz	1.2-6 cm/s (at 1 m/s)	0.7-65 m	–
KVH DSP-3000 1-Axis FOG	Yaw rate	100 Hz	1-6° /h	±375°/s	4°/h/√Hz
Desert-Star SSP-1 300PSIG Digital Pressure Transducer	Depth	0.0625-4 Hz	0.2% of FS†	0-20.4 atm	–
Applied Acoustics USBL	XYZ position	1-10 Hz	±0.1 m (Slant Range)	1000 m	–
OWTT* Nav (Modem + PPS)	Slant range	Varies	18.75 cm (at 1500 m/s)	Varies	<1.5 m/14 h
•WHOI Micro-modem	Communication	Varies	–	Varies	–
•Seascan SISMTB v4 PPS Clock	Time	1 Hz	1 µs	–	<1 ms/14 h
Microstrain 3DM-GX1 AHRS	Attitude	1-100Hz	2° (Hdg), 2° (Roll/Pitch)	360°	–
	Angular rate	1-100 Hz	3.5°/s	±300°/s	210°/h/√Hz

†Full scale.
‡In development.
*One-way travel time.

through the use of lightweight materials such as acrylonitrile butadiene styrene (ABS), Delrin, and aluminum, and through careful center of buoyancy and center of mass computations. The entire vehicle was modeled using SolidWorks solid modeling software, and the extensive use of these computer-aided design (CAD) models provided optimal arrangements of internal components prior to actual installation (Figure 7).

The addition of a redesigned SLAM nose cone and sensor payload shifted both the original center of buoyancy and center of gravity. New positions were estimated using the CAD models and refined during ballast tests at the UMich Marine Hydrodynamics Laboratory (MHL). The vehicle is ballasted to achieve approximately 0.11 kg (0.25 lbs) of reserve buoyancy for emergency situations when the vehicle must surface without power. Vehicle trim is set neutral to achieve passive stability and to optimize both diving and surfacing operations.

The interior component arrangement within the main body took into account mass, geometry, heat dissipation, and electrical interference considerations when determining the spatial layout and arrangement of sensors, computing, and electronics in the main tube. Because of the high density of sensors and other devices in the pressure housing, the components with the highest heat radiation, such as computers and DC-DC converters, were placed in direct contact with the aluminum chassis to allow better heat dissipation. Also, sensors that are prone to electrical noise from surrounding electronics were spatially separated in the layout (e.g., the Micro-Electro-Mechanical Systems (MEMS) Microstrain 3DM-GX1 is located in the nose cone tip, the furthest point from the motor and battery pack influence).

Electrically, the vehicle is powered by a 665 Wh Li-ion battery pack made up of seven 95 Wh laptop batteries. This battery pack is managed by an Ocean-Server Intelligent Battery and Power System module. The additional sensors and PC104 computing added by PeRL draw less than 40 W total. This load is in addition to the original 12 W nominal vehicle hotel load and 110 W propulsion load of the stock Iver2, which results in a combined maximum total power draw of approximately 162 W (this assumes full hotel load and the motor at full power). The estimated run time at full load is 4.1 h; however, taking into account a more realistic assessment of propulsion load for photo transect survey conditions, the continuous run time will be closer to 5.2+ h at a 2 knot (i.e., 75 W propulsion) survey speed.

FIGURE 7

Mechanical layout.

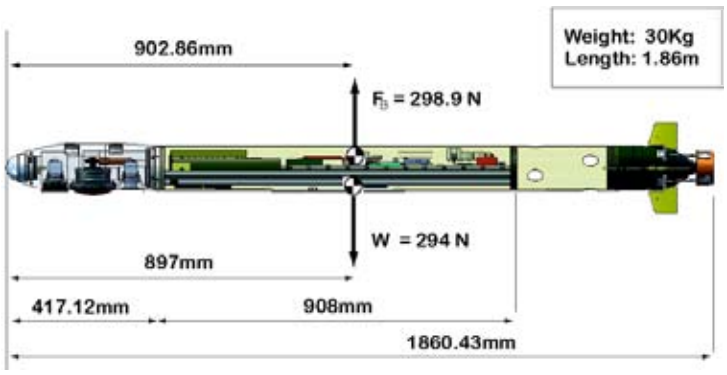

SLAM Nose Cone

In order to support the real-time visual SLAM objectives of PeRL, a down-looking stereo-vision system was added to the Iver2 vehicles. A dual camera arrangement was chosen because it provides greater flexibility for visual SLAM research. For example, using a stereo-rig allows for the measurement of metrical scale information during pairwise image registration and, thereby, can be used to improve odometry estimation by observing velocity scale error in DVL bottom-track measurements. Additionally, the dual camera arrangement can be used to run one of the cameras in a low-resolution mode suitable for real-time image processing (e.g., VGA or lower), whereas the second camera can be run at its native 1.6 megapixel resolution for offline processing. At depth, illumination will come from a LED array mounted at the aft of the vehicle. The array will provide optimal illumination over a 2-4 m imaging altitude at up to 4 fps strobe rate with a camera-to-light separation distance of approximately 1.25 m.

To accommodate the two-camera vision system and the DVL transducer, a new nose cone was designed and fabricated. The UMich custom-designed nose cone (Figure 8) was fabricated from Acetron GP (Delrin) because of the material's high tensile strength, scratch resistance, fatigue endurance, low friction, and low water absorption. Threaded inserts are installed in the nose cone to prevent stripped threads, and stainless fasteners with a polytetrafluoroethene paste (to prevent corrosion issues) are used in all locations.

FIGURE 8

(top) Exploded and transparent view of PeRL's redesigned nose cone. (bottom) The fabricated nose cone as installed.

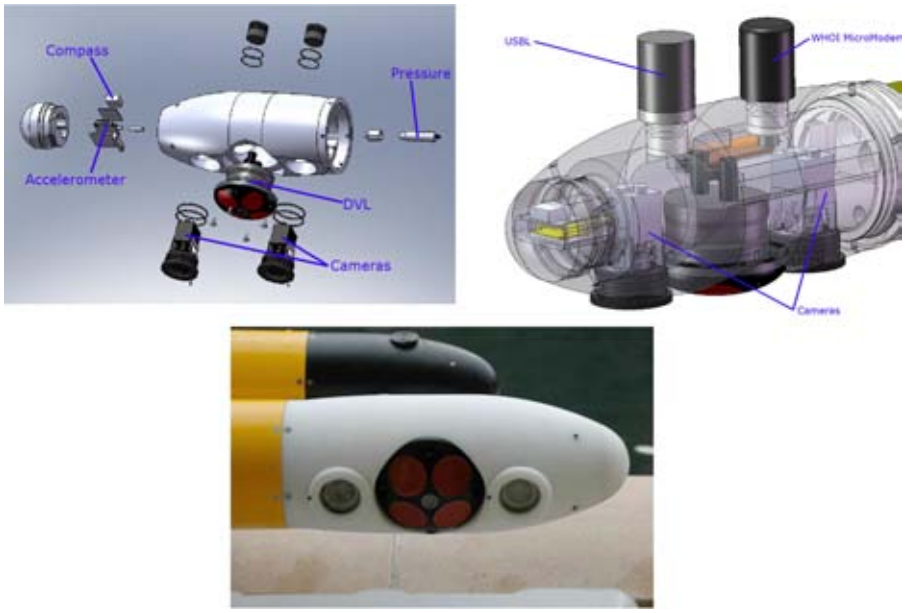

The designed working depth of the nose cone is 100 m (to match the full rating of the Iver2). Calculations were performed according to the ASME Section VIII Boiler and Pressure Vessel Code to verify the wall thickness in each of the nose cone sections. A minimum factor of safety of at least 2.64 was attained for all sections of the nose cone. Pressure tests, conducted at Woods Hole Oceanographic Institution, demonstrated the structural integrity of the nose cone to 240 m water depth. Three short duration tests of 12 min each were made to 24.5 atm (240 m salt water equivalent), and one long duration test of 5 h was made to 24.5 atm.

The Teledyne RDI 600 kHz Explorer DVL is integrated into the nose cone using fasteners to attach the DVL head to threaded inserts in the nose cone material. The limited internal cavity space of the Iver2 nose precludes the use of RDI's recommended clamp attachment method. Instead, self-sealing fasteners are used to eliminate a fluid path through the mounting holes of the DVL to the interior of the nose cone. The associated DVL electronics module is mounted in the main chassis of the vehicle just behind the forward bulkhead. The electronics module and transducer head are connected by RDI's recommended shielded twisted-pair cabling to reduce stray electromagnetic field effects.

Two nose cone plugs were designed for camera integration. These plugs include a sapphire window and two mounting brackets each (Figure 8). The synthetic sapphire window was custom designed and fabricated by the Optarius Company of the U.K. Sapphire was chosen because of its high scratch resistance and superior tensile strength to that of plastic or glass materials. The mounting brackets were designed in CAD and printed in ABS plastic using a Dimension Fused Deposition Modeling (FDM) Elite rapid prototype machine. Static face and edge o-ring seals prevent water ingress through the plug around the sapphire window.

A Desert Star SSP-1 pressure transducer is mounted to an internal face of the nose cone and is exposed to the ambient environment through a 1/8 in. shaft drilled perpendicular to the nose cone wall to reduce the flow noise influence on the sensor. The Microstrain 3DM-GX1 is integrated into the nose cone tip by mounting the Ocean-Server OS5000 compass on top of the 3DM-GX1 and milling a cavity in the tip to allow additional vertical clearance. All o-rings installed in the nose cone are of Buna-N (acrylonitrile-butadiene) material and are lightly lubricated with Dow Corning #4 prior to installation.

Mission Planning and Control

The stock Iver2 control computer is a 500 MHz AMD Geode CPU running Windows XP Embedded for the operating system. Ocean-Server provides a Graphical User Interface (GUI) mission planning module called VectorMap (Figure 11) and a vehicle control software called Underwater Vehicle Control (UVC). The VectorMap mission planning software allows the user to graphically layout a mission trajectory over a geo-registered image or nautical navigation chart and to specify parameters such a depth, speed, goal radius, timeout, and other attributes for each waypoint. The output of VectorMap is an ASCII waypoint file that the UVC loads and executes within a Proportional-Integral-Derivative (PID) control framework (Leveille, 2007). Additionally, the UVC supports a backseat driver Application Programming Interface (API) interface for user-level control from a host client. This API supports two control primitives: (1) a

high-level control interface where the host specifies the reference heading, speed, and depth set points, and (2) a low-level control interface where the host specifies servo commands for the thruster and control surfaces.

The modified PeRL vehicle uses a Digital-Logic ADL945 1.2 GHz Core-Duo PC104 for backseat control and data logging. The ADL945 runs less than 10 W in power consumption, has Gigabit Ethernet for interfacing with the Prosilica GigE cameras, and runs 32-bit Ubuntu Linux. The host stack records data from the cameras and navigation sensors, performs online state estimation, and directs the real-time control of the Iver2 via the backseat driver API. For ease of software development and modularity, we have adopted a multi-process software paradigm that uses the open-source LCM inter-process communication library developed by the Massachusetts Institute of Technology (MIT) Defense Advanced Research Projects Agency (DARPA) Urban Grand Challenge team (Leonard et al., 2008; LCM, 2009).

Missions and Testing

Current missions and testing conducted by PeRL include testing at the UMich MHL tow tank, automated visual ship-hull inspection (conducted at AUV Fest 2008), field testing at the UMich Biological Station, and archaeological surveys of shipwrecks in the Thunder Bay National Marine Sanctuary.

UMich Marine Hydrodynamics Laboratory

The UMich MHL provides a controlled experimental environment for testing real-time underwater visual SLAM algorithms. The freshwater physical model basin measures 110 m × 6.7 m × 3.0 m (Figure 9) and can achieve prescribed vehicle motions via the electronically controlled tank carriage. Trajectory ground-truth is obtained from the encoder measured carriage position and will be used to validate real-time visual SLAM pose estimates derived from registering the imagery of the tank floor. For ease of real-time algorithm development, we can attach a wet-mateable wired Ethernet connection to a vehicle bulkhead so that imagery and sensor data can be streamed live to a topside desktop computer. This allows for greater flexibility in real-time software development, visualization, and debugging. The use of the test facility has been beneficial for early development and testing of our Iver2 hardware and real-time underwater visual SLAM algorithms.

AUV Fest 2008

The Iver2 serves as a testbed for real-time visual autonomous port and hull inspection algorithm research at UMich. We use the Iver2 as a proxy for visual hull inspection by developing and testing our algorithms to navigate over the seafloor (because the underlying visual navigation algorithm is fundamentally the same in the two scenarios). This allows us to use the Iver2 to validate the accuracy of our visually augmented navigation method, and to test and implement our real-time algorithms on the type of embedded system hardware typically found on AUVs.

Meanwhile, to test our VAN algorithms in a real hull-inspection scenario, PeRL collaborated with MIT and Bluefin Robotics at AUV Fest 2008 to put one of our camera systems on the Hovering Autonomous Underwater Vehicle (HAUV) (Vaganay et al., 2005). In this experiment, we collected imagery of the hull of the USS Saratoga—a decommissioned U.S. aircraft carrier stationed at Newport, Rhode Island (Figure 10a). PeRL packaged and mounted a calibrated Prosilica GC1380HC camera (the same camera system used in the Iver2 SLAM nose cone) and a flash strobe light system on the HAUV hull inspection vehicle. Boustrophedon survey imagery was collected by the HAUV of the hull of the USS Saratoga. The

FIGURE 9

Vehicle testing at MHL tow tank.

FIGURE 10

Hull inspection results from AUV Fest 2008. (a) Depiction of the AUV Fest 2008 experimental setup. (b) The camera-derived pose constraints are shown as red and green links. Each vertex represents a node in the pose-graph enclosed by its 3σ covariance uncertainty ellipsoid. Because of the change of the visual feature richness along the hull, the uncertainty ellipsoid inflates when the vehicle is not able to build enough pose constraints but then deflates once VAN creates camera constraints with previous tracklines. Three small figure insets depict the typical feature richness for different regions of the hull. (c) Triangulated 3-D points are fitted to obtain a smooth surface reconstruction and then texture mapped to create a 3-D photomosaic. The six white dots are targets that were manually placed on the hull and used to verify the utility of the visual hull inspection algorithm.

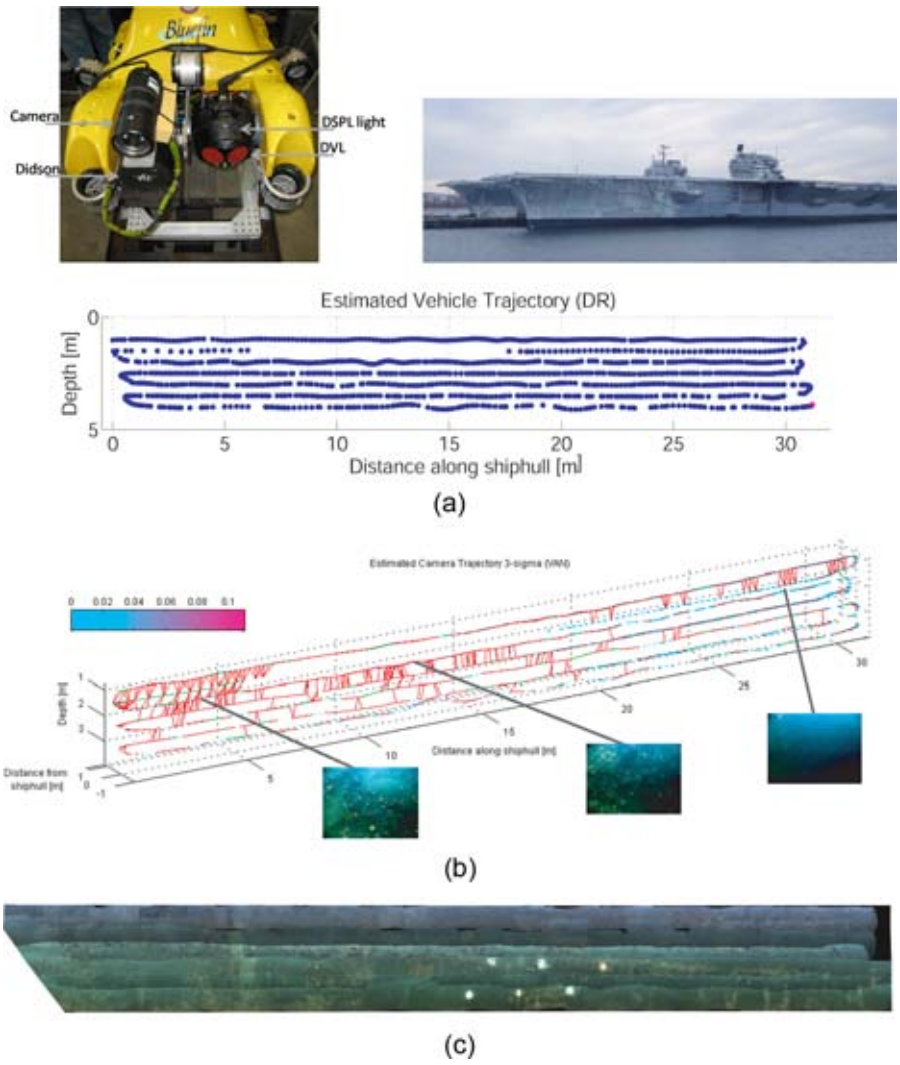

HAUV is equipped with a 1200 kHz DVL, a FOG, and a depth sensor, all of which are comparable to the sensor suite integrated into PeRL's Iver2 testbed.

Preliminary results for visual hull-relative navigation are shown in Figure 10 (Kim and Eustice, 2009). Here, we see a pose-graph of the camera constraints generated through pairwise registration of overlapping imagery. These constraints are fused with navigation data in an extended information filter framework to provide a bounded error precision navigation estimate anywhere along the hull. Each node in the network corresponds to a digital-still image taken along the hull (over 1300 images in all). Note the discrete dropout of imagery along the second leg in the region of 5 m to 20 m along the hull axis. Because of a logging error, we did not record any imagery during this time; however, this gap in the visual data record actually highlights the utility of our hull-referenced visual navigation approach. Because we are able to pairwise register views of the hull taken from different times and locations, the camera-based navigation algorithm is able to "close-the-loop" and register itself to earlier imagery from the first leg of the survey—thereby resetting any incurred DVL navigation error during the data dropout period. It is precisely this hull-referenced navigation capability that allows the AUV to navigate *in situ* along the hull without the need for deploying any external aiding (e.g., acoustic-beacon transponders).

UMich Biological Station

Field trials were held on Douglas Lake at the UMich Biological Station (UMBS) in Pellston, Michigan, during July 2008. Four days of on-water testing demonstrated maneuverability, vehicle speed, dead-reckon navigation, wireless Ethernet communication, sidescan sonar functionality, digital compass, and manual surface joystick operation modes as summarized in Table 2.

Launch and recovery were conducted from shore, dock, and from a pontoon boat. A full sidescan sonar survey of the southeastern bay at Douglas Lake was run from the UMBS docks (Figure 11). After completion of the mission, the vehicle was manually driven under joy-stick con-

TABLE 2

Results of testing stock Iver2 at UMBS.

Attribute	Performance
Maneuverability	1.5 m altitude bottom following
	25 cm depth band control
	4.5 m turning radius
Speed	0.5-1.5 m/s
DR navigation accuracy *(DR = prop counts + compass u/w; GPS when on surface)*	10% distance traveled
802.11g Wi-Fi	100 m range (on surface)

trol from a portable wireless station back to the dock for recovery. This onshore launch and recovery capability facilitates the ease of experimental field testing with the Iver2.

Thunder Bay National Marine Sanctuary

In August 2008, PeRL collaborated with the National Oceanic and Atmospheric Administration (NOAA) Thunder Bay National Marine Sanctuary (TBNMS) researchers to map unexplored areas outside the Sanctuary's current boundaries (Figure 12a). Established in 2000, the TBNMS protects

FIGURE 11

VectorMap mission-planning interface for the Iver2. The depicted tracklines are for a sidescan sonar survey of a portion of Douglas Lake. Launch and recovery of the Iver2 were performed from a dock on shore.

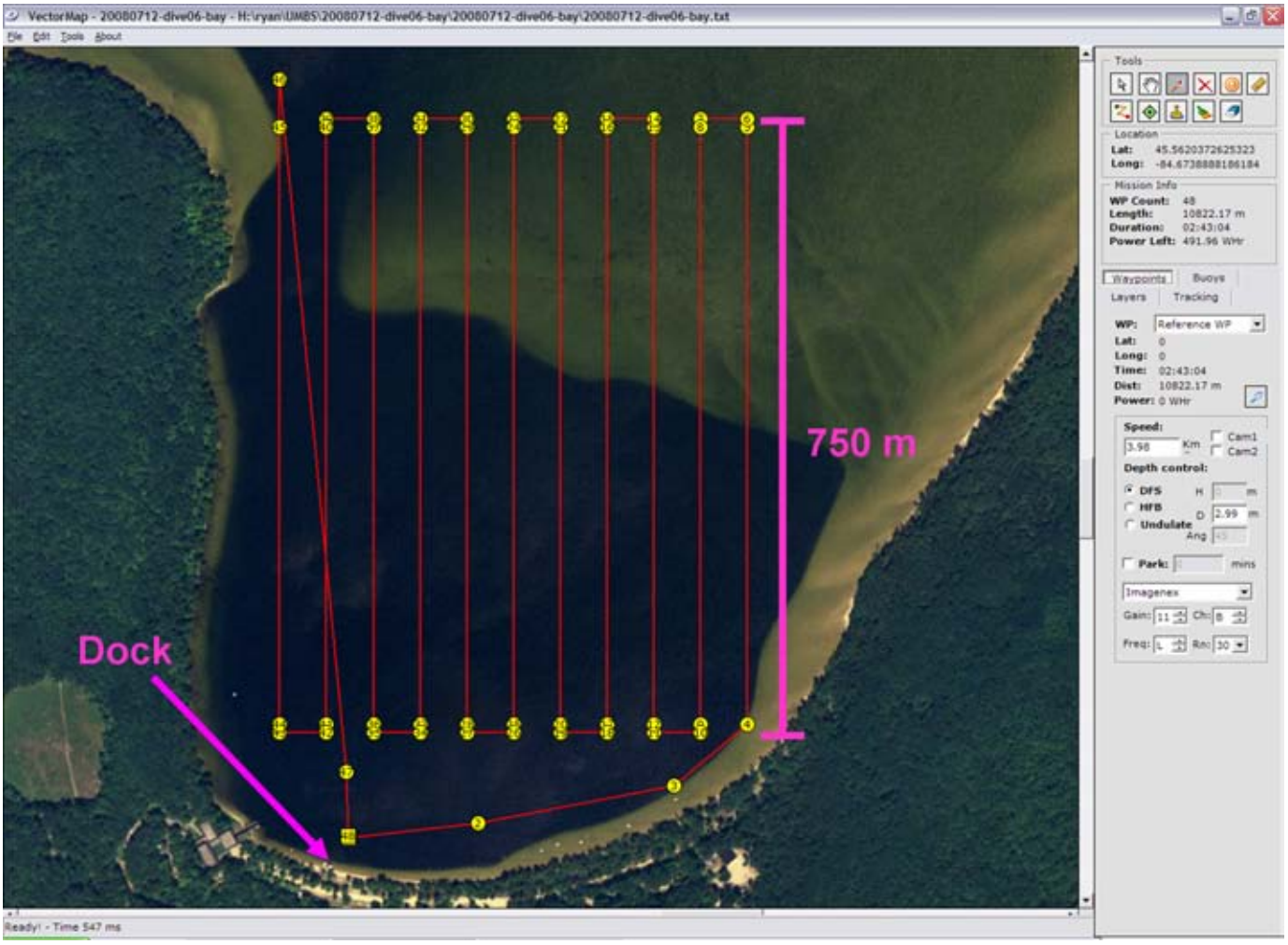

FIGURE 12

Sidescan sonar mapping results from the 2008 summer field season in TBNMS. (a) Thunder Bay National Marine Sanctuary facility. (b) A large area search was conducted first to locate the target wreck indicated in the white box (survey tracklines are shown in green). A second finer-scale survey was then conducted to map the target at higher resolution (tracklines overlaid in gray). (c) Target imagery found using 330 kHz sonar. (d) Detailed target imagery using 800 kHz sonar.

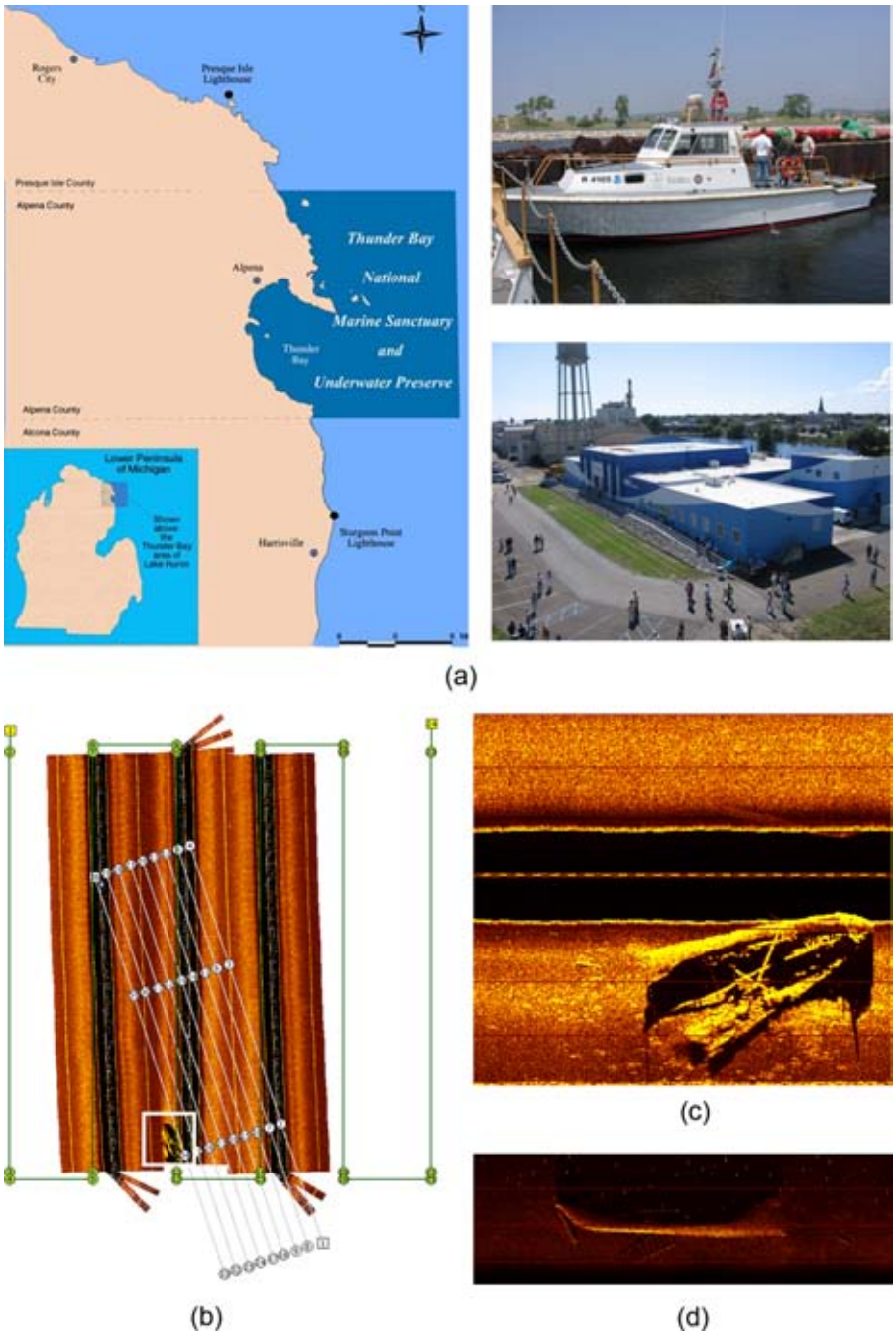

one of the nation's most historically significant collections of shipwrecks. Located in the northeast corner of Michigan's Lower Peninsula, the 448 mi^2 sanctuary contains 40 known historic shipwrecks. Archival research indicates that over 100 sites await discovery within and just beyond the sanctuary's current boundaries. This fact, coupled with strong public support and the occurrence of dozens of known shipwrecks, provides the rationale for the sanctuary's desire to expand from 448 mi^2 to 3,662 mi^2 (an eightfold increase). To date, however, a comprehensive remote sensing survey has not been conducted in the potential expansion area. Moreover, significant portions of the existing sanctuary have not been explored.

PeRL is engaged in a 5-year collaboration effort with TBNMS to use the Sanctuary as a real-world engineering testbed for our AUV algorithms research. TBNMS provides in-kind support of ship time and facilities and in return receives SLAM-derived archaeological data products ranging from 3-D photomosaics of shipwrecks to sidescan sonar maps of the Sanctuary seafloor. In addition, PeRL is engaged in public outreach efforts in collaboration with TBNMS to educate the general public in the use and technology of underwater robotics. In development is an AUV technology display in their state-of-the-art Great Lakes Maritime Heritage Center, (a 20,000 ft^2 building featuring a 100-seat theater, 9,000 ft^2 of exhibit space, and distance learning capabilities), which will consist of an Iver2 AUV hull, a multimedia kiosk, and maps and data products derived from PeRL's field testing in the Sanctuary.

This past August, as part of an NOAA Ocean Exploration grant, PeRL fielded one of its two Iver2 AUVs to collect sidescan sonar imagery in unmapped regions of the Sanctuary seafloor. Figure 12 shows survey tracklines and sonar imagery collected of a newly found wreck outside of the Sanctuary's boundaries in approximately 50 m of water depth.

Conclusion

This paper provided an overview of PeRL's AUV algorithms research and testbed development at UMich. To summarize, PeRL's main research thrusts are in the areas of (1) real-time visual SLAM, (2) cooperative multi-vehicle navigation, and (3) perception-driven control. Toward that goal, we reported the modifications involved in preparing two commercial Ocean-Server AUV systems for SLAM research at UMich. PeRL upgraded the vehicles with additional navigation and perceptual sensors, including 12-bit stereo down-looking Prosilica cameras, a Teledyne RDI 600 kHz Explorer DVL for 3-axis bottom-lock velocity measurements, a KVH single-axis FOG for yaw rate, and a WHOI Micro-modem for communication, along with other sensor packages. To accommodate the additional sensor payload, a new Delrin nose cone was designed and fabricated. An additional 32-bit embedded CPU hardware was added for data-logging, real-time control, and *in situ* real-time SLAM algorithm testing and validation. Our field testing and collaboration with the TBNMS will provide a validation of the proposed navigation methodologies in a real-world engineering setting, whereas a new museum exhibit on underwater robotics at their visitor center will disseminate the findings and results of this research to the general public.

Acknowledgments

This work is supported in part through grants from the National Science Foundation (Award #IIS 0746455), the Office of Naval Research (Award #N00014-07-1-0791), and an NOAA Ocean Exploration grant (Award #WC133C08SE4089).

References

Anderson, B., Crowell, J. 2005. Workhorse AUV—A cost-sensible new autonomous underwater vehicle for surveys/soundings, search & rescue, and research. In Proc. of the IEEE/MTS OCEANS Conference and Exhibition. pp. 1228-1233. Washington, D.C.: IEEE.

Bailey, T., Durrant-Whyte, H. 2006. Simultaneous localization and mapping (SLAM): Part II. IEEE Robot. Autom. Mag. 13(3): 108-117.

Ballard, R.D. (ed). 2008. Archaeological Oceanography. Princeton, New Jersey: Princeton University Press. 296 pp.

Bourgault, F., Furukawa, T., Durrant-Whyte, H. 2004. Decentralized Bayesian negotiation for cooperative search. In Proc. of the IEEE/RSJ International Conference on Intelligent Robots and Systems. pp. 2681-2686. Sendai, Japan: IEEE.

Durrant-Whyte, H., Bailey, T. 2006. Simultaneous localization and mapping: Part I. IEEE Robot. Autom. Mag. 13(2):99-110.

Eustice, R.M. 2008. Toward real-time visually augmented navigation for autonomous search and inspection of ship hulls and port facilities. In: International Symposium on Technology and the Mine Problem. Monterey, CA: Mine Warfare Association (MINWARA).

Eustice, R.M., Singh, H., Leonard, J.J. 2006a. Exactly sparse delayed-state filters for view-based SLAM. IEEE Trans. Robot. 22(6):1100-1114.

Eustice, R.M., Singh, H., Leonard, J.J., Walter, M.R. 2006b. Visually mapping the RMS Titanic: Conservative covariance estimates for SLAM information filters. Int. J. Rob. Res. 25(12):1223-1242.

Eustice, R.M., Whitcomb, L.L., Singh, H., Grund, M. 2006c. Recent advances in synchronous-clock one-way-travel-time acoustic navigation. In Proc. of the IEEE/MTS OCEANS Conference and Exhibition. pp. 1-6. Boston, MA: IEEE.

Eustice, R.M., Whitcomb, L.L., Singh, H., Grund, M. 2007. Experimental results in synchronous-clock one-way-travel-time acoustic navigation for autonomous underwater vehicles. In Proc. of the IEEE/RSJ International Conference on Intelligent Robots and Systems. pp. 4257-4264. Rome, Italy: IEEE.

Eustice, R.M., Pizarro, O., Singh, H. 2008. Visually augmented navigation for autonomous underwater vehicles. IEEE J. Oceanic Eng. 33(2):103-122.

Fleischer, S. 2000. Bounded-error vision-based navigation of autonomous underwater vehicles. PhD thesis, Stanford University.

Foley, B., DellaPorta, K., Sakellariou, D., Bingham, B., Camilli, R., Eustice, R., Evagelistis, D., Ferrini, V., Hansson, M., Katsaros, K., Kourkoumelis, D., Mallios, A., Micha, P., Mindell, D., Roman, C., Singh, H., Switzer, D., Theodoulou, T. 2009. New methods for underwater archaeology: The 2005 Chios ancient shipwreck survey. J. Hesperia. In press.

Freitag, L., Grund, M., Singh, S., Partan, J., Koski, P., Ball, K. 2005a. The WHOI micro-modem: an acoustic communications and navigation system for multiple platforms. In Proc. of the IEEE/MTS OCEANS Conference and Exhibition. pp. 1086-1092. Washington, D.C: IEEE.

Freitag, L., Grund, M., Partan, J., Ball, K., Singh, S., Koski, P. 2005b. Multi-band acoustic modem for the communications and navigation aid AUV. In Proc. of the IEEE/MTS OCEANS Conference and Exhibition. pp. 1080-1085. Washington, D.C.: IEEE.

Hunt, M., Marquet, W., Moller, D., Peal, K., Smith, W., Spindel, R. 1974. An acoustic navigation system. Woods Hole Oceanographic Institution Technical Report WHOI-74-6.

Kim, A., Eustice, R.M. 2009. Pose-graph visual SLAM with geometric model selection for autonomous underwater ship hull inspection. In: IEEE/RSJ International Conference on Intelligent Robots and Systems. Submitted for publication.

Kinsey, J.C., Eustice, R.M., Whitcomb, L.L. 2006. Underwater vehicle navigation: Recent advances and new challenges. In Proc. of the IFAC Conference on Maneuvering and Control of Marine Craft. Lisbon, Portugal: International Federation of Automatic Control (IFAC).

LCM. 2009. Lightweight Communications and Marshalling. http://code.google.com/p/lcm/ (Accessed April 15, 2009).

Leonard, J., How, J., Teller, S., Berger, M., Campbell, S., Fiore, G., Fletcher, L., Frazzoli, E., Huang, A., Karaman, S., Koch, O., Kuwata, Y., Moore, D., Olson, E., Peters, S., Teo, J., Truax, R., Walter, M., Barrett, D., Epstein, A., Maheloni, K., Moyer, K., Jones, T., Buckley, R., Antone, M., Galejs, R., Krishnamurthy, S., Williams, J. 2008. A perception-driven autonomous urban vehicle. J. Field Robot. 25(10):727-774.

Leveille, E.A. 2007. Analysis, redesign and verification of the Iver2 autonomous underwater vehicle motion controller. Masters thesis, University of Massachusetts Dartmouth.

Milne, P. 1983. Underwater acoustic positioning systems. Houston: Gulf Publishing Company. 284 pp.

Neira, J., Tardos, J. 2001. Data association in stochastic mapping using the joint compatibility test. IEEE Trans. Robot. Autom. 17(6):890-897.

Newman, P.M., Leonard, J.J. 2003. Pure range-only sub-sea SLAM. In Proc. of the IEEE International Conference on Robotics and Automation. pp. 1921-1926. Taipei, Taiwan: IEEE.

Olson, E., Leonard, J.J., Teller, S. 2006. Robust range-only beacon localization. IEEE J. Oceanic Eng. 31(4):949-958.

Ong, L.L, Upcroft, B., Bailey, T., Ridley, M., Sukkarieh, S., Durrant-Whyte, H. 2006. A decentralised particle filtering algorithm for multi-target tracking across multiple flight vehicles. In Proc. of the IEEE/RSJ International Conference on Intelligent Robots and Systems. pp. 4539-4544. Beijing, China: IEEE.

Partan, J., Kurose, J., Levine, B. N. 2006. A survey of practical issues in underwater networks. In: Proc. of the ACM International Workshop on Underwater Networks. pp. 17-24. New York: ACM Press.

Rekleitis, I., Dudek, G., Milios, E. 2003. Probabilistic cooperative localization and mapping in practice. In Proc. of the IEEE International Conference on Robotics and Automation. pp. 1907-1912. Taipei, Taiwan: IEEE.

Ridley, M., Nettleton, E., Sukkarieh, S., Durrant-Whyte, H. 2002. Tracking in decentralised air-ground sensing networks. In Proc. of the IEEE International Conference on Information Fusion. pp. 616-623. Annapolis, Maryland: IEEE.

Roman, C., Singh, H. 2005. Improved vehicle based multibeam bathymetry using submaps and SLAM. In Proc. of the IEEE/RSJ International Conference on Intelligent Robots and Systems. pp. 2422-2429. Edmonton, Alberta, Canada: IEEE.

Smith, S., Kronen, D. 1997. Experimental results of an inexpensive short baseline acoustic positioning system for AUV navigation. In Proc. of the IEEE/MTS OCEANS Conference and Exhibition. pp. 714-720. Halifax, Nova Scotia, Canada: IEEE.

Stewart, W. 1991. Remote-sensing issues for intelligent underwater systems. In Proc. of the IEEE Conference on Computer Vision and Pattern Recognition. pp. 230-235. Maui, HI, USA: IEEE.

Vaganay, J., Elkins, M., Willcox, S., Hover, F., Damus, R., Desset, S., Morash, J., Polidoro, V. 2005. Ship hull inspection by hull-relative navigation and control. In Proc. of the IEEE/MTS OCEANS Conference and Exhibition. pp. 761-766. Washington, D.C.: IEEE.

Walter, M.R., Leonard, J.J. 2004. An experimental investigation of cooperative SLAM. In Proc. of the IFAC/EURON Symposium on Intelligent Autonomous Vehicles. Lisbon, Portugal: International Federation of Automatic Control (IFAC).

Williams, S.B., Dissanayake, G., Durrant-Whyte, H. 2002. Towards multi-vehicle simultaneous localisation and mapping. In Proc. of the IEEE International Conference on Robotics and Automation. pp. 2743-2748. Washington, D.C.: IEEE.

PAPER

Multi-Objective Optimization of an Autonomous Underwater Vehicle

AUTHORS

M. Martz
W. L. Neu
Department of Aerospace and Ocean Engineering, Virginia Tech

ABSTRACT

The design of complex systems involves a number of choices, the implications of which are interrelated. If these choices are made sequentially, each choice may limit the options available in subsequent choices. Early choices may unknowingly limit the effectiveness of a final design in this way. Only a formal process that considers all possible choices (and combinations of choices) can insure that the best option has been selected. Complex design problems may easily present a number of choices to evaluate that is prohibitive. Modern optimization algorithms attempt to navigate a multidimensional design space in search of an optimal combination of design variables. A design optimization process for an autonomous underwater vehicle is developed using a multiple objective genetic optimization algorithm that searches the design space, evaluating designs based on three measures of performance: cost, effectiveness, and risk. A synthesis model evaluates the characteristics of a design having any chosen combination of design variable values. The effectiveness determined by the synthesis model is based on nine attributes identified in the U.S. Navy's Unmanned Undersea Vehicle Master Plan and four performance-based attributes calculated by the synthesis model. The analytical hierarchy process is used to synthesize these attributes into a single measure of effectiveness. The genetic algorithm generates a set of Pareto optimal, feasible designs from which a decision maker(s) can choose designs for further analysis.

Keywords: Genetic Algorithm, Analysis of Alternatives, Synthesis Model, Multi-disciplinary Design Optimization, Autonomous Underwater Vehicle Design

I. Introduction

Traditionally, the autonomous underwater vehicle (AUV) design process has been largely "ad hoc" with designs governed by experience and rules of thumb. Multi-disciplinary design optimization has been increasingly used in conceptual design problems in many fields. Of particular interest here is its use in the ship and aircraft fields (e.g., Neu et al., 2000; Brown and Salcedo, 2003) where a system level approach at the conceptual design stage can yield significant design improvements. The design of any vehicle involves a myriad of choices of design attributes. These choices are inevitably inextricably linked in complicated ways that may bridge the traditional disciplinary breakdown of the design analysis process. These choices are typically made one at a time as the design spiral proceeds sequentially through each disciplinary process until a converged design emerges. Unfortunately, each decision in this sequential process limits the range of possibilities for future decisions, virtually guaranteeing a sub-optimal resulting design. The higher-level or system-level characteristics, such as gross dimensions and characteristics of the major onboard systems, have the greatest influence on the utility or effectiveness of a given design. These are the first to be set and, once set, are the largest limiters of subsequent design choices. The promise of multi-disciplinary design optimization is that if we can identify the range of all of these system-level design choices and if we are able to explore the design space formed by the confluence of any permissible combination of these choices, then we can pick that set of choices, which leads to the "best" design as defined by some chosen criterion. The approach taken for this work is closely modeled after the ship and submarine design work being done at Virginia Tech. The process begins with the construction of a synthesis model for the vehicle being optimized. This model needs to calculate system-level characteristics and capabilities of a particular design from specified vehicle characteristics (the design variables, which are allowed to vary within a permissible range during the process) and design parameters that arise from the environment the vehicle needs to operate in (these remain fixed). A mathematical optimization scheme alters the values of the design variables with the goal of opti-

mizing one or more of the outputs of the synthesis model.

There are many optimization schemes to choose from. Saitou et al. (2005) contained a good overview of the range of schemes currently in use. There are brute-force search schemes (generally intractable because of the size of the resulting calculation), gradient-descent schemes, and population-based schemes, such as genetic schemes or particle swarm schemes, to form an incomplete list. For vehicle design problems, there are almost always a number of constraints to be considered so we dismiss the consideration of unconstrained optimization techniques (although, it is often possible, and indeed often advantageous, to formulate some constraints in terms of objectives). The choice of schemes hinges largely on two factors: the presence of discrete vs. continuous design variables and whether the problem has one or multiple objectives to be optimized. Often, multiple objectives are combined into a single objective by choosing weighting factors according to the importance of each and them summing them into a single value. One usually finds that the a priori choice of these weighting factors is difficult. It is often better to allow the trade-offs between objectives to fall out of the optimization scheme's exploration of the design space through the use of a multi-objective optimization algorithm. Gradient-based schemes are usually the most computationally efficient schemes; however, they rely on design variables being continuous so that those gradients exist. Design variables often represent choices between alternate technologies or a quantity of items to be included in a design and are inherently discrete in nature. The presence of these types of design variables will eliminate gradient-based schemes from consideration unless the discrete variable(s) can be adequately approximated by a continuous quantity as was done by Neu et al. (2000).

The objective attributes or measures of performance (MOPs) considered for this work are cost, risk, and effectiveness. Each design is optimized to maximize effectiveness and minimize both cost and risk. The effectiveness classifications are defined using the U.S. Navy's Unmanned Undersea Vehicle (UUV) Master Plan (U.S. Navy, 2004) as a baseline. The measure of effectiveness is calculated following Brown and Salcedo (2003). Cost is calculated as a sum of material and component costs. Risk is based on a procedure developed by Mierzwicki and Brown (2004) that includes both a probability of occurrence and a consequence level for major risk events. These attributes are different enough from one another that they cannot be rationally combined into a single overall measure.

The process developed herein uses a multiple objective genetic optimization (MOGO) algorithm. This genetic algorithm searches the design space for the set of non-dominated, feasible designs that form the non-dominated frontier called a Pareto front. A non-dominated solution, for a given problem and set of constraints, is a feasible solution for which no other feasible solution exists, which is better in one objective attribute and at least as good in all others. The non-dominated frontier, or Pareto front, indicates optimal trade-offs between multiple, distinct objectives. From this set of designs, decision makers can make an informed choice of a baseline design for further development.

Both the synthesis model and multi-objective optimization are implemented in ModelCenter 8.0 from Phoenix Integration, Inc. ModelCenter is a computer-based design integration environment that includes tools for linking design model components, visualizing the design space, performing trade studies and optimization, developing parametric models of the design space, and archiving results from multiple studies. ModelCenter provides a visual environment in which design processes can be assembled as a series of linked applications with a single interface in order to easily perform multi-disciplinary analysis. It facilitates the communication of data from one application to the next, producing an automated multi-disciplinary design environment. An example optimization for the design of a small AUV used primarily for oceanographic observations is presented.

II. AUV Synthesis Model

A schematic of the model and its data flow is shown in Figure 1. The model is composed of an input module, three primary AUV synthesis model modules, a feasibility (constraint) module, three objective modules, and a genetic algorithm optimization module. The Darwin MOGO plug-in, version 1.2.3, is a genetic algorithm optimization module for ModelCenter

FIGURE 1

AUV synthesis model in ModelCenter.

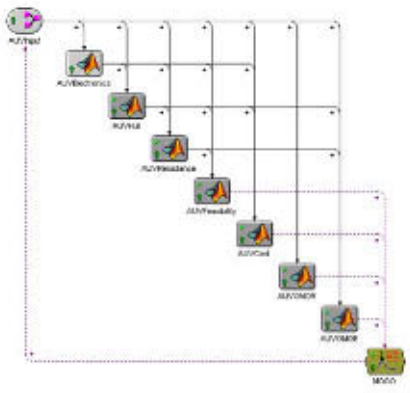

designed to solve engineering optimization problems with multiple objectives and any number of constraints. Darwin is capable of handling both discrete and continuous design variables; however, continuous variables are modeled internally as discrete.

Risk and effectiveness are two relatively abstract objectives that are based largely on expert opinion. The effectiveness of a few concepts can be analyzed using complex models or war-gaming exercises, but for an AUV model that has to rigorously analyze hundreds of models, this is impractical. This synthesis model uses a methodology for calculating the overall measure of effectiveness (OMOE) and the overall measure of risk (OMOR) indices using expert opinion and the analytical hierarchy process (Saaty, 1980) to synthesize diverse inputs such as mission requirements and experience.

A. Input Module

The first module serves one main purpose: to collect the values of the input variables before providing them to specific modules. The values within this module are the design variables (DVs) and design parameters (DPs). The MOGO module output connects as an input to this module, allowing the optimizer to adjust input variables for different designs.

Design parameters and design variables define the environment the AUV operates in and the characteristics of the AUV (respectively). A list of the design parameters is given in Table 1, and a list of the design variables is given in Table 2.

B. Electronics Module

The electronics module computes the overall electrical power requirements. First, non-payload power consumption is calculated by summing individual components based on individual voltages and current requirements. This value is then combined with the payload consumption to obtain the maximum functional load.

The maximum functional load is not the average load that the components will encounter. It is used so that a conservative estimate of range and lifetime of the AUV can be considered. In a similar manner to the maximum functional load, the module also calculates the total power available. The module calculates the "port feasibility" for the feasibility module because of a limitation of ModelCenter. Port feasibility assesses whether or not the electronics and payload packages of the AUV have enough of the right kind of data ports.

TABLE 1

Design parameters used in the AUV synthesis model.

DP Name	Description
PC	Propulsive coefficient
Eta	Motor efficiency
Vsmin	Minimum sprint speed (knots)
Vsgoal	Goal sprint speed (knots)
Vemin	Minimum endurance speed (knots)
Vegoal	Goal endurance speed (knots)
MinDuration	Minimum duration at endurance speed (hours)
GoalDuration	Goal duration at endurance speed (hours)
MinBallast	Minimum ballast mass (kg)
GoalBallast	Goal ballast mass (kg)
PR	Performance risk weight
SR	Schedule risk weight
CR	Cost risk weight
EW1	Effectiveness weight (ISR)
EW2	Effectiveness weight (oceanography)
EW3	Effectiveness weight (CN3)
EW4	Effectiveness weight (mine countermeasures)
EW5	Effectiveness weight (anti-submarine warfare)
EW6	Effectiveness weight (inspection/identification)
EW7	Effectiveness weight (payload delivery)
EW8	Effectiveness weight (information operations)
EW9	Effectiveness weight (time critical strike)
EW10	Effectiveness weight (sprint speed)
EW11	Effectiveness weight (endurance speed)
EW12	Effectiveness weight (endurance duration)
EW13	Effectiveness weight (ballast/expandability)

TABLE 2

Design variables used in the AUV synthesis model.

DV Name	Description
D	Vehicle diameter
LtoD	Length-to-diameter ratio
nf	Forward shape coefficient
na	Aft shape coefficient
Ve	Endurance speed
CommConf	Communication configuration
PayConf	Payload configuration
PropConf	Propulsion configuration
BatConf	Battery configuration
ElecConf	Electronics configuration
WallType	Hull wall thickness/material

C. Hull Geometry and Arrangement Module

An axisymmetric teardrop hullform with parallel mid-body was selected for use. The advantages of the axisymmetric hull are its producibility, low resistance, and structural efficiency. The hullform model is based on the MIT hull model (Jackson, 1992) shown in Figure 2 where

$$\begin{aligned} Y_f &= D/2\left[1-\left(X_f/L_f\right)^{n_f}\right]^{1/n_f} \\ Y_a &= D/2\left[1-\left(X_a/L_a\right)^{n_a}\right] \end{aligned} \tag{1}$$

In equation (1), n_f and n_a are the forward and aft shape coefficients. They are used as DVs in the synthesis model, and they adjust the fullness of the forward and aft sections. This module assigns the length of the forward and aft sections each to be 25% of the overall length, with the parallel mid-body being the remaining 50%.

The hull code does a preliminary arrangement of hull items using a "box stacking" algorithm developed for this synthesis model. It begins by ensuring the components are aligned in the appropriate direction, with the longest dimension in line with the longitudinal direction and the second largest dimension aligned with the beam direction. Components are then sorted by weight, with the heaviest objects being placed first. Objects are always placed as low as possible in the AUV. If the first object placed leaves room below it for the second object, the second object will be placed below it. The MATLAB function "inpolygon" is used to ensure that two objects do not occupy the same space.

Once the first section area is filled, the code steps forward in the AUV to the next free space. If object 1 is the longest object of the group and is 30 cm long, then the code steps forward 30 cm and tries to start another object at its end. This process repeats (while checking to make sure nothing overlaps) until all of the objects are placed. With all of the objects placed, the code finds the total length (or "compressed length") of the objects. The feasibility module compares this length with the length of the vehicle (see Section II.E).

FIGURE 2

Hull model with a parallel mid-body (Jackson, 1992).

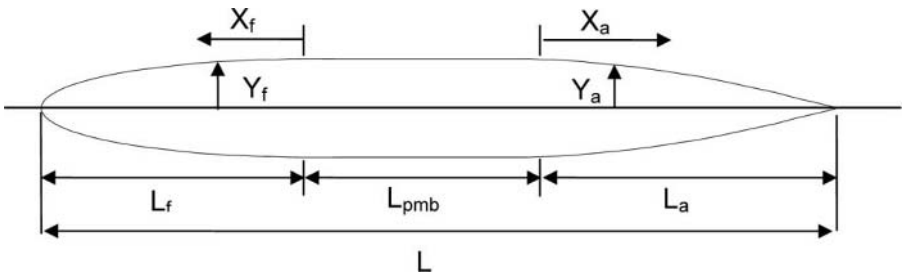

D. Resistance Module

This module calculates resistance, speed, and endurance. The total resistance of the AUV is estimated based on the shape of its hull. Resistance is calculated for fully submerged conditions only. The bare hull power is then calculated, and the shaft power is determined.

The bare-hull skin friction coefficient, C_f, is found from the 1957 ITTC line (Lewis, 1988)

$$C_F = \frac{0.075}{\left(\log_{10}R_n - 2\right)^2} \tag{2}$$

where R_n is the Reynolds number based on the length of the AUV. The coefficient of viscous resistance for the smooth bare hull is then found using equation (3) from Gillmer and Johnson, 1982

$$C_{V_{BH}} = C_F\left[1 + 0.5\left(\frac{1}{LtoD}\right)^{1.5} + 3\left(\frac{1}{LtoD}\right)^{3}\right] \tag{3}$$

where *LtoD* is the length-to-diameter ratio. From this, the effective power, *PE,* and shaft power, *PS,* can be calculated

$$PE = \frac{\rho V^3}{2}[(C_{V_{BH}} + C_A)S_{BH} + \Sigma C_{V_{AP}} S_{AP}]$$

$$PS = PE/PC \tag{5}$$

where ρ is the density of water, V is the velocity, C_A is the roughness allowance for full-scale resistance estimates made without model tests, S_{BH} is the bare-hull surface area, PC is the propulsive coefficient, and C_{VAP} and S_{AP} are the appendage viscous coefficient and surface areas, respectively. It is common to use a value of 0.0002 for C_A. C_{VAP} and S_{AP} are found using either experimental data or computational fluid dynamics calculations.

This process is then used in reverse to calculate the maximum speed of the vehicle, given the maximum effective power output of the motor. The *PS*, *PE*, and R_n are all functions of the velocity. *PS* is compared to the effective power output of the motor (motor rating times efficiency of motor). The speed at which these two values match is the sprint speed of the AUV.

E. Feasibility Module

Characteristics such as speed, range, duration, ballast, etc., are all examined to determine feasibility. In order for a specific design to be feasible, all feasibility ratios must be greater than zero and in some circumstances be below a certain threshold. Feasibility ratios are defined as

$$FR = \frac{C - C_{\min}}{C_{\min}} \tag{6}$$

where C is the constraint in question and C_{min} is the minimum for that constraint. The module returns values of the various comparisons, demonstrating which aspects of the design are feasible and which are not. Table 3 is a list of the constraints considered by this module. F_TL, the total length constraint, and F_TB, the total ballast constraint, also have upper bounds. F_TL requires the total compressed length of the AUV to be less than 80% of the length of the AUV overall. F_TB requires that the density of the total ballast must be below the density of brass, or 8750 kg/m^3. This ensures that a reasonable material will be used to ballast the AUV.

F. Cost Module

This module calculates the total component purchase cost. Materials cost is included in this calculation. Man-hours and development time are not included. The basic cost of construction (BCC) is the output of this module. It is calculated by taking the sum of the cost of components plus the materials cost:

$$BCC = 6W_{cap}(2.952) + AV_{mid}^{1+B} + \Sigma C_i$$

where W_{cap} is the end cap weight, V_{mid} is the midsection volume, and A and B are the constants, which were found to fit the material type with its cost per volume. C_i is the component cost.

G. Overall Measure of Risk Module

The risk module calculates the OMOR. The calculation considers three types of technology risk: performance, cost, and schedule. Summing these three values of risk for applicable risk events and multiplying each type of risk by its associated weight factor result in the OMOR. Weight factors were determined using an analytical hierarchy process (Saaty, 1980).

The OMOR function's purpose is to provide a quantitative measure of technology risk for a specific design based on the selection of components. These components are specified by DVs in Table 2. The calculation of the value of risk for any given variable, R_i, is the probability of failure, P_i, multiplied by the consequence of said failure, C_i.

Risk events are associated with specific design variables. P_i and C_i are estimated using Table 4 and Table 5. In order to be considered in the risk factors, the event must have a major impact on performance, cost, or schedule.

TABLE 3

Constraints used in the AUV synthesis model.

Name	Description
F_TB	Total ballast requirement
F_BW	Ballast weight requirement
F_VE	Endurance speed requirement
F_TL	Total length requirement
F_ED	Endurance duration requirement
F_PR	Port availability requirement
F_VS	Sprint speed requirement

TABLE 4

Event probability estimate.

Probability	What is the Likelihood this Event will Occur?
0.1	Remote
0.3	Unlikely
0.5	Likely
0.7	Highly likely
0.9	Near certain

TABLE 5

Event consequence estimate.

Consequence	Given the Risk is Realized, What is the Magnitude of Impact?	
Level	*Performance*	*Schedule*
0.1	Minimal or no impact	Minimal or no impact
0.3	Acceptable with some reduction in margin	Additional resources required; able to meet dates
0.5	Acceptable with significant reduction in margin	Minor slip in key milestones; not able to meet need date
0.7	Acceptable; no remaining margin	Major slip in key milestone or critical path impacted
0.9	Unacceptable	Cannot achieve key team or major program milestone

Each event is then documented with its given value of risk and associated design variable or variables. Values for weight (W_{pe}, W_{sc}, and W_{co}) were given to the three types of risk according to a pair-wise comparison by expert opinion on the subject. The value for the OMOR is determined as

$$OMOR = W_{pe}\frac{\sum P_i C_i}{\sum_i (P_i C_i)_{\max}} + W_{sc}\frac{\sum P_j C_j}{\sum_j (P_j C_j)_{\max}} + W_{co}\frac{\sum P_k C_k}{\sum_k (P_k C_k)_{\max}} \quad (8)$$

The weight factors and risk register are given in Section III.B.

H. Overall Measure of Effectiveness Module

This module calculates the OMOE for a specific design based on its measures of effectiveness (MOEs). The OMOE function must include all important effectiveness/performance attributes, both discrete and continuous, and must ultimately be used to assess an unlimited number of AUV alternatives. Expert opinion and the analytical hierarchy process (Saaty, 1980) are used to integrate these diverse inputs and assess the value or utility of the AUV MOEs.

MOEs critical to AUV missions are identified with goal and threshold values for each. The MOEs are organized into an OMOE hierarchy, and weights are found for each using pair-wise comparison and the analytical hierarchy process. The weights for each MOE are used in the OMOE function:

$$OMOE = \sum_{i=1}^{9}\left[\frac{\sum MOE_j}{\sum (MOE)_{\max}} W_i\right] + \sum_{i=10}^{13} W_i MOE_i \quad (9)$$

where the MOE_j are pre-determined component MOEs for the nine areas identified by the UUV Master Plan (U.S. Navy, 2004). The MOE_i for i = 10 to 13 are calculation-based MOEs related to speed, duration, and expandability. These are evaluated based on goals and thresholds set for each attribute. If the calculated attribute is below the threshold, it is given an MOE value of 0, or if it is equal to or greater than the goal, it is given an MOE of 1.0. Values in between the threshold and goal are scaled between 0 and 1. Goals are considered the point of diminishing return. Designs with attribute calculations greater than the goals do not provide an added benefit because the MOE will not go above 1.0. These goal and threshold values are design parameters.

I. Discussion of the Synthesis Model

The synthesis model developed here is still quite crude. Many additions and improvements could be made but always at the cost of added computational time. For example, the arrangement algorithm could arrange the entire AUV and also adjust the placement of objects to optimize the center of gravity (which also contributes to the controllability of the AUV).

Propeller design and optimization could be integrated directly into the resistance module of the synthesis model. Two approaches are the most likely to be implemented. Approach 1 would optimize the propeller for the AUV's sprint speed and endurance velocity. Approach 2 would have a database of propellers, and the propeller would be a part of the configuration files. Approach 1 would be more computationally intensive than Approach 2.

Computational Fluid Dynamics (CFD) could be used to provide better power and drag estimates. An analysis that could assist in the evaluation and ranking of vehicle dynamics and control could possibly be done. The major drawback with computational fluid dynamics is that it is computationally intensive and likely would not allow for realistic development times. A way around this issue is to use response surface calculations as a

surrogate for a complete CFD analysis of each design. This would involve performing the CFD analysis for a range of designs spanning the design space and fitting a mathematical model (the response surface) to approximate the results for the rest of the design space (or a portion thereof). Controls design/analysis is a major component of AUV design. Controllability of the AUV could tie into the risk and/or effectiveness of the AUV.

Structural analysis is another AUV design component that is lacking. The depth attainable by a particular design is unknown in the present model and may be very important to decision makers. Finite-element models could be used in the structural analysis, but this would also increase the computation time for each model. Response surface models could also be used for the structural analysis, but it may be easier to develop a model based on structural weight and attainable depth. Depth attainability could be integrated into both the risk and effectiveness MOPs.

III. Example Optimization Run

In the following, the framework discussed above is applied to the design of a small AUV used primarily for oceanographic observations. The intended use is determined from expert interviews and incorporated into the optimization through the effectiveness weights that are determined from this input.

A. Component Specification

Components are the working parts of the AUV, whether they are electrical or mechanical in nature. There are three tab-delimited input files associated with the components: Input.txt, Config.txt, and OMOE.txt.

The "Input.txt" file is a master database of all of the components. It stores all of the component characteristics, which include the following:

- Component name
- Component type
- Payload
- Propulsion
- Electronic
- Power
- Communications
- Component number
- Voltage required
- Negative value if it receives
- Positive value if it provides
- Current used/provided
- Port availability
- Negative value if it needs
- Positive value if it provides
- Ports:
- USB
- Firewire
- RS-232
- RS-485
- SPI
- I2C
- 1-wire
- Bluetooth
- 802.11 a/b/g/n (Wi-Fi)
- Ethernet
- Fiber optic
- Component mass (in kg)
- Component X, Y, and Z, dimensions
- Components center of gravity locations (X, Y, and Z directions)
- Location in the AUV
- Nose
- Midsection
- Tail
- External
- Propulsion (motor rating)
- Added drag (input as * *SAP*, see Section II.D)
- Component cost

The "Config.txt" file organizes the components into configuration lists. It is separated by component type (payload, propulsion, electronics, power, communications) and assigns component numbers to configuration numbers. For example, payload configuration 1 might use components 1, 3, and 5, whereas payload configuration 2 uses components 2 and 4.

The 'OMOE.txt' file includes the effectiveness and risk registers for the component configurations. For each component type configuration (e.g., payload configuration 1, power configuration 3, etc.), the "OMOE.txt" file stores the nine effectiveness ratings from the UUV Master Plan (U.S. Navy, 2004) and three risk types. The risk and effectiveness values were judged by expert opinion.

B. Optimization Initialization

Design parameters are generated by the decision makers and define the characteristics about how the AUV operates and the environment it operates in. The risk and effectiveness weights are design parameters and have a large effect on how and if a particular AUV design will survive to the next generation of the genetic optimization. Table 6 gives the values of the DPs used for this analysis. They were chosen based on expert experience and opinion.

The effectiveness importance and the risk importance, also based on a survey of experts, are broken down according to Figures 3 and 4, respectively.

Design variables make up the DNA of the AUV design. The MOGO varies with each DV between its lower and upper bounds. Table 7 lists the lower and upper bounds considered for this optimization run.

Figure 5 is the optimization parameter window used by the Darwin MOGO module. For this analysis, a population size of 200 was chosen.

TABLE 6

Design parameter initialization.

DP Name	Value	Description
PC	0.6	Propulsive coefficient
Eta	0.9	Motor efficiency
Vsmin	5	Minimum sprint speed (knots)
Vsgoal	6	Goal sprint speed (knots)
Vemin	2.5	Minimum endurance speed (knots)
Vegoal	4	Goal endurance speed (knots)
MinDuration	4	Minimum duration at endurance speed (hours)
GoalDuration	6	Goal duration at endurance speed (hours)
MinBallast	0	Minimum ballast mass (kg)
GoalBallast	0	Goal ballast mass (kg)
PR	0.47956	Performance risk weight
SR	0.11496	Schedule risk weight
CR	0.40548	Cost risk weight
EW1	0.19928	Effectiveness weight (ISR)
EW2	0.17499	Effectiveness weight (oceanography)
EW3	0.10284	Effectiveness weight (CN3)
EW4	0.028626	Effectiveness weight (mine countermeasures)
EW5	0.023392	Effectiveness weight (anti-submarine warfare)
EW6	0.019135	Effectiveness weight (inspection/identification)
EW7	0.019135	Effectiveness weight (payload delivery)
EW8	0.066494	Effectiveness weight (information operations)
EW9	0.017981	Effectiveness weight (time critical strike)
EW10	0.083953	Effectiveness weight (sprint speed)
EW11	0.099519	Effectiveness weight (endurance speed)
EW12	0.15633	Effectiveness weight (endurance duration)
EW13	0.0083279	Effectiveness weight (ballast/expandability)

FIGURE 5

Genetic algorithm optimization parameters used for the example run.

It was decided to preserve 50 designs as parents for the next generation. The convergence method chosen was to allow the model to go 50 generations without improvement before stopping.

C. Optimization Results

The entire final generation from the optimization of the small, oceanographic observation AUV is shown in Figure 6. Figure 6 is a three-dimensional view of the objective function space, and each point on the figure represents a different AUV design. The gray points are infeasible

FIGURE 3

Effectiveness importance breakdown. (Color versions of figures available online at: http://www.ingentaconnect.com/content/mts/mtsj/2009/00000043/00000002.)

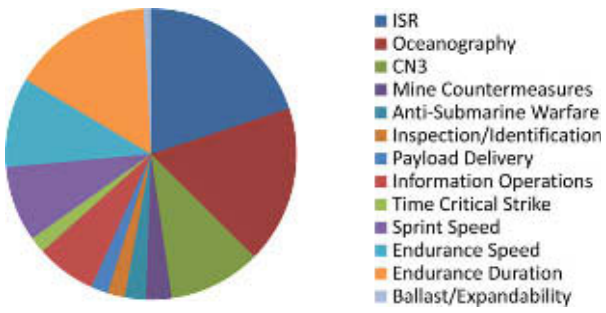

FIGURE 4

Risk importance breakdown.

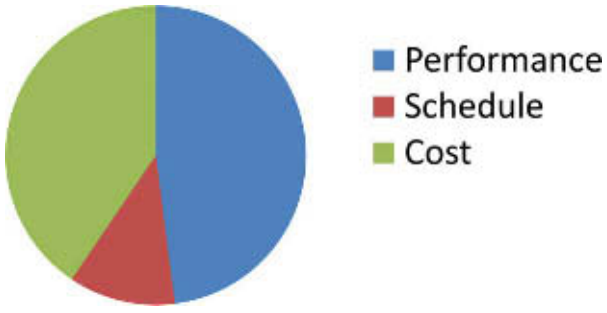

TABLE 7

Design variable initialization.

DV Name	Lower	Upper	Description
D	0.05	1.0	Vehicle diameter (m)
LtoD	1.0	20.0	Length-to-diameter ratio
nf	2.0	2.5	Forward shape coefficient
na	2.5	3.0	Aft shape coefficient
Ve	2.0	5.0	Endurance speed
CommConf	1	1	Communication configuration
PayConf	1	12	Payload configuration
PropConf	1	9	Propulsion configuration
BatConf	1	8	Battery configuration
ElecConf	1	3	Electronics configuration
WallType	1	4	Hull wall thickness/material

designs. The optimization algorithm retains infeasible points within a specified tolerance of satisfying a constraint in order to keep desirable features of these designs in the population. Figure 7 shows only the non-dominated, feasible designs from this final generation. These points form an approximation of the Pareto front.

Figures 8, 9, and 10 compare the three MOPs against one another. The graphs have one MOP on each of the two axes and are colored based on the third unused MOP. The Pareto designs are highlighted using black plus signs.

The Pareto designs show that, generally, as cost and risk go up, the effectiveness also goes up. This trend is stronger for cost than for risk as can clearly be seen in the two-dimensional plots presented. The relationship, among the Pareto designs, is strongest between cost and effectiveness, and that between cost and risk is less well defined.

"Knees" in the Pareto front indicate possibly attractive designs. "Knees" are the locations on the Pareto front where significant changes in the slope occur. For example, two trend lines have been added to Figure 8, which indicate the relative slope of the Pareto front. The location where the two trend lines intersect would be a "knee" in the curve. Along the blue line, the additional cost per unit of additional effectiveness is small compared to that along the red line. The following section uses this method to pick candidate AUV designs from among the generated Pareto designs.

D. Comparison of Designs from the Pareto Front

The five Pareto designs highlighted in Figure 11 were chosen to com-

FIGURE 6

Entire final population in objective function space. Infeasible designs are in grey.

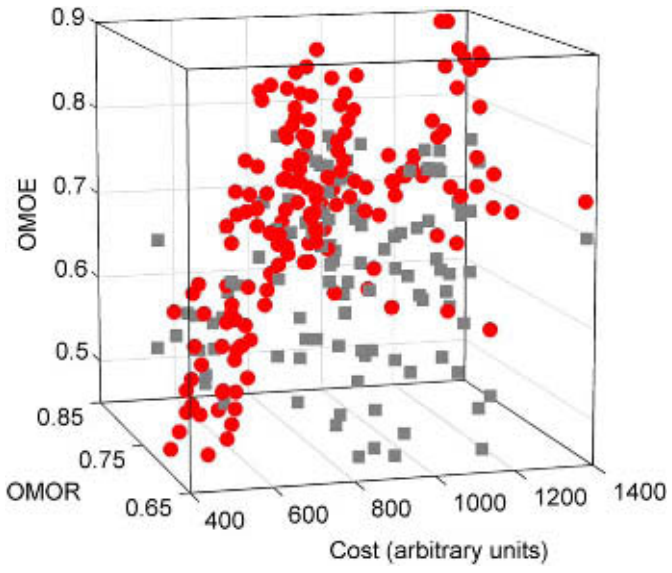

FIGURE 7

Non-dominated, Pareto designs from the final population.

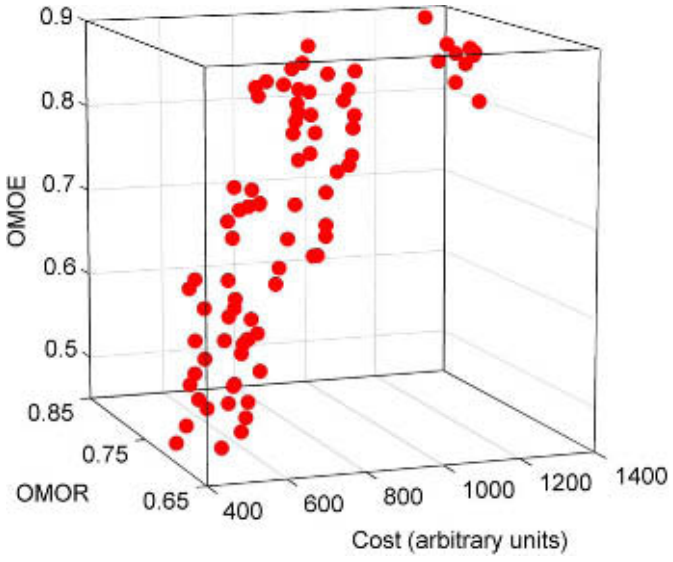

FIGURE 8

Effectiveness vs. cost of the final generation designs. Risk is colored blue (low) to red (high), and the Pareto designs are highlighted. Trend lines are added to indicate a 'knee' in the Pareto front.

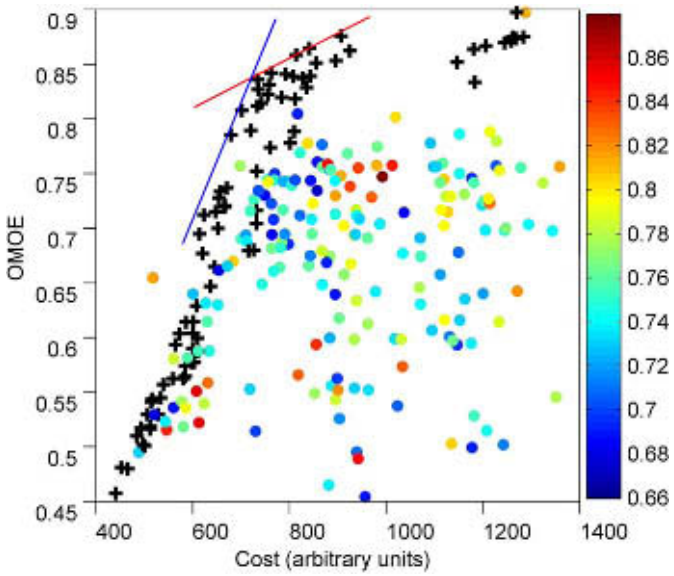

FIGURE 9

Risk vs. cost of the final generation designs. Effectiveness is colored blue (low) to red (high), and the Pareto designs are highlighted.

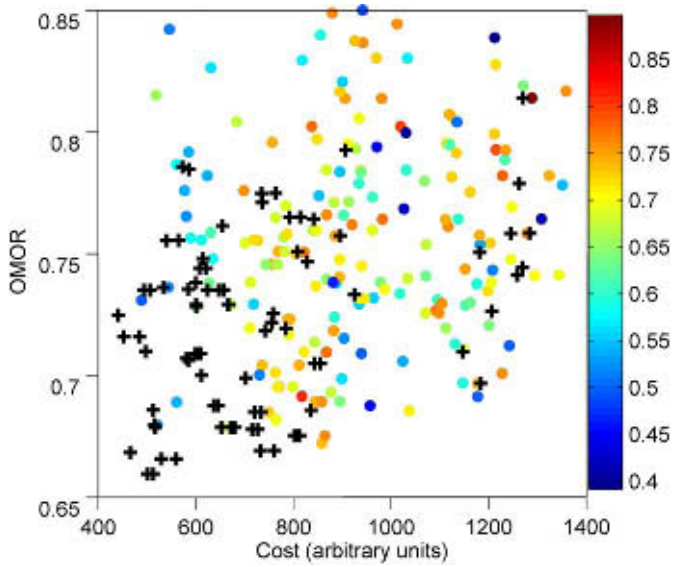

pare and analyze. Table 8 gives the traits that caused them to be chosen and their MOP and constraint results. The extremes for each of the MOP and constraint values among the chosen designs are highlighted green and red for best and worst, respectively. Table 9 gives the values of their DVs.

The values of some of the design variables of the five selected designs are similar, and others are quite dissimilar. The diameters are all approximately 0.11 m. The length-to-diameter ratios have a larger range, going from 8.02 to 11.21. The aft shape coefficients, n_a, vary somewhat but remain toward the lower end of the possible range. The forward shape coefficients, n_f,

FIGURE 10

Effectiveness vs. risk of the final generation designs. Cost is colored blue (low) to red (high), and the Pareto designs are highlighted.

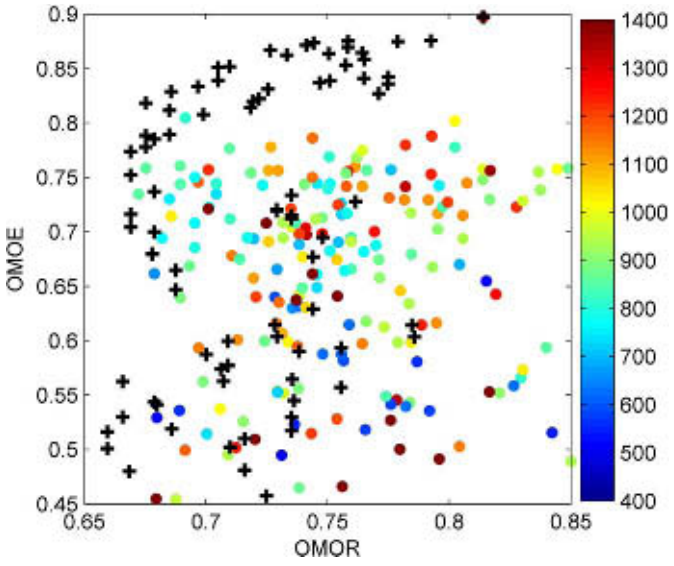

FIGURE 11

Designs selected among the Pareto set for analysis and comparison.

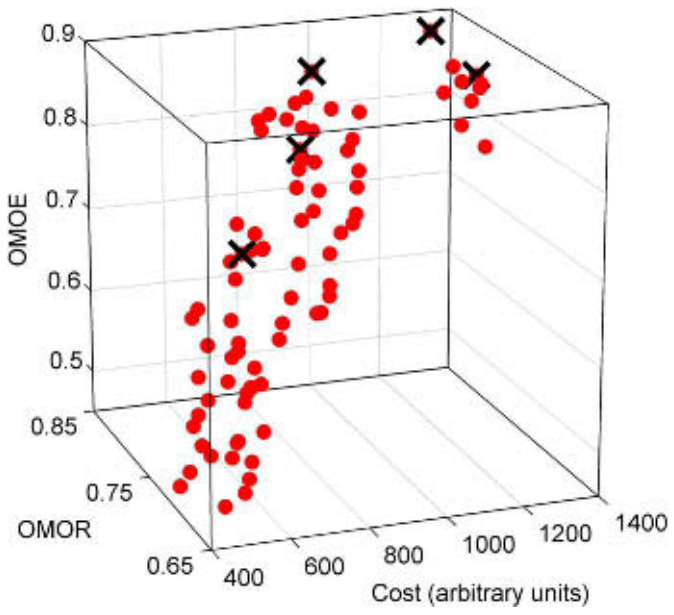

TABLE 8

Traits, measures of performance, and constraint values for the selected Pareto designs.

Design	**33**	**56**	**72**	**82**	**83**
Trait	*Best cost*	*Best OMOR*	*Knee*	*Best OMOE*	*Highest cost*
OMOE	0.712	0.831	0.876	0.897	0.875
OMOR	0.735	0.726	0.793	0.814	0.758
BCC	624	759	907	1270	1284
F_TB	331	359	349	350	126
F_BW	2.15	2.83	2.49	2.49	0.65
F_TL	0.638	0.472	0.683	0.680	0.755
F_VE	0.52	0.6	0.64	0.64	0.44
F_VS	1.14	2.05	3.55	3.54	3.77
F_PR	1.5	0.667	0.667	1.667	1.667
F_ED	0.843	0.642	0.554	0.551	0.896

are more diverse than the aft shape coefficients but also remain toward the lower end of the possible range.

The component configurations are diverse. No two designs had the same component configurations. All designs used the same communications payload. Payload and battery configurations have two sets of repeating configurations. The designs with the best OMOE all use the most powerful motors available in the component database, and the battery configurations are the batteries with the highest capacity. The electronic component configuration was fairly diverse, considering there are only three electronic configurations available to choose from.

The wall types are not all the same. Four of the five designs used the 0.0625-in. thick polycarbonate material because it was the cheapest. This synthesis model does not account for structural strength, which would have an effect on material selection, but if it did, Design 83 would have a thicker hull.

TABLE 9

Values of design variables for the selected Pareto designs.

Design	**33**	**56**	**72**	**82**	**83**
D (m)	0.11	0.11	0.12	0.12	0.11
LtoD	9.4	11.21	8.02	8.06	8.3
nf	2.18	2.0	2.21	2.22	2.04
na	2.68	2.6	2.5	2.5	2.6
Ve (knots)	3.8	4	4.1	4.1	3.6
CommConf	1	1	1	1	1
PayConf	1	3	4	4	3
PropConf	3	6	9	9	9
BatConf	1	1	3	3	3
ElecConf	3	1	1	2	2
WallType	1	1	1	1	2

Design 72 has MOPs that fall in the midrange of the five selected designs. The only major difference in its design variables is the Payload, Propulsion, and Battery configurations. It also has less expandability (fewer data ports available).

Design 56 has the highest ballast weight of all the designs, but it also has the highest risk and second slowest sprint speed. A mass of 2.83 kg is required to ballast this vehicle, but this mass could take the form of additional payload. It should be noted, however, that because of the choices made on the desired characteristics of the optimum AUV, very little effectiveness weight was given to expandability. It is the longest AUV, which causes the compressed length feasibility constraint to be the lowest. This might infer that this would be the easiest design to arrange.

Design 33 has the lowest cost and second lowest risk but is the least effective design. It also has the second slowest endurance speed of the five selected designs.

Design 82 has the highest effectiveness of the five chosen designs, but it also has the highest risk. It has 2.49 kg of ballast weight available for additional payload, and it also has the greatest number of ports available for payload. This design has the lowest endurance duration but a good sprint speed.

Design 83 has the highest cost but also has the highest sprint speed. Because of the thicker hull, it has the least amount of ballast weight available. It, along with Design 82, does have the most ports available, but

arrangement may be a factor because the hull arrangement algorithm calculated this design to have the worst compressed length among the five chosen. It has the F_TL closest to 80% of the total overall length, which is the upper bound for the constraint. So it has the port availability, but payloads to use the ports may not fit inside the hull.

With the potential designs chosen, it is now up to the decision maker(s) to choose the design that best fits their preferences. The MOPs need to be carefully weighed against the vehicle attributes, which include the DVs and the results of the feasibility/constraint analysis. The decision maker(s) also need to take into account the limitations of the model with respect to the structural performance of the AUV and the controllability of the AUV. Both are beyond the scope of this project.

Although the design optimization process may provide an intelligent filtering of the broad range of options presented by the design space, it is not a substitute for sound engineering judgment. The authors' favorite choice is Design 72, the "knee" design. It offers a good blend of cost, capability, and risk. It would be prudent, however, to choose several designs for a more detailed analysis before a final decision is made. In addition to the characteristics discussed above, the design variable choices used in this design include a number of specific components. Those components include an acoustic modem, an RF modem, an acoustic transducer and an RF antenna, an attitude and heading reference system, a GPS, a depth sensor, and a standard CPU with a serial expansion board and an analog input board. Propulsion and power components include a 1666-W brushless electric motor, a gear box, a motor controller, four fin actuation servos and a servo controller, one 12-V 8 A-hr battery stack, one 24-V 5 A-hr battery stack, and a power controller board.

E. Design Variable Study

ModelCenter has a built-in data explorer that includes a Variable Influence Profiler. A part of this profiler is the Main Effects plot, which can be drawn for each design parameter. It shows quantitatively how the selected output variable changes (on average) as each design parameter is varied from its lower bound to its upper bound. The influence of all the other design parameters is averaged out. The designs from the last generation available are used for this analysis. Table 10 shows how each of the design variables affects each of the MOPs of the AUV.

The length-to-diameter ratio, *LtoD*, and propulsion configuration are the primary items that affect the effectiveness of the AUV. These two variables both affect the speed and duration aspects of the OMOE. *LtoD* has an effect on the resistance of the AUV. The propulsion configuration selects the motor to be used, which can affect the sprint speed and endurance duration.

The electronics configuration is the primary DV that affects the risk of the AUV. The DVs having the next greatest effect on risk are the diameter, length-to-diameter ratio, and the propulsion configuration. The diameter and length-to-diameter ratio can affect what electronic components could fit into the AUV. The component configurations are the only things associated with risk, and the electronic and propulsion configurations have the highest potential risks associated with them. The other DVs may force or eliminate the selection of certain components because of size or weight constraints.

Diameter, length-to-diameter ratio, and the wall type are the three major DVs that drive the cost, accounting for 62% of the main effect of cost. This would imply that the hull material and cost of material are the principle contributors. Large diameters and length-to-diameter ratios would lead to the requirement of more hull material, which would lead to a greater cost.

TABLE 10

Percentage of the variation in each MOP attributable to each DV.

Design	OMOE	OMOR	BCC
D (m)	10	**17**	**27**
LtoD	**20**	**16**	**18**
nf	3	2	9
na	10	12	2
Ve (knots)	11	6	0
CommConf	0	0	0
PayConf	10	3	8
PropConf	**19**	**17**	13
BatConf	7	3	2
ElecConf	6	**23**	4
WallType	5	1	**17**

IV. Conclusions

The goal of the concept design process is to identify non-dominated concepts so the decision makers can base their selection on the objective attributes. There should be no bias for particular vehicle characteristics. Vehicle characteristics are only parameters that lead to the calculation of the objective attributes of the AUV.

Multi-disciplinary design optimization is essential for the design of highly integrated systems, such as AUVs, because it integrates multiple

disciplines so that effective system-wide decisions can be made. The optimal system design is often something unique or non-intuitive, and the use of MDO increases the confidence that the optimal combination of design variables has been used to achieve the best design possible.

The use of an optimizer to efficiently search the design space has an obvious advantage over using a systematic or random brute-force approach. Genetic algorithms are most appropriate to the optimization of designs, which require discrete choices such as the AUV design considered here.

Multiple objective problems yield a set of non-dominated designs. Once this set has been generated, it is the job of the decision makers to choose potential candidates for further evaluation. The synthesis model and optimizer do the heavy lifting of the analysis work cutting down millions of design combinations into tens of designs in the form of a Pareto front. Looking at the "knees" in the Pareto front allows the decision makers to narrow this down even further. Once a set of candidate designs have been identified, their design details can be refined beyond the basic level of the synthesis model used for the optimization. Additional analysis and experience should then be applied to arrive at a final choice of design.

Each of these points has been illustrated in this paper through the application of this design optimization process to a hypothetical AUV design. A simple synthesis model was constructed, which illustrated the process. Methods of formulating overall MOEs and risk were presented. These, along with a cost measure, served as objectives of the optimization.

An example optimization calculation was formulated and executed. The results of the process are documented, and the process by which candidate designs can be chosen from among the Pareto set is illustrated by example. Five candidate designs are chosen, and their defining characteristics are discussed.

References

Brown, A., Salcedo., J. 2003. Multiple objective genetic optimization in naval ship design. Nav. Eng. J. 115(4): 49-61.

Gillmer, T.C., Johnson., B. 1982. Introduction to Naval Architecture, 2nd print with revisions. Annapolis, MD: U.S. Naval Institute Press.

Jackson, H. A., 1992. MIT Professional Summer Course "Submarine Design Trends".

Lewis, E. V., ed. 1988. Principles of Naval Architecture, 2nd revision. Jersey City, NJ: Society of Naval Architects and Marine Engineers.

Mierzwicki, T., Brown, A. 2004. Risk metric for multi-objective design of naval ships. Nav. Eng. J. 116(2): 55-71.

Neu, W. L., Mason, W.H. , Ni, S. , Lin, Z., Dasgupta, A. , Chen, Y. 2000. A multidisciplinary design optimization scheme for containerships. In: 8th AIAA/USAF/NASA/ISSMO Symposium on Multidisciplinary Analysis and Optimization, Long Beach, CA, AIAA-2000-4791. Reston, VA: American Institute of Aeronautics and Astronautics.

Saaty, T.L. 1980. The Analytic Hierarchy Process, Planning, Priority Setting, Resource Allocation. New York: McGraw-Hill. 287 pp.

Saitou, K., Izui, K., Nishiwaki, S., Papalambros., P. 2005. A survey of structural optimization in mechanical product development. J. Comput. Inf. Sci. Eng. 5: 214-226.

U.S. Navy. 2004. The Navy Unmanned Undersea Vehicle (UUV) Master Plan. http://www.navy.mil/navydata/technology/uuvmp.pdf (accessed 14 May 2009).

PAPER

Design Requirements for Autonomous Multivehicle Surface-Underwater Operations

AUTHORS

Brian S. Bingham
University of Hawaii at Manoa

Eric F. Prechtl
Axis Engineering Technologies, Inc.

Richard A. Wilson
Aurora Flight Sciences Corporation

ABSTRACT

Future autonomous marine missions will depend on the seamless coordination of autonomous vehicles: unmanned surface vehicles (USVs), unmanned underwater vehicles (UUVs) and unmanned aerial vehicles (UAVs). Such coordination will enable important inter-vehicle applications such as autonomous refueling, high-throughput data transfer and periodic maintenance to extend the mission length. A critical enabling capability is the autonomous capture, retrieval and deployment of a UUV from a USV platform. As a first step toward solving this problem, we propose a performance specification that quantifies the necessary motion compensation required to safely and reliably operate a USV and UUV in concert in the dynamic marine environment. To accomplish this, we use a model-based approach to predict the motion of typical vehicles under the influence of the same sea conditions. We summarize the predictions succinctly using a scalar performance metric, the *peak-to-peak vertical displacement*, as a function of vehicle type, sea-state and vehicle formation.

To substantiate this model-based approach experimentally, we present sea-trial data and compare the empirical observations to model predictions. The results show that although simple three degree-of-freedom models do not capture the full complexity of an actual six degree-of-freedom ship motion, they can prove expedient in an engineering context for quantifying the design requirements of a USV-UUV capture, deployment and retrieval system.

Keywords: USV, UUV, sea-state, vehicle dynamics, Pierson-Moskowitz spectrum

Introduction

Soon, unmanned surface vehicles (USVs) will autonomously capture, recover and deploy unmanned underwater vehicles (UUVs), creating a heterogeneous vehicle network. The Navy has already voiced a need for this capability. The current USV Master Plan calls for moving beyond the situation where, "today's fielded autonomous systems consist of individual vehicles that provide data for follow-on decision making." Instead, "future USV systems may deploy UUVs to gain the advantage of higher area coverage rates through multiple, simultaneous operations" (U.S. Navy, 2007).

The ability of a USV to autonomously capture, recover and deploy a UUV is a foundational technology, enabling a variety of mission-specific applications. For example, UUVs of today operate with limited endurance. In the future, UUVs will autonomously refuel from the nearest USV. As endurance limits expand, maintenance and repair requirements will become the binding constraints to UUV mission length. Autonomous maintenance and repair are one way of addressing this constraint, and a critical enabling technology will be UUV capture, recovery and deployment from a USV platform. Another example that could leverage autonomous deployment and recovery capabilities is the mine countermeasure mission. The Navy envisions both "remotely operated vehicle (ROV)-type neutralizers automatically deployed by the USV" as part of future neutralization systems and "stationary explosive charge delivered to the mine danger area and deployed by the USV transporter" (U.S. Navy, 2007).

Approach

Any successful USV-UUV capture, recovery and deployment system must compensate for the relative motion between the surface platform and submerged vehicle. We propose a first step in addressing this technological need—a sea-state-dependent performance requirement based on the seakeeping dynamics of two such vessels and their formation geometry. We use a single metric to summarize the motion compensation requirement, the *peak-to-peak vertical displacement* (PVD). The PVD is the maximum amplitude of the alternating component of the vertical offset between the USV and UUV when acted upon by a common sea condition. This measurement summarizes the worst-case peak-to-peak displacement over a statistically significant time-history.

Quantifying this dynamic inter-vehicle motion provides designers with a key parameter for evaluating the feasibility of a potential launch and recovery solution. As an illustration, we might consider one particular scenario: an 11-m Fleet Class USV (11 m) attempting to capture and recover a Man Portable UUV (2 m) in sea-state 4. The USV could utilize an existing design such as commercially available stern-mounted or crane-based launch and recover systems. However, a new solution might directly address the challenge of executing this operation autonomously. In either case, a PVD value of 1.25 m for this scenario would specify that any successful solution would need to actively compensate for displacement between the two vehicles of 1.25 m. As a design requirement, this quantitative measure of performance will guide development and can be used to quickly ascertain the feasibility of potential solutions.

In this article, we describe a model-based approach to quantify the design requirements for autonomous USV-UUV capture, recovery and deployment. The predictive modeling combines stochastic representations of sea-state with the three degree-of-freedom dynamic responses of the surface (USV) and submerged (UUV) platforms. This quantitative analysis leads to both frequency-domain and time-domain descriptions of the motion of both platforms. Figure 1 illustrates our modeling process.

Our view is that a model can only be expected to *approximate* reality and not duplicate it. Thus, we do not claim that the simple models used in this analysis are absolutely precise, but that they are useful in bounding the design requirements of a USV-UUV coordination system. We substantiate this claim of utility by comparing our model predictions to experimental evidence.

FIGURE 1

Flowchart illustration of the modeling process to derive design parameters based on the relative motion of a USV and UUV.

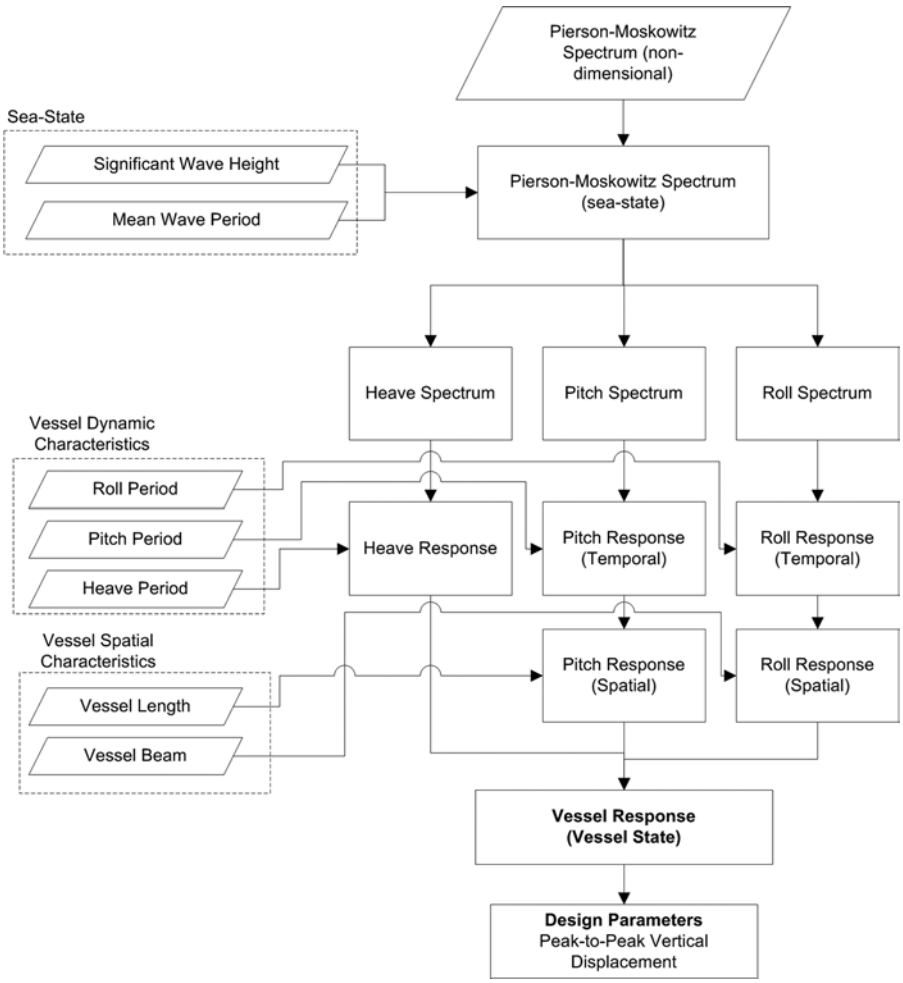

Related Work

Engineering models are used to aid in design decisions by providing a surrogate for costly experimentation and prototype development. Much of the current research on dynamic models for USVs and UUVs is aimed at aiding the design of feedback control algorithms. For surface vehicles, these models, based on naval architecture techniques, predict the response to thrust and rudder commands to predict the stability and performance of guidance and control techniques. The quality of the predictions can be determined by carefully instrumented sea trials to identify the hydrodynamic characteristics of the vessel (Krishnamurthy et al., 2005; Caccia et al., 2008). Similar model identification approaches have been used to aid in developing flight controllers for UUVs where accurate system parameter estimates are used to improve the control performance (Prestero, 2001; Rentschler et al., 2006). Such models make use of standard techniques from the hydrodynamics

community to improve the maneuvering of single vehicles. This type of model relies on detailed treatments of the kinematic and hydrodynamic aspects of the model and uses stochastic disturbance models to capture the impact of environmental factors such as waves, wind and current.

Another topic of research interest has been the modeling and control of multiple coordinating vehicles. In contrast to the detailed hydrodynamic models for single vehicles, research on multivehicle control makes use of simplifying assumptions to analyze questions of stability and controllability. For example, coordinating underwater gliders for the Autonomous Ocean Sampling Network (AOSN II) program required developing control laws for formation flying and feature tracking. Analysis of this complex situation required assuming point mass dynamics for each vehicle and full actuation (Fiorelli et al., 2006; Zhang et al., 2007). Similar control theoretic approaches have been proven useful in determining the required communication to realize the stabilizing decentralized control of a set of UUVs (Stilwell and Bishop, 2001).

This work is situated between these two extremes in the literature. We use vehicle models much simpler than the full hydrodynamic studies of single platforms because we are interested in aggregate summations of behavior for design instead of predicting the performance or stability of an individual controller. However, because we are interested in how the vehicle dynamics and environmental forcing functions drive our design choices, we do use vessel dynamics and sea-state models which are of greater complexity than those typically used for multiple underwater vehicles. This compromise is motivated by the need to predict the performance currently available by operational assets working in a complex, dynamic ocean environment.

Modeling for Design

As illustrated in Figure 1, we use simple models to describe the sea height, which simultaneously drives both the USV and UUV response, each in three degrees of freedom. This section describes our implementation of the Pierson-Moskowitz (PM) wave spectrum and the frequency-domain response in heave, pitch and roll for both the surface and submerged vessel.

Statistical Description of Surface Waves

The notion of sea-state concisely describes the wind and wave conditions with a single number (see Table 1). Our goal is to translate a sea-state specification to a stochastic time-domain representation of the sea surface, which drives the vessel response. We make this connection using the PM spectra for a fully developed sea (Pierson and Moskowitz, 1964), a standard description in the ocean engineering community (S. Committee and International Towing Tank Conference, 1984; Waves and International Towing Tank Conference, 2002).

The PM spectrum captures the sea surface characteristics as a stationary random process based on a two key parameters: significant wave height ($H_{1/3}$) and mean wave period (T_1). These parameters describe a power spectral density ($S(\omega)$) as a function of the temporal frequency (ω), for a particular sea-state (Faltinsen, 1990).

$$\frac{S(\omega)}{H_{1/3}^2 T_1} = \frac{0.11}{2\pi}\left(\frac{\omega T_1}{2\pi}\right)^{-5} \exp\left[-0.44\left(\frac{\omega T_1}{2\pi}\right)^{-4}\right] \tag{1}$$

By sampling the PM spectrum in equation (1), we build a description of the surface height ($h(t,x)$) as the sum of N discrete spatio-temporal waveforms.

$$h(t,x) = \sum_{j=1}^{N} A_j \sin\left(\omega_j t - k_j x + \varepsilon_j\right) \tag{2}$$

where A_j is the amplitude of the wave spectral component determined by the PM wave spectrum, k_j is the spatial wave number (inverse of wave length) and ε_j is a random phase component. The spatial wave number and temporal

TABLE 1

Pierson-Moskowitz spectra parameters for sea-state 2 to 5.

Sea-State	2	3	4	5
Significant wave height (m)	0.3	0.88	1.88	3.25
Mean wave period (s)	7.5	7.5	8.8	9.7
Wind speed (knots)	8.5	13.5	19	24.5

frequency are related by the following dispersion relation based on the free surface boundary condition (Newman J. N., 1977).

$$k_j = \frac{\omega_j^2}{g} \tag{3}$$

where g is the acceleration of gravity. These three equations (1-3) provide a stochastic description of sea surface based on the general idea of sea-state. This spatio-temporal description of the free surface is the driving input for the USV and UUV response.

Pitch and Roll Spectra

In the same way that the sea surface height drives the heave response, the sea surface angle drives the pitch (and roll) response. The spatial derivative of the height expression in equation (2) leads directly to an expression of the sea surface pitch angle response ($\phi(t,x)$).

$$\phi(t,x) = \tan^{-1}\left(\sum_{j=1}^{N}\left[(-A_jK_j)\cos(\omega_j t + k_j x + \varepsilon_j)\right]\right) \tag{4}$$

Similarly, the y wave height spectrum in the transverse direction results in an expression for the sea surface roll angle.

Motion at Finite Depth

The sea-state simultaneously drives both the surface and the submerged vessel motion. To capture the subsurface fluid motion, we use the commonly accepted expression for the exponential decay of the wave motion with increasing depth expressed as

$$\delta = e^{-k_j d} \tag{5}$$

where k_j is the wave number component and d is the depth. To account for vessel depth, this multiplicative factor (δ) is applied to the heave, pitch and roll forcing functions.

Vehicle Modeling

We predict the vehicle response in heave, pitch and roll by using the fluid motion expressions to drive lumped parameter models that capture the temporal and spatial characteristics of USVs or UUVs. Concurrently, predicting the motion of both vehicles in the same sea-state allows us to characterize the relative motion between the USV and UUV—the key factor for guiding the design of capture and retrieval motion.

Temporal Response: Heave, Pitch and Roll

The temporal response of each of the three degrees of freedom for both the USV and UUV is modeled as a second-order linear system. Damping in heave, pitch and roll is unknown and can vary for different hull types and vessel characteristics. The results that follow are based on a general assumption that the linear damping ratio will be between 0.1 and 0.707. We find that the resulting design parameters are insensitive to damping values in this range.

The key determining parameter is the natural period (frequency) for each degree of freedom. We also assume that there is no coupling between heave, pitch and roll, i.e., each degree of freedom is independent. The natural period in heave (T_{n3}) depends on the mass of the vessel (M), the added mass (A_{33}) and the waterplane area (A_w) (Faltinsen, 1990).

$$T_{n3} = 2\pi\sqrt{\frac{M + A_{33}}{\rho g A_w}} \tag{6}$$

where ρ is the fluid density. The natural period of pitch T_{n5} is

$$T_{n5} = 2\pi\sqrt{\frac{Mr_{55}^2 + A_{55}}{\rho g V(GML)}} \tag{7}$$

where GML is the longitudinal metacentric height, V is the displaced volume, r_{55} is the pitch radius of gyration and A_{55} is the added moment of inertia. The natural period in roll T_{n4} is

$$T_{n4} = 2\pi\sqrt{\frac{Mr_{44}^2 + A_{44}}{\rho g V(GMT)}} \tag{8}$$

where GMT is the transverse metacentric height, r_{44} is the roll radius of gyration (typically 0.35 times the beam) and A_{44} is the added roll moment of inertia.

Figure 2 shows an example of this temporal response in two degrees of freedom. The particular example shows the wave height spectrum for sea-state 4 along with the temporal heave and pitch response. Using equation (4), the wave height spectrum leads directly to the pitch spectrum shown in the lower set of axes.

FIGURE 2

Temporal response spectra for sea-state 4 shown as the power spectral density for heave and pitch, i.e., squared amplitude per unit frequency as a function of frequency. The vessel response is determined by the heave/pitch natural periods (T_{n3} = T_{n5} = 7.5 *s* (0.13 Hz)) and highly damped heave/pitch damping (ζ = 0.707). (Color versions of figures available online at: http://www.ingentaconnect.com/content/mts/mtsj/2009/00000043/00000002.)

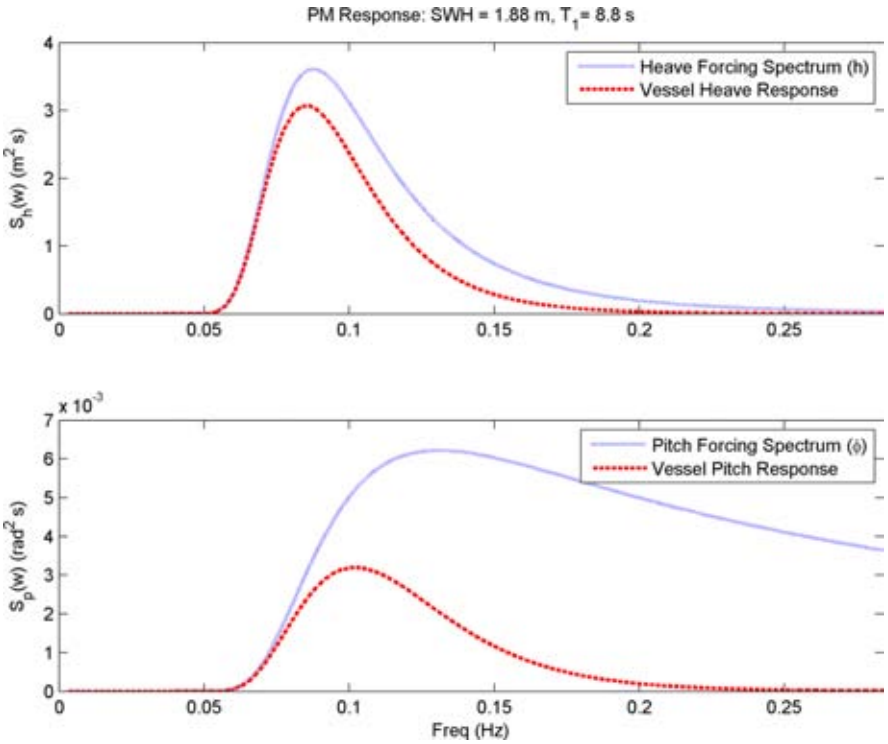

Spatial Response: Pitch and Roll

In addition to the temporal response, the spatial extent of the vessel modulates the pitch and roll movement. We use a first-order spatial response filter to capture this behavior. In the pitch direction, the wave number spectral cutoff is $K_c = \frac{1}{L}$ where L is the length at the waterline. In the roll direction, the spectral cutoff is $K_c = \frac{1}{B}$ where B is the vessel beam.

Summarizing Performance Requirements

Using modeling tools described above, we can predict the motion of a USV and UUV in a common sea condition. The output of this process is a time-history of the three degrees of freedom, USV heave, pitch and roll, and the same three degree-of-freedom solution for a coordinated UUV. To characterize the design requirements, we predict the motion of the USV-UUV system for a variety of operational scenarios. This sensitivity analysis results in an ensemble of simulation results, which allow us to infer the influence of a variety of key performance factors: sea-state, USV type, UUV type and USV-UUV formation. The final result is a measure of the sensitivity of the design requirement with respect to changes in the system, an important tool when the designer weighs various tradeoffs. The key design configurations we examine include the following factors:

- **Sea-state:** We consider sea-state 2 through sea-state 5 using the parameters listed in Table 1.
- **USV Type:** Based on the Navy's standard USV classes, we model the dynamics of three classes of USV: the Fleet Class (11 m), the Harbor Class (7 m), and the X-Class (3 m) (U.S. Navy, 2007).
- **UUV Type:** Based on the Navy's standard UUV classes, we model the dynamics of three classes of UUV: the Heavy Weight Vehicle (HWV) (21-in. diameter, approximately 3,000 lbs), the Light Weight Vehicle (LWV) (12.75-in. diameter, approximately 500 lbs) and the Man-Portable Vehicle (MPV) (no standard diameter, 25-100 lbs) (U.S. Navy, 2004).
- **USV-UUV Formation:** In contrast to the factors listed above, the relative geometric configuration, i.e., the formation, of the two platforms is not standardized. Therefore, we propose three particular relative geometric configurations, shown in Figure 3, to capture the variety of possible configurations.
  1. *Amidships*: In this arrangement, the vessels are aligned vertically, i.e., the UUV is directly below the USV. Relative heave motion dominates the relative displacement.
  2. *Astern*: In this arrangement, the bow of the UUV is directly below the stern of the USV. Relative heave and the pitch of each vessel dominate the relative displacement.
  3. *Alongside-Astern*: In this arrangement the bow of the UUV is directly below the stern of the USV and the starboard side of the UUV is directly below port side of the USV. All three degrees of freedom (heave, pitch and roll) contribute to the relative displacement.

FIGURE 3

Illustration of the three USV-UUV configurations considered as possible capture and recovery scenarios: Amidships, Astern and Alongside-Astern.

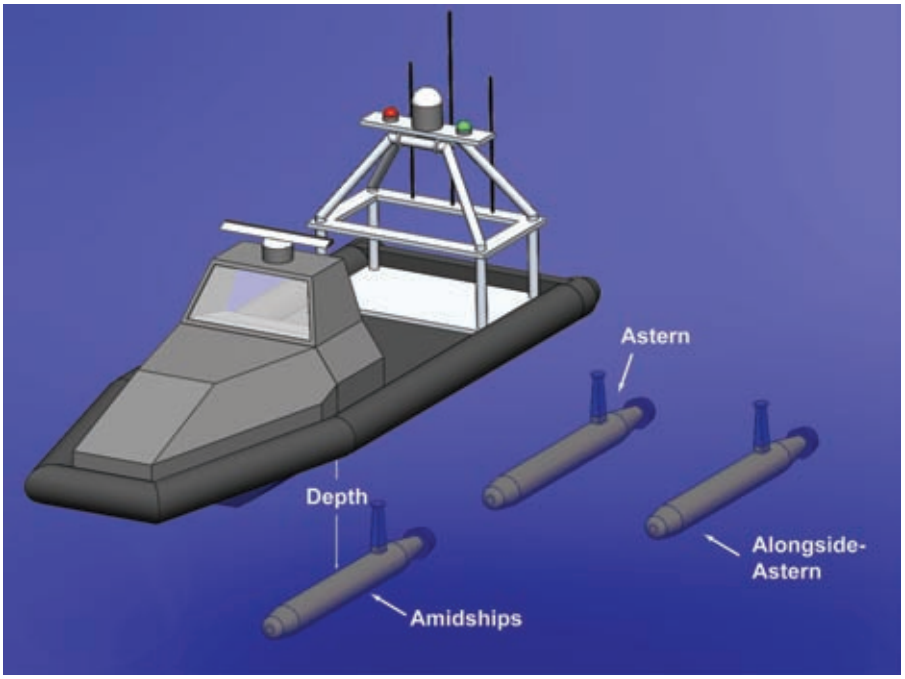

TABLE 2

Particular parameters used for dynamics example.

Variable	Value
Sea-state	4
USV class	Fleet Class
USV length	11 m
USV beam	2.0 m
USV heave period	1.0 s
USV pitch period	1.0 s
USV roll period	6.0 s
UUV class	Man portable
UUV length	2.0 m
UUV beam	0.5 m
UUV heave period	3.0 s
UUV pitch period	3.0 s
UUV roll period	35.0 s
Geometric configuration	Amidships
Mean vertical offset	2 m

USV, unmanned surface vehicle; UUV, unmanned underwater vehicle.

To summarize the pertinent simulation results, we use the PVD metric defined above as the maximum peak-to-peak amplitude of the alternating component of the vertical offset between the USV and UUV. Because this succinct, scalar performance metric summarizes the relative displacement time-history, the PVD must be obtained from a statistically significant sample. In each case, the simulation results used to estimate the PVD include at least 150 cycles of the dominant period (Waves and International Towing Tank Conference, 2002), resulting in a simulated time-history of roughly 25 min for each design scenario. This metric quantifies the requisite motion cancellation to safely and repeatedly capture, retrieve and deploy a UUV from a USV platform.

Illustrative Examples

The following examples illustrate the method of simulating the vessel response to particular sea conditions. The first example shows the time-history results from considering one particular combination of sea-state, USV type, UUV type and geometric configuration. Next, we show how we expand this treatment to examine how sea-state and geometric configuration influence the vessel dynamics and the relative displacement between the USV and UUV.

Particular Example

The key parameters for one particular example are shown in Table 2. The heave natural period is calculated from the actual physical parameters (equation (6)), but the pitch and roll periods are estimated. The pitch natural period is assumed to be similar to the heave natural period (Faltinsen, 1990). The roll natural period is estimated based on typical vessels of similar size and shape.

One output of the simulation is a concurrent time-history of the state of both the USV and UUV in response to the sea conditions. This record of heave, pitch and roll is one possible instance of these results, generated from the stochastic characterization of sea-state and the vessel dynamics. Figure 4 shows a snapshot of the time-history to illustrate the particular configuration. This time-history provides an estimate of the relative motion on the USV and UUV and the bases for calculating the PVD metric.

Sensitivity with Respect to Geometric Configuration and Sea-State

Each particular case, such as the one described above, results in a PVD metric that summarizes the USV-to-UUV motion for that set of parameters. Next, we present a set of sensitivity studies that build on these individual configurations to quantify how

FIGURE 4

Illustration of the combined heave/pitch/roll temporal response for sea-state 4. The vessel characteristics are listed in Table 2. Notice that the USV has a large roll response, whereas the UUV has almost no roll response. This lack of UUV roll response is because of the large roll period (T_{n4}) of a submerged vessel.

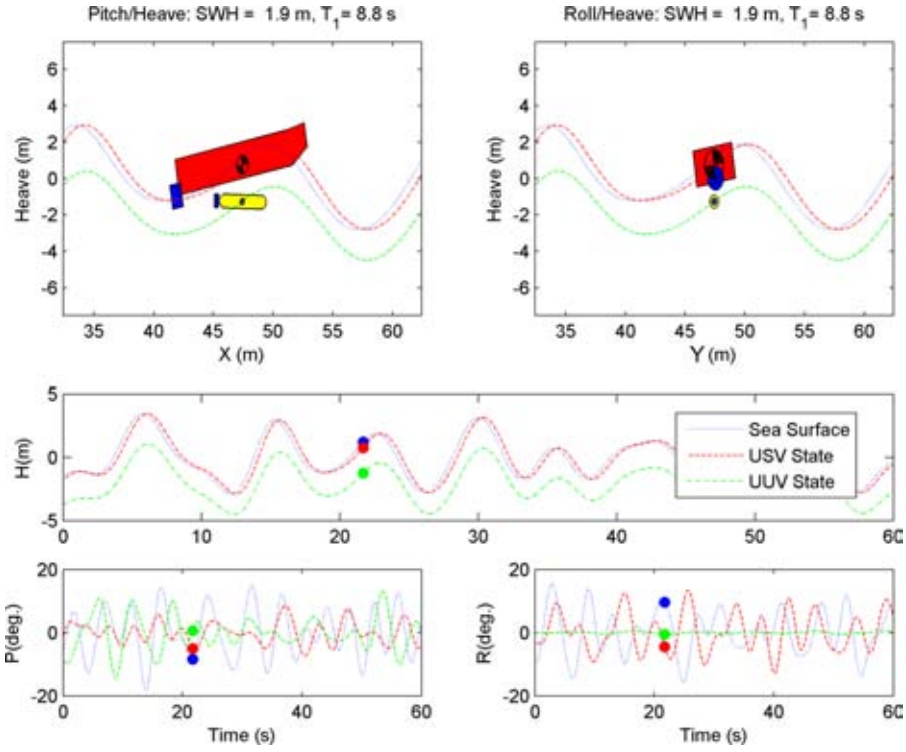

sea-state, vehicle type and geometric formation affect the requirements for capture, recovery and deployment. For example, based on the results of the previous section, we can begin to ask questions such as, "How does the choice of UUV type influence the relative displacement between USV and UUV?" or "How does the USV-UUV formation influence the relative displacement?"

Figure 5 illustrates the relative vertical displacement between the Fleet Class USV of Table 2 and three types of UUV for the three possible USV-UUV formations. Here, we notice that the variation across various UUV platforms is small. The small manportable vehicle and the heavy weight vehicle each have a similar relative displacement relative to the USV. In contrast, the geometric configuration has a larger effect on the relative displacement. We can see in the lower two plots that the Astern and Alongside-Astern configurations have a much larger relative displacement between the USV and UUV. The reason for this larger relative displacement is that, in the Astern and Alongside-Astern configurations, the relative displacement is measured from the stern of the USV. In such cases, the pitch response of the USV causes an increase in the relative displacements.

Proposed Design Parameters

To elucidate the important system trades in the design of a capture, retrieval and deployment system, we performed a full set of sensitivity studies, exploring variation in sea-state, USV type, UUV type and geometric configuration. Similar to the examples above, each configuration was examined by predicting the time response through simulation and then summarizing the time response using the PVD performance metric. Based on these results, we propose the set of design parameters listed in Table 3.

In addition to the summary design in Table 3, exploring the sensitivity of the PVD requirement to the configuration parameters also provides insight into how the configuration choices affect the challenge of autonomous capture, recovery and deployment. The influence of these factors is listed below in order of impact:

- **Sea-State** has the largest impact on the PVD requirement. This is evident across the rows of Table 3.
- **USV-UUV Formation** also has a large impact on the relative vertical displacement. The columns of Table 3 quantify this sensitivity with respect to vessel to vessel configuration. Notice that the Astern PVD values are almost as large as the values for the Alongside-Astern configuration for a given sea-state condition. The Alongside-Astern configuration requires much more dynamic range (a factor of three) than the simple vertical alignment. This result indicates that the pitch response dominates the vertical displacement for the USVs and UUVs considered; the roll response is less important.
- **USV Class** has a moderate impact on the relative displacement, mostly because an increase in length corresponds to a longer moment arm, amplifying the pitch contribution to vertical displacement. This is especially true for the Astern and Alongside-Astern configurations. In the Amidships configuration, the vessels are vertically aligned, and the

FIGURE 5

Sensitivity of relative vertical displacement with respect to variation in UUV type (MP, LWV, HWV) and geometric configuration (Amidships, Astern, Alongside-Astern). The vertical axis of each plot shows the displacement between the UUV and USV position. The PVD is calculated directly from such a time-series but with a much longer record.

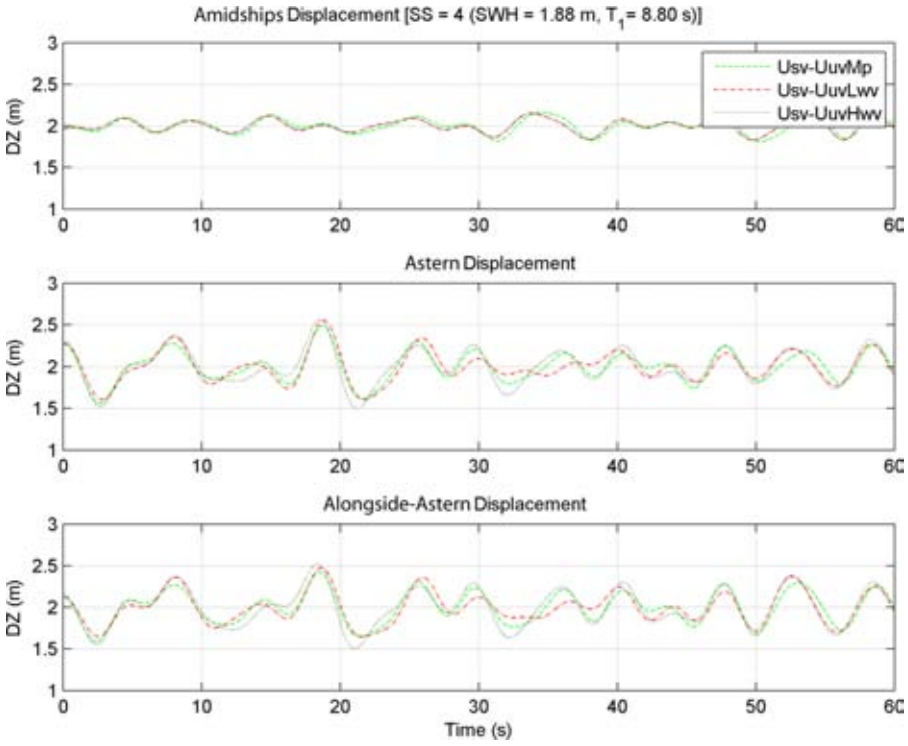

pitch, and hence the vessel length, does not affect the displacement.

- **UUV Class** has the least impact on the vertical displacement requirements. This is because the UUVs are relatively short, so their length does cause as much amplification of the pitch response. Submerged vessels also have a substantially smaller roll response than surface vessels.

TABLE 3

Design parameters as PVD values for four sea-states and three USV-UUV formations. These values are valid for all three classes of UUV (man-portable, light weight and heavy weight) when operating in concert with a Fleet Class 11-m USV.

Environmental Inputs				
Sea-state	2	3	4	5
SwH (m)	0.3	0.88	1.88	3.25
Average period (s)	7.5	7.5	8.8	9.7
Design Parameter (Peak Vertical Displacement (PVD) in meters)				
Amidships	0.25	0.5	0.75	1.0
Astern	0.4	1.0	1.25	2.25
Alongside-Astern	0.5	1.0	1.5	2.5

SwH, Significant Wave Height.

It should be noted that the UUV depth is not a major factor in determining the PVD metric. Because the metric focuses on the amplitude of the alternating displacement, and not the mean offset, the depth has only a small influence on the PVD results.

Experimental Results

We do not claim that the models for sea-state and vessel response absolutely duplicate reality, but only that they provide a useful representation of the aggregate vessel motion for designing a USV-UUV capture, recovery and deployment system. To substantiate this claim of utility, we present model predictions of a vessel response compared to experimental measurements of a small coastal vessel undergoing near-shore sea trials. This comparison between model and experiment is made based on three response characteristics: the dominant response amplitude, the dominant response period and the overall spectra power. The aim of this comparison is to determine the efficacy of the two most important portions of our approach:

1. The applicability of PM spectra for capturing sea conditions that are not fully developed
2. The applicability of the simple uncoupled, lumped parameter vessel dynamics to predict the response for a given sea condition

Experimental Setup

The experimental evidence we use to evaluate the utility of our approach is a set of sea trials conducted on a small coastal vessel (see Table 4) near Boston Harbor. The trial consisted of a set of short tests where the ship navigated on a single course at a single speed for approximately 10 min. The vessel was instrumented with GPS

TABLE 4

Characteristics of coastal surface vessel used in sea trials.

Variable	Value
Mass	10,909 kg
Length	12.2 m
Beam	4.12 m
Wetted area	40.15 m^2
Heave period	1.52 s
Pitch period	1.52 s
Roll period	3.0 s

and attitude sensors to record the position, speed and attitude information. This protocol produced a set of 20 data records, one for each distinct trial. Because the sea trials were conducted near a NOAA data buoy (Station 44013, 16 nm east of Boston, MA), we also have real-time observations of the aggregate sea-state during the trials.

To evaluate the utility of the sea-state and vessel response models, we consider four particular sea trials (numbered 9, 10, 15 and 16 in the arbitrary sequence of the experiment). These four trials were chosen because they were conducted at the lowest vessel speeds (4.0 and 2.5 knots).[1]

Input: Summarizing Wave Spectra

One reason for the experimental consideration is to determine the applicability of PM spectra for capturing sea conditions that are not fully developed. Table 5 shows the observations summarizing the sea-state. The coastal sea condition during the sea trials consists of two fundamental wave types: short period wind-driven waves combined with a long period swell. To capture this condition, we combined two PM spectra as shown in Figure 6. During the 4-h experiment, the sea condition, as reported by the buoy, was statistically constant.

[1]The forward speed of the vessels is not directly considered. This assumption is because of the small speeds of typical UUVs (6 knots), indicating that most launch and recovery tasks will take place at minimal speeds. Significant forward speed will have the effect of decreasing the period of motion and increasing the bandwidth requirement.

TABLE 5

Summary sea-state statistics taken from NOAA data buoy during vessel sea trials (Station 44013, 16 nm east of Boston, MA).

Parameter	Value
Swell height (SwH)	0.48 m
Swell period (SwP)	11.2 s
Wind wave height (WWH)	0.7 m
Wind wave period (WWP)	3.6 s

Experimental Results: Comparison of Model Predictions and Experimental Observations

To compare the model and experiment, we examine the power spectral density estimates for heave, pitch and roll. The experimental values are calculated directly from the attitude sensor time records for the four pertinent experiments. The model predictions are a result of using the combined PM spectrum in Figure 6 to drive the dynamic model of the surface vessel.

The heave spectra, predicted and experimental, are plotted together in Figure 7. From this image, we can see that the dominant heave period and amplitude of the experimental results are within 10% of the predicted response. However, the predicted spectrum is wider than the experimental power spectral density, indicating

FIGURE 6

Illustration of the "Combined" spectrum created by summing two Pierson-Moskowitz (PM) spectra: the "Swell" component (11.2-s period) and the "Wind" component (3.6 s).

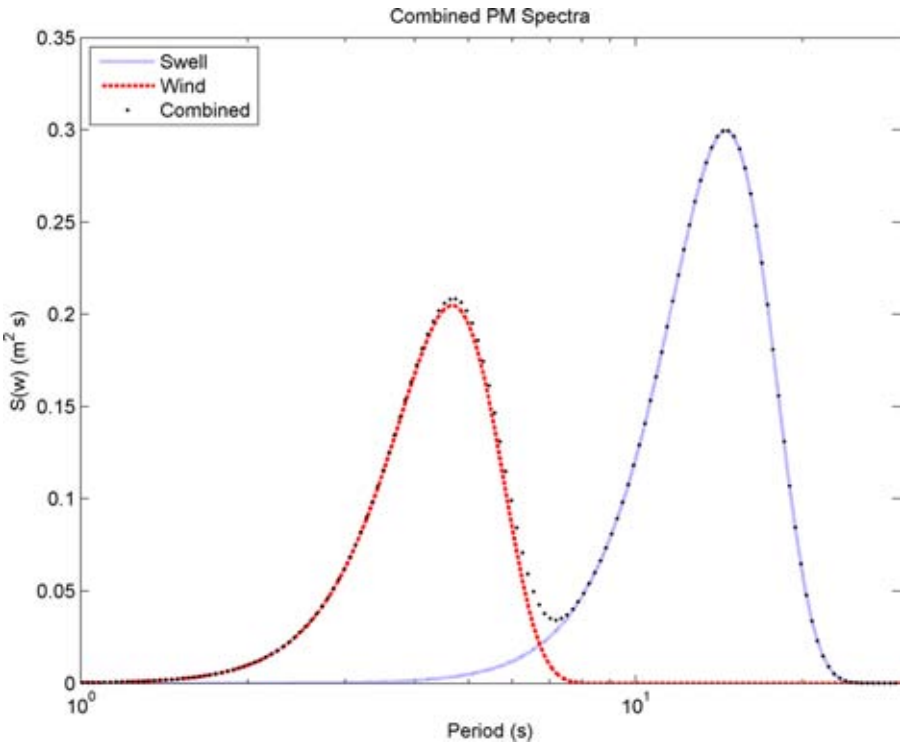

that more power is present in the predicted response. One possible cause of this difference is the assumed level of damping in the vessel heave response. This dynamic characteristic is challenging to estimate empirically, and overestimating the parameter would result in a widening of the spectrum, as shown in Figure 7.

The pitch and roll spectra also exhibit encouraging correspondence between the model prediction and experimental evidence. Figure 8 illustrates the power spectral density comparison for the pitch response.[2] In both cases, the amplitude and power (spectrum width) give rise to similar time histories. Also, in both cases, the dominant period of the predicted model is shorter than the empirical evidence. The likely reason for this discrepancy is the rough estimate of vessel characteristics used to make the prediction, where the distribution of mass on the vessel is likely a critical factor. Presumably, the heave, pitch and roll periods would be available from vessel testing. It is important to note that this mismatch does not affect the overall results. Although it is important to match the dominant period, it is more important that the model predicts the aggregate power of the pitch and roll signals.

Figure 9 presents anecdotal evidence of the efficacy of the predictive model to help interpret the spectra. It is neither possible nor advisable to have a phase agreement between these time histories; the model is inherently probabilistic. As such, the instance shown is only a visual representation of the more fundamental spectral characterization. However, these time histories serve to qualitatively illustrate the model and experimental agreement.

[2]The roll response is very similar and omitted for brevity.

FIGURE 7

Heave spectra for a simple model and four trials. The dominant period and spectra amplitude both correlate extremely well for all four experimental cases.

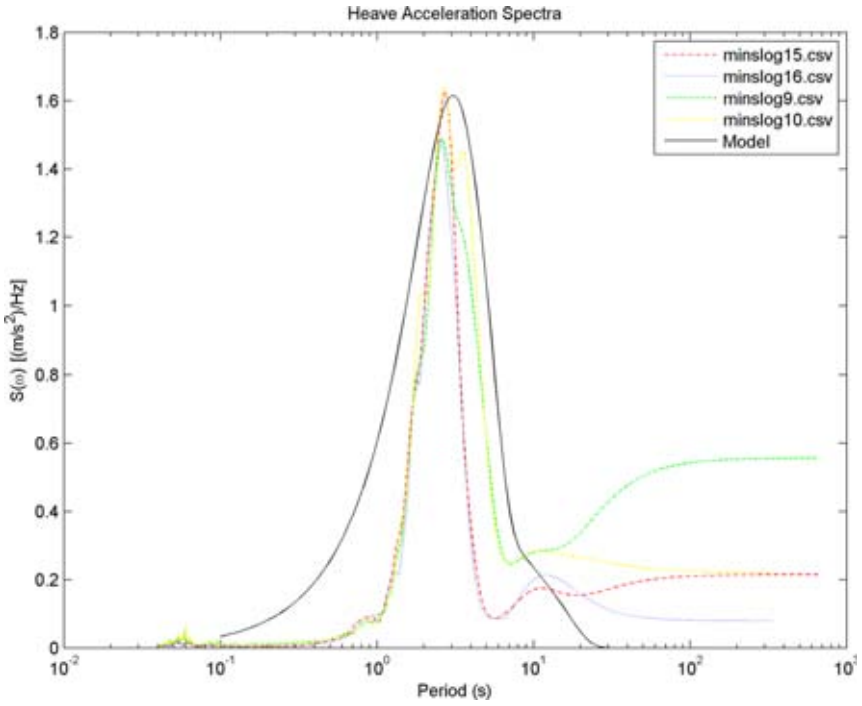

FIGURE 8

Pitch spectra for a simple model and four trials. Notice the variance in the experimental spectra amplitude. The model amplitude correlates well. The model underpredicts the dominant pitch period.

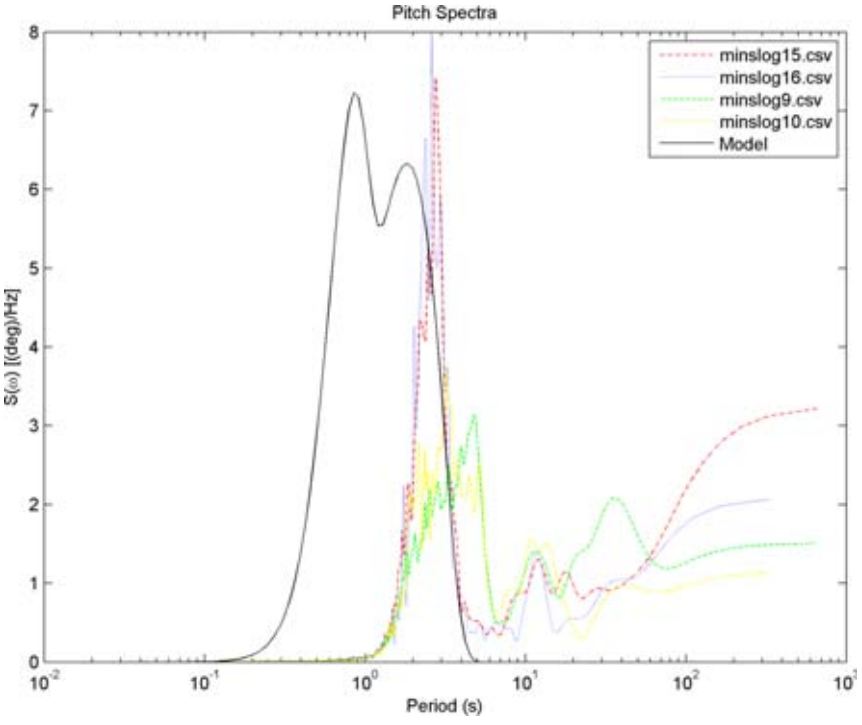

FIGURE 9

Snapshot of the time-history from one particular trial shown with one possible outcome of the stochastic model. This figure is qualitative and is meant to illustrate the comparison between the empirical data and model prediction.

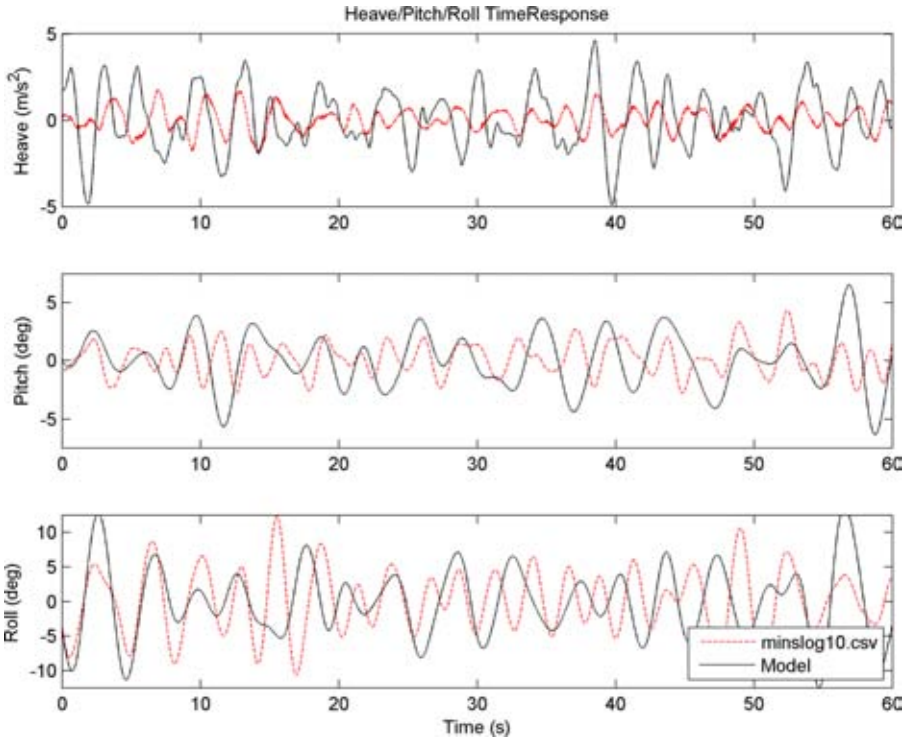

Summary of Experimental Results

These results illustrate the agreement between the model predictions and the sea-trial evidence. This agreement is best quantified by considering the vessel response spectra in heave, pitch and roll. More specifically, we consider three spectral characteristics when making comparisons between model-predicted and empirical spectra:

1. Dominant Spectrum Amplitude
2. Dominant Spectrum Period
3. Average Spectrum Power

The amplitude and spectral power are shown to agree between four pertinent sea trials and an approximate model. The difference in amplitude and spectral power is typically 10-20%. For the heave spectra, the dominant period also agrees well within 10%. However, the dominant period of the pitch and roll spectra shows a difference between the model and evidence of a factor of 2 or a factor of 4. This variation is not unexpected given coarse estimates of the pitch and roll period available from the ship parameters. Importantly, this disparity does not have a large effect on the temporal results and the resulting performance predictions because of the high agreement in overall pitch and roll spectral power. These experimental results, along with the standard methods used in creating the models, substantiate the summary performance requirements previously proposed.

Anecdotally, this process of matching the experiment and model results has shown that the modeling approach is insensitive to changes in the vessel characteristics. Instead, the sea-state parameters (significant wave height and average period) dominate the model output. This insensitivity is a very positive quality for a theoretical model used to guide performance constraints and design decisions.

Discussion and Conclusions

This document describes the model-based development of quantifiable design parameters to support autonomous USV-UUV capture, recovery and deployment. The culmination of this effort is a set of proposed design parameters—quantified requirements that must be met by any proposed design for capturing a UUV from a USV platform. The scalar performance metric is reported as the peak-to-peak vertical displacement to summarize the required motion cancellation for a candidate solution. These results are summarized in Table 3 for sea-state 2 to 5 and three USV-UUV formations.

The predictive models are based on simplifying assumptions: the wave conditions are modeled as a well-developed sea-state using the PM spectrum, the spatial and temporal vessel responses are modeled as lumped parameter systems and the dynamic characteristics of these systems are calculated (or estimated) from basic vessel specifications. To assess the utility of these modeling assumptions, we compared model predictions to experimental evidence from sea trials. This comparison showed sufficient agreement to justify bounding the design requirements using the simulation results. This empirical agreement serves to substantiate the model predictions, enabling the design decisions to be based on the succinct design requirements listed in Table 3.

The objective of this work is to present guidance for the development of coordinating technologies for simultaneous USV-UUV operations. The PVD performance metrics provide a quantitative tool for evaluating the applicability of candidate solutions to this important problem.

Future Work

A natural next step in this effort is to examine the coordination of an unmanned aerial vehicle (UAV) with a USV. Unlike the USV-UUV modeling presented here, the UAV and USV models will likely be uncoupled. Such models would provide bounding design parameters to guide designs for USV-UAV capture, retrieval and deployment.

Also, refining the predictive models and performing more detailed experiments would likely result in better agreement between model and experiment. It is our belief that the level of model complexity presented here is suitable for understanding and quantifying the design environment, but more detail will certainly be required as the technology for autonomous capture, retrieval and deployment continues to develop. For example, the model could take into account the ship wave and boundary flow around the USV. Because the capture and recovery evolution will likely occur at slow speeds, this would likely be a secondary consideration. Similarly, it would be ideal to repeat the sea-trial experiments with a USV and UUV simultaneously instead of just the coastal vessel data used in this work.

Acknowledgments

The authors wish to thank Aurora Flight Sciences Corporation for their support of this work. The authors also wish to thank Mr. Joe Holler for his contributions, particularly with Figure 3. Finally, the authors would like to thank the MTS Journal reviewers for their thoughtful comments, which improved this manuscript.

References

Caccia, M., Bruzzone, G., Bono, R. 2008. A practical approach to modeling and identification of small autonomous aurface craft. IEEE J. Oceanic Eng. 33(2), 133-145.

Faltinsen, O. M. (1990). Sea Loads on Ships and Offshore Structures. Cambridge University Press. IEEE J. Oceanic Eng. Durham, NH.

Fiorelli, E., Leonard, N.E., Bhatta, P., Paley, D.A., Bachmayer, R., Fratantoni., D.M. 2006. Multi-AUV control and adaptive sampling in Monterey Bay. IEEE J. Oceanic Eng. 31(4), 935-948.

Krishnamurthy, P., Khorrami, F., Fujikawa, S. 2005. A modeling framework for six degree-of-freedom control of unmanned sea surface vehicles. In: 2005 European Control Conference. Seville, Spain. pp. 2676-2681.

Newman, J.N. 1977. Marine Hydrodynamics. Cambridge, MA USA.

Pierson, W.J., Moskowitz., L. 1964. A proposed spectral form for fully developed wind seas based on the similarity theory of S. A. Kitaigorodski. J. Geophys. Res. 69, 5184-5203.

Prestero, T. 2001. Development of a six-degree of freedom simulation model for the REMUS autonomous underwater vehicle. In: OCEANS MTS/IEEE Conference. pp. 450-455. Washington, D.C.: Oceans 2000 MTS/IEEE Conference Committee.

Rentschler, M.E., Hover, F.S., Chryssostomidis., C. 2006. System identification of open-loop maneuvers leads to improved AUV flight performance. IEEE J. Oceanic Eng. 31(1), 200-208.

S. Committee and International Towing Tank Conference. 1984. Report of the Seakeeping Committee. In: 17th International Towing Tank Conference (ITTC). Goteborg: International Towing Tank Conference.

Stilwell, D.J., Bishop., B.E. 2001. Platoons of underwater vehicles: Communication feedback, and decentralized control. Control Syst. Mag. 20(6), 45-52.

U.S. Navy. 2004. The Navy Unmanned Undersea Vehicle (UUV) Master Planning. Department of the Navy. Available from www.navy.mil/navydata/technology/uuvmp.pdf.

U.S. Navy. 2007. The Navy Unmanned Surface Vehicle (USV) Master Planning. Department of the Navy. Available from www.navy.mil/navydata/technology/usvmppr.pdf.

Waves Technical Committee. 2002. Final report and recommendation to the 23rd ITTC. In: National Academy Press. Washington, DC.

Zhang, F., Frantantoni, D.M., Paley, D.A., Lund, J.M., Leondard., N.E. 2007. Control of coordinated patterns for ocean sampling. Int. J. Control. 80(7), 1186-1199.

PAPER

The NOAA Ship *Okeanos Explorer*: Continuing to Unfold the President's Panel on Ocean Exploration Recommendation for Ocean Literacy

AUTHORS

Paula Keener-Chavis
NOAA Ocean Exploration and Research Program

Liesl Hotaling
Beacon Institute for Rivers and Estuaries

Susan Haynes
NOAA Ocean Exploration and Research Program

ABSTRACT

The NOAA Ship *Okeanos Explorer*, commissioned as the first federal vessel dedicated solely to ocean exploration, will offer unparalleled opportunities to the scientific and education communities for "reaching out in new ways to stakeholders to improve the literacy of learners of all ages with respect to ocean issues" (The President's Panel on Ocean Exploration, 2000) and for enhancing awareness of Ocean Literacy Essential Principle #7 — "The ocean is little explored." Using a systematically mission-driven exploration protocol and advanced technological instrumentation and systems to explore little-known or unknown regions of the ocean, the ship will employ an integrated telepresence system that will provide broadband satellite transmission of data and discoveries in real time for science, education, and outreach. This paper describes the capabilities and assets of the ship, begins to address some of the opportunities that the ship will offer for "learning in new ways," describes the *Okeanos Explorer* Education Forum held in the summer of 2008, and addresses some of the issues that will be taken into consideration in using real-time data in a variety of learning environments as the education program for the ship unfolds.

Keywords: *Okeanos Explorer*, Ocean Science Literacy

> *"There are a number of good arguments for mounting as many of these [technological] systems as possible on a … flagship for the Ocean Exploration Program. A properly equipped flagship will also facilitate multidisciplinary data management and educational outreach by centralizing much of the data collection and outreach technologies on a dedicated platform."*—Discovering Earth's Final Frontier: A U.S. Strategy for Ocean Exploration

The NOAA Ship *Okeanos Explorer*: A Flagship for Ocean Exploration

It was August 13, 2008 in Seattle, almost eight years to the day of the first meeting of the President's Panel on Ocean Exploration (President's Panel) held on our opposite coast in Washington, D.C., and yet another Panel recommendation was becoming a reality. As they took their seats on Pier 66 for the commissioning ceremony of the NOAA Ship *Okeanos Explorer*, the first federal ship dedicated to ocean exploration, members of the President's Panel must have reflected on conversations they had eight short years ago about "a flagship for the Ocean Exploration Program." In front of them was a majestic 224-foot white ship decorated with international signal flags and red, white, and blue bunting: the realization of a bold idea. Those highly energetic conversations had focused on how such a vessel would journey with multidisciplinary science and education teams to the most unexplored areas of the global ocean, and how the ship would deploy the newest technologies into the deepest reaches of the ocean. That vision declared that this new "properly equipped flagship will also facilitate multidisciplinary data management and educational outreach by centralizing much of the data collection and outreach technologies on a dedicated platform through telepresence" (Figure 1).

After the Navy transferred the ship to the National Oceanic and Atmospheric Administration (NOAA), and

FIGURE 1

The NOAA Ship *Okeanos Explorer* prior to her commissioning in Seattle, Washington. Image courtesy of NOAA.

after undergoing an extensive two-year phased conversion in two shipyards in the Pacific Northwest, the *Okeanos Explorer* is nearing completion of the integration of state-of-the-art instrumentation that includes a hull-mounted deepwater "next generation" multibeam mapping system, a dedicated dual-body 6,000-m-rated science class remotely operated vehicle (ROV) system, and an integrated telepresence system. This integrated telepresence system will provide broadband satellite and high-speed Internet transmission of data and discoveries in real time for science, education, and outreach. The ship's prominent very small aperture terminal (VSAT) dome enables high-bandwidth satellite communications between explorers ashore and afloat and provides multiple high-definition video streams for wide dissemination via multicast protocols. The manufacturer describes the system as the world's largest and highest-power commercial VSAT stabilized terminal.

Visualizations and communication of images, data, and discoveries will be sent via Internet 2 to scientists and educators standing watch at shore-based Exploration Command Centers (ECCs) currently installed at five locations throughout the country. Through telepresence, the ECCs will enable multidisciplinary teams of identified scientists and educators to participate in "remote science" explorations live from ashore via intercom communications with the *Okeanos Explorer* when discoveries are made, adding intellectual capital to ocean exploration for ocean science discoveries and ocean science literacy on a global scale (Figure 2).

Systematically Mission-Driven Exploration Protocol

The mission of NOAA's flagship for ocean exploration is unique and bold, calling for the *Okeanos Explorer* to be "a dedicated ship of exploration

FIGURE 2

Telepresence technology will enable images from the seafloor to be sent via satellite and the Internet to Exploration Command Centers for remote science, education, and outreach operations. Image courtesy of Paul Oberlander, WHOI.

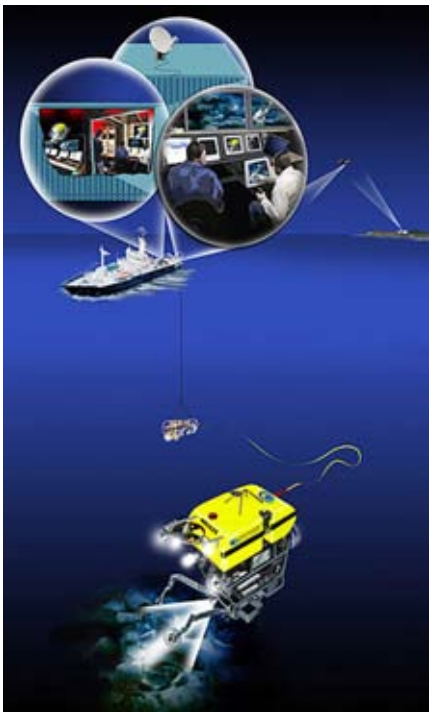

intended to carry out a *systematic global program of exploration* in the ocean linked in real time through satellite and Internet telepresence technology to the scientific community, educators, the media and the general public." In further carrying out the President's Panel recommendations, the exploration operations on board the *Okeanos Explorer* are fundamentally and uniquely different from other "project-driven" operations executed onboard most oceanographic research vessels in that they are *systematically mission-driven*. Operating under a novel exploration regime, the *Okeanos Explorer* will provide a foundation of information that will benefit multiple exploration projects as opposed to in-depth investigations designed to meet the objectives of a single project or hypothesis. Leaders

of the multidisciplinary oceanographic community developed this new approach to ocean exploration during workshops held over the past two years at the National Geographic Society and Monterey Bay Aquarium Research Institute. These workshops were facilitated by the NOAA Ocean Exploration Advisory Working Group, a working group of the NOAA Science Advisory Board.

Systematic mission-driven exploration onboard the *Okeanos Explorer* will be executed through three exploration regimes: 1) Reconnaissance, 2) Water Column Exploration, and 3) Site Characterization. The primary exploration regime will be Reconnaissance as the *Okeanos Explorer* transits through unknown or poorly-known regions of the ocean with the express purpose of making a discovery using the multibeam mapping capabilities of the ship. Water Column Exploration will be conducted at periodic stops during Reconnaissance transits in an effort to enhance the understanding of water column dynamics, to search for anomalies during Reconnaissance regime modes, and to maximize exploration efforts during transits. Once a discovery is made, or a unique feature or anomaly is found, Site Characterization will employ most of the ship's sensors and systems, including ROV capabilities and telepresence, and will consist of a 3-D characterization of the site. Standard Exploration Procedures for Reconnaissance, Water Column Exploration, and Site Characterization are under development.

Currently, the *Okeanos Explorer* is engaged in a series of final shipboard integration procedures and at-sea shakedown operations, to be followed by field trials designed to test, evaluate, and refine each of the three exploration regimes described above.

The NOAA Ship *Okeanos Explorer* Education Vision and Education Forum

The Education Vision for the *Okeanos Explorer* is that she is the ship upon which learners of all ages embark together on scientific voyages of exploration to poorly known or unexplored areas of the global ocean to participate in innovative ways as ocean explorers in breakthrough discoveries that lead to increased scientific understanding and enhanced literacy about our ocean world. NOAA and its partners in the ocean science education community and the science community at large are working together to achieve this bold education vision. As a first step to achieving this vision and in celebration of the commissioning, a two-day *Okeanos Explorer* Education Forum was held at the NOAA Pacific Marine Environmental Laboratory Western Regional Center Campus in Seattle, with the goal of developing the building blocks for a five-year education program. The Forum focused on how best to reach students, teachers, and other audiences in novel ways with the excitement of ocean exploration in light of the new assets and capabilities brought to the NOAA Ocean Exploration and Research Program (OER) by the *Okeanos Explorer*.

Forum participants represented areas of expertise that were unique to the conceptual design of the Forum. They included ocean scientists; technicians; precollege, undergraduate, and graduate and informal educators; evaluators; experts in the use of real time data and in the science of how people learn; Web designers; experts working with traditionally underserved and underrepresented groups; and experts in multimedia and virtual learning environments. Keynote presentations targeted many of these thematic areas. Large and small group discussions focused on teacher professional development, K-12 education (formal and informal), higher education, underrepresented/underserved groups, the use of real time data and new media and virtual environments, and working with informal science centers and aquariums (Figure 3).

The two guiding principles for the Forum were 1) to continue the commitment of unfolding the fourth key objective in the President's Panel Report of "reaching out in new ways to stakeholders to improve the literacy of learners of all ages with respect to ocean issues" and 2) to enhance awareness of Ocean Literacy Essential Principle # 7 – "The ocean is largely unexplored." (http://www.coexploration.org/oceanliteracy/documents/OceanLitChart.pdf). A large group brainstorm at the beginning of the Forum focused on what is meant by "reaching out in new ways." Forum participants were asked to focus on how to most effectively capture and deliver the compelling and extraordinary ocean science content and real time exploration data the ship will collect given the wide range of multimedia and other technological applications through which information might be delivered. Specifically, they were asked to frame their discussions within the construct of their key audiences, such as informal K-12, higher education, and traditionally underrepresented/underserved groups. They were also asked to identify what these various audiences were prepared to receive in their teaching and learning environments, and what

FIGURE 3

Education Forum participants in front of the NOAA Ship *Okeanos Explorer* after a tour of the ship. Image courtesy of S. Haynes.

those users would want to achieve with the information provided. Participants provided recommendations for short-term (two years) and long-term (five years) products and services. Indicators of success and unique partnerships/collaborations were also identified. Although this information is currently under review, a few items came to the forefront as overall recommendations and include:

- virtual tours of the *Okeanos Explorer*;
- development of an online learning community;
- review of existing Ocean Explorer lessons and revision as appropriate for use with the *Okeanos Explorer*; and
- increasing diversity by establishing partnerships with key organizations.

Opportunities identified during the Forum will be prioritized, and strategies addressing these opportunities will eventually form the blueprint for the NOAA Ship *Okeanos Explorer* Education Program. Already, the NOAA OER is discussing the development of a virtual tour of the ship, which will incorporate interviews with officers and crew members and information on careers connected with the vessel. The tour will also include links to the popular OceanAGE component of the Ocean Explorer Web site (http://www.oceanexplorer.noaa.gov/edu/oceanage/welcome.html).

Also under development in partnership with the College of Exploration is an Ocean Exploration Virtual Learning Community, which uses the *Okeanos Explorer* as the platform for engaging people in ongoing group conversations about ocean science teaching and learning. OER has also begun sponsoring online professional development for teachers and the development of an

FIGURE 4

A Second Life image of the NOAA Ship *Okeanos Explorer* and a visiting avatar. Image courtesy of S. Haynes and E. Hackathorn, NOAA.

Okeanos Explorer Leaders' Guides focused on "Why Do We Explore?," "How Do We Explore?," and "What Do We Expect to Find?" (Figure 4).

Exploring Ocean Science Literacy "In New Ways"

Technology enables each advancement made in exploration from the poles to the deepest reaches of the ocean to Mars and beyond. Discovery of new life forms at hydrothermal vents was made possible by submersible vehicle technology, and continued enhancements in satellite sensor and system technologies provide ever-improving documentation of climate and other planetary-scale changes, including those taking place in the deepest parts of the ocean. With the unprecedented advancements in all areas of technology, learning is no longer restricted to a place and time, and students, more than any other segment of our society, are perhaps the most profoundly affected by this distance learning evolution.

Is it well known in the field of science education that children learn science best by having opportunities to explore science and to construct their own understandings of scientific processes in the same way that scientists "do" science. As children learn and as

scientists conduct research, they build upon existing knowledge and build new cognitive foundations for understanding the world around them. Add to this the increased accessibility to the Internet and visualization technologies and you have a very innovative, inquiry-based strategy through which to teach ocean science topics to learners of all ages in ways that enable them to participate in mindful learning as they explore, discover, and construct their own knowledge in an environment facilitated by a skilled and talented teacher or one that enables self-guided learning and exploration any place and any time (Figure 5).

The *Okeanos Explorer* will present the ocean science education community with an unparalleled new national ocean-based venue through which to continue to implement the President's Panel recommendation of "reaching out in new ways to learners." Quite possibly, the ship will foster learning environments not yet thought about or explored.

Real-Time Data: Considerations in the Development of the NOAA Ship *Okeanos Explorer* Education Program

Trends reported by the National Science Board (NSB) show that there are not enough students in the pipeline today to support the science, technology, engineering, and mathematics (STEM) workforce of tomorrow (NSB 2003, 2004, 2006). The graying trend in the ocean science-related workforce adds to the urgency of training new ocean professionals (Piktialis and Morgan, 2003). Developing curricula that incorporate real world ocean technology-enabled systems, tools, data, and services helps to nurture a STEM workforce for the future.

Beyond building a necessary STEM workforce for the future, advantages to using real-time data in the classroom include:

- increasing students' science and mathematics literacy through the infusion of inquiry-based learning (Eisenhower Regional Consortia for Mathematics and Science Education, 1995);
- fostering problem-solving skills and improving test scores (Rowand and Jessup 2000; O'Sullivan et al., 2003);
- addressing several learning styles (Klicek and Susac, 2003);
- increasing student relevance (Bransford et al., 2003); and
- assisting English language learners (Warschauer et al., 2000).

Technology-based and data-enhanced educational experiences are important tools for student learning. In particular, these types of learning experiences prepare and empower students to address real-world complex problems; develop students' ability to use scientific methods; teach students how to critically evaluate the integrity and robustness of data or evidence and of their consequent interpretations or conclusions; and provide training in scientific, technical, quantitative, and communication skills (Hotaling, et al., 2006). However, for technology-based and data-enhanced educational experiences to become incorporated into classrooms, the experiences must be meaningful, engaging, dovetail into standard STEM curricula, and address educational standards.

The *Okeanos Explorer* will promote a wide range of opportunities

FIGURE 5

Children learn science best by having opportunities to explore science and construct their own understandings of scientific processes in the same way that scientists "do" science. Image courtesy of P. McKeever.

for interaction with the ship and the data collected. Notices of upcoming explorations, planned objectives, and anticipated data sets will be published to alert and entice participants to join in the voyage. Collected data will be available in real time and archived for use when data are not available and for comparative purposes. Tools will be available for users to combine data sets into customized products. In addition, physics, chemistry, biology, and geology educational materials based on shipboard operations will be available for educators. The data products and tools aim to engage the potential STEM workforce of tomorrow by capturing the feel for day-to-day life on board the ship and the awe of discovery of those fortunate enough to be the "first to discover."

At the same time, the use of real-time data in and of itself presents unique challenges to the task of unfolding a successful strategy for any education program, especially when it comes to accessibility, usability, and connectivity; preparation and professional development opportunities; and screen design and display. To broaden and strengthen the pipeline of STEM students, it is essential to provide data and services accessible to non-expert audiences. Following a traditional definition of accessible, data and tools produced by the *Okeanos Explorer* should be available to the education community (capable of being reached), easy to communicate, and capable of being used and understood (understanding at-a-glance) by non-expert audiences.

To permeate classrooms, data should be available to potential users 24 h a day, seven days a week. If data are reliable, engaging, well-organized, and easy to interpret, users will return. Classrooms are in session 24 h a day around the world so there is a steady stream of potential users. Another important aspect of implementation of Internet-based resources in classrooms is connectivity, specifically access, type of connection, and support. Reliable access and support are key components of a successful integration of any Internet-based resource in the classroom.

An essential step in preparing a future STEM workforce for the oceanographic field is raising the comfort level of K-12 educators and thus, their students with the use and application of real-time data from the *Okeanos Explorer*. Educators who are knowledgeable and comfortable with the technology and data from real-time exploration help their students learn and engage more effectively. Teachers educated in the use of real-time data in the classroom (Yepes-Baraya, 2003)

- tend to feel better prepared to teach problem-solving skills;
- tend to spend less time lecturing;
- tend to report an improved ability to teach complex concepts;
- are better able to conduct small group learning activities;
- can more easily implement cooperative learning approaches; and
- are more effective in managing diverse learning styles.

Too often, computers are provided for teachers with little or no associated professional development. Consequently, efforts to use or integrate computers in classrooms have been focused on simplistic uses such as drill and practice programs instead of effective, inquiry-based programs. In an effort to improve educator understanding of data, lessons supporting the use of real time data and classroom implementation, more effective professional development opportunities, either face to face, online, or a hybrid of the two, must be provided to educators.

NOAA OER and its partners will work to ensure that a large portion of the population (non-expert audiences) will be able to access, understand, and apply data and information to real life situations. If a large portion of the population enters college with this resident knowledge, then the preparation of the students to use real-time data will potentially occur at a much quicker pace, adding to the pool of a qualified workforce of scientists, technicians, engineers, and mathematicians to more quickly satisfy the ever increasing demands for a competitive and diverse STEM workforce.

The Internet has revolutionized the use of and access to real-world data. The effective display of real-world data for non-expert audiences is now of critical importance in a number of different arenas, for example

- public education and awareness;
- K-12 classrooms;
- policy and decision makers;
- emergency management; and
- time critical interagency operations.

Clear representation of technical information and data from the *Okeanos Explorer* on Web sites, in kiosks, and possibly ECC "hybrids" that could be developed for use in aquaria and informal science centers will generate and sustain users, help them make informed decisions, and increase awareness of and support for real-time exploration data. It is also critical for the scientific community that non-expert members of the general public be able to understand and engage with scientific exploration and discoveries. Helping scientists to understand and address the ways in which the public accesses, assimilates, and uses the products of their exploration and research will increase the awareness of, support for, and number of providers and users of that data. Proper representation

FIGURE 6

NOAA Ship *Okeanos Explorer* Telepresence Control Room, the "nerve center" of the ship.

of information technology-enabled systems, tools, and services is critical for addressing these STEM workforce training needs and will have a profound impact on the practice of science, engineering research, industry, and global citizenry (Figures 6 and 7).

FIGURE 7

Dr. Deborah Kelley at an Exploration Command Center located at the University of Washington remotely directs science activities during the Lost City Expedition with the NOAA Ship *Ron Brown* just off the Mid-Atlantic Ridge. Image courtesy of University of Washington.

The NOAA Ship *Okeanos Explorer* and the America COMPETES Act

The *Okeanos Explorer* Education Forum participants discussed at length the importance of making the *Okeanos Explorer* "come alive" by capturing the enthusiasm of the ship's officers and crew as they live and work onboard the nation's first dedicated ship for ocean exploration. This is of particular importance in fulfilling NOAA's Education Mission to "advance environmental literacy and promote a diverse workforce in ocean, coastal, Great Lakes, weather, and climate sciences encouraging stewardship and increasing informed decision making for the Nation." The America COMPETES Act (2007) mandates that NOAA build on its role in stimulating excellence in the advancement of ocean and atmospheric science and engineering disciplines and provide opportunities and incentives for the pursuit of academic studies in STEM content areas. The educational program developed for the *Okeanos Explorer* clearly will offer outstanding opportunities to address the requirements of the America COMPETES Act and will be in direct alignment with NOAA's Education Strategic Plan. NOAA's Education Strategic Plan has two goals: 1) environmental literacy and 2) workforce development and its Implementation Plan is currently under development by the NOAA Education Council.

The NOAA Ship *Okeanos Explorer* Education Program and Partnerships

Chapter 3 of *Discovering Earth's Final Frontier: A U.S. Strategy for Ocean Exploration* (President's Panel,

FIGURE 8

NOAA Ship *Okeanos Explorer*. Image courtesy of NOAA.

2000) is entitled "Ocean Exploration Partnerships." The President's Panel acknowledged that partnerships were critical in unfolding the vision for a bold national ocean exploration program and included multidisciplinary partnerships in planning, uses of exploration platforms, sharing of assets and information, and partnerships in education. The *Okeanos Explorer* with her state-of-the-art telepresence capabilities and with premier scientists and educators building the exploration, education, and outreach efforts from sea and ashore will have a profound impact on ocean literacy in this country as we strive to understand our intrinsic connections with the ocean more fully and why it is called the "lifeblood of Earth." The vision for education for the ship, as mentioned previously in this paper, cannot be unfolded by one agency working alone. Extensive partnerships must continue to be developed if the full potential of what the *Okeanos Explorer* can bring to the forefront of ocean science literacy is to be realized. This is why the *Okeanos Explorer* Education Forum participants were asked, "Are there partnerships or collaborations that are unique to unfolding any of the recommendations that you have made during this Forum?" And they had novel ideas and suggestions that will be explored as we begin to open up a virtual world of exploration on America's first flagship of ocean exploration (Figure 8).

References

Bransford, J., Brown, A., Cocking, R. 2003. How People Learn: Brain, Mind, Experience and School. Washington D.C: National Academy Press.

Eisenhower Regional Consortia for Mathematics and Science Education: Eisenhower National Clearinghouse (ENC); U.S. Department of Education (DED), Office of Educational Research and Improvement. 1995. Promising Practices in Mathematics and Science Education 1995: A Collection of Promising Educational Programs and Practices from the Eisenhower Mathematics and Science Regional Consortia. Reform in Math and Science Education. Eisenhower National Clearinghouse, U.S. Department of Education.

Hotaling, L., Matsumoto, G., Herrington, T. 2006. Using real world data in education. In: Marine Technology Society Oceans Conference Proceedings, Boston, MA, Marine Technology Society, September 2006. (https://www.mtsociety.org/conferences/proceedings.aspx (accessed 26 March 2009).

Klicek, B., Susac, M. 2003. Toward integrated and revised learning styles supported by Web and multimedia technologies. In: 8th Annual Conference of the European Learning Styles Information Network (ELSIN), University of Hull, Hull, England. (ELSIN), July 2003. http://www.hull.ac.uk/elsin/programme.htm (accessed 16 June 2006; 26 March 2009).

National Science Board. 2003. The Science and Engineering Workforce: Realizing America's Potential. National Science Foundation. http://www.nsf.gov/nsb/documents/2003/nsb0369/nsb0369.pdf (accessed 16 June 2006; 26 March 2009).

National Science Board. 2004. An Emerging and Critical Problem of the Science and Labor Force. National Science Foundation. http://www.nsf.gov/statistics/seind04/ (accessed 16 June 2006; 26 March 2009).

National Science Board. 2006. Science and Engineering Indicators 2006. Two Volumes, Arlington, VA: National Science Foundation (volume 1, NSB 06-01; volume 2, NSB 06-01A).

O'Sullivan, C., Lauko, M., Grigg, W., Qian, J., Zhang, J. 2003. The Nation's Report Card: Science 2000. National Center for Education Statistics, Washington, DC.

Piktialis, D., Morgan, H. 2003. The aging of the U.S. workforce and its implications for employers. Compens. Benefits Rev. 35(1):57-63.

The President's Panel on Ocean Exploration. 2000. Discovering Earth's Final Frontier: A U.S. Strategy for Ocean Exploration. http://oceanpanel.nos.noaa.gov, 61p. (accessed 16 June 2006; 26 March 2009).

Rowand, C., Jessup, M.D. 2000. Teacher Use of Computers and the Internet in Public Schools. Washington, D.C.: National Center for Education Statistics, NAEP (Rep. No. NCES 2000090, FRSS 70), April 2000.

Warschauer, M., Shetzer, H., Meloni, C. 2000. Internet for English Teaching. Teachers of English to Speakers of other Languages, Inc. (TESOL) Publications.

Yepes-Baraya, M. 2003. Minority student retention and academic achievement. Alliance+ Mid-Point Evaluation Report (unpublished).

UPCOMING MTS JOURNAL ISSUES

Summer 2009

General Issue

Fall 2009

The Legacy of Underwater Munitions Worldwide: Policy and the Science of Assessment, Impacts and Potential Responses

Guest Editors: Lisa C. Symons, Office of National Marine Sanctuaries, NOAA; and Geoff Carton, Office of the Deputy Assistant Secretary of the Army for Environment, Safety and Occupational Health

Winter 2009

Into the Trench: Marine Technology Opens the World Below 6 km

Guest Editor: Kevin Hardy, DeepSea Power & Light

Future *MTS Journals* will include special issues on Offshore Wind Power, Aquaculture, and an annual collection of papers by student authors.

Check the Society Web site for future Journal topics.
www.mtsociety.org

ADVERTISING RATES

SPACE	INSERTION RATE (US$)			SPACE DIMENSIONS	
	1x	2x	4x	Width	Depth
Full Page	551.25	498.75	456.75	7”	10”
Half Page					
Vertical	367.50	336.00	315.00	3 1/2”	10”
Horizontal	367.50	336.00	315.00	7”	4 1/2”
One-Quarter	215.25	194.25	168.00	3 1/2”	4 1/2”
One-Eighth	141.75	120.75	110.25	3 1/2”	2”

CALL FOR PAPERS

The *MTS Journal* includes technical papers, notes and commentaries of general interest in most issues.

Contact Managing Editor Amy Morgante (morganteeditorial@verizon.net) if you have material you would like considered.

Specifications for submitting a manuscript are on the MTS Web site under the Publications menu.

www.mtsociety.org

E-mail:
morganteeditorial@verizon.net

Or visit our homepage at

www.mtsociety.org

Marine Technology Society Publications Listing

The following **Marine Technology Society** publications are available for purchase. Prices for 2009 are listed below.
Members are granted a discount of 10% off the purchase order.
You can purchase publications by doing one of the following:

- Calling MTS at 410-884-5330 with your publication(s) order and credit card number. Reference 43.2.
- Logging on to our Web site at **www.mtsociety.org**, selecting the Store.
- Circling the items and filling out the form below, then mailing it to MTS.

JOURNALS

Student Authors: The Next Wave of Marine Technology Professionals $20
Global Lessons Learned from Regional Coastal Ocean Observing Systems $20
Offshore Wind Energy $20
The State of Technology in 2008 ..... $20
Advances in Animal-Borne Imaging $20
Societal Benefits of Marine Technology $20
Stemming the Tide of Coastal Disasters, Part 2 .. $20
Stemming the Tide of Coastal Disasters, Part 1 .. $20
Tales of Not-So-Ancient Mariners: Review From the MTS Archives $20
Promoting Lifelong Ocean Education $20
State of Technology: Marine Technology in 2005 ..... $20
Acoustic Tracking of Marine Fishes: Implications for Design of Marine Protected Areas $20
Final Report from the U.S. Commission on Ocean Policy: Implications and Opportunities $20
Underwater Pollution Threats to Our Nation's Marine Resources $20
Innovations in Ocean Research Infrastructure to Advance High Priority Science $20
Human-generated Ocean Sound and the Effects on Marine Life $20
Ocean Observing Systems $20
Science, Technology and Management in the National Marine Sanctuary Program $20
Ocean Energy—an Overview of the State of the Art $20
Marine Archaeology and Technology—A New Direction in Deep Sea Exploration $20
Technology in Marine Biology $20
Ocean Mapping—A Focus of Shallow Water Environment $20
Oceanographic Research Vessels $20
Technology as a Driving Force in the Changing Roles of Aquariums in the New Millennium $20
Submarine Telecoms Cable Installation Technologies $20
Deep Ocean Frontiers $20
A Formula for Bycatch Reduction $16
Marine Science and Technology in the Asia Region, Part 2 ..... $16
Marine Science and Technology in the Asia Region, Part 1 ..... $16
Major U.S Oceanographic Research Programs: Impacts, Legacies and the Future $16
Marine Animal Telemetry Tags: What We Learn and How We Learn It $16
Scientific Sampling Systems for Underwater Vehicles $16
U.S. Naval Operational Oceanography $16
Innovation and Partnerships for Marine Science and Technology in the 21st Century $16
Marine Science and Technology in Russia $16
Public-Private Partnerships For Marine Science & Technology (1995) $16
Oceanographic Ships (1994–95) $16
Military Assets for Environmental Research (1993–94) $16
Oceanic and Atmospheric Nowcasting and Forecasting (1992) $12
Education and Training in Ocean Engineering (1992) $12
Global Change, Part II (1991–92) $10
Global Change, Part 1 (1991) $10

MARINE EDUCATION

Guide to Marine Science and Technology Programs In Higher Education (2008) $25
Operational Effectiveness of Unmanned Underwater Systems $99
State of Technology Report—Ocean and Coastal Engineering (2001) ..... $7 dom ..... $9For.
State of Technology Report—Marine Policy and Education (2002) ..... $7 dom ..... $9 For.

PROCEEDINGS

Oceans 2008 MTS/IEEE (CDROM) $80
Oceans 2007 MTS/IEEE (CDROM) $80
Oceans 2006 MTS/IEEE (CDROM) $80
Oceans 2005 MTS/IEEE (CDROM) $50
Oceans 2004 MTS/IEEE (CDROM) $50
Oceans 2003 MTS/IEEE (CDROM) $50
Oceans 2002 MTS/IEEE (CDROM) $50
Oceans 2001 MTS/IEEE (CDROM) $50
Artificial Reef Conference $25
Oceans 2000 MTS/IEEE CD-ROM $50
Oceans 1999 MTS/IEEE '99 Paper Copy $80
Oceans 1999 MTS/IEEE CDROM $40
Ocean Community Conference '98 ..... $100
Underwater Intervention 2002 ..... $50
Underwater Intervention 2000 ..... $50
Underwater Intervention '99 ..... $50
Underwater Intervention '98 ..... $50
500 Years of Ocean Exploration (Oceans '97) $130
Underwater Intervention '97 ..... $50
The Coastal Ocean—Prospects for The 21st Century (Oceans '96) $145
Underwater Intervention '96 ..... $50
Challenges of Our Changing Global Environment (Oceans '95) $145
Underwater Intervention '95 ..... $75
Underwater Intervention '94 ..... $95
Underwater Intervention '93 ..... $95
MTS '92 ..... $140
ROV '92 ..... $105
MTS '91 ..... $130
ROV '91 ..... $95
1991–1992 Review of Developments in Marine Living Resources, Engineering and Technology $15
ROV '90 ..... $90
The Global Ocean (Oceans '89) $75
ROV '89 ..... $65
Partnership of Marine Interest (Oceans '88) ... $65
The Oceans–An International Workplace (Oceans '87) $65
Organotin Symposium (Oceans '87, Vol. 4) ... $10
ROV '87 ..... $40
Technology Update–An International Perspective (ROV '85) $35
Ocean Engineering and the Environment (Oceans '85) $45
Ocean Data: Sensor-to-User (1985) $33

MTS PUBLICATIONS ORDER FORM–REF: 43.2

Please print

Mr./Ms./Dr. First name Last name

Address

City State Zip Country

Telephone FAX

E-mail

PAYMENT: Make checks payable to Marine Technology Society (U.S. funds only)
Credit card: ❑ Amex ❑ Mastercard ❑ Visa ❑ Diners Club

Card Number Exp. Date Signature

SEND ORDER FORM TO:

Marine Technology Society
5565 Sterrett Place
Suite 108
Columbia, Maryland 21044
FAX: (410) 884-9060

Please call MTS at 410-884-5330 for an MTS Membership Application or see the following pages for an Application.

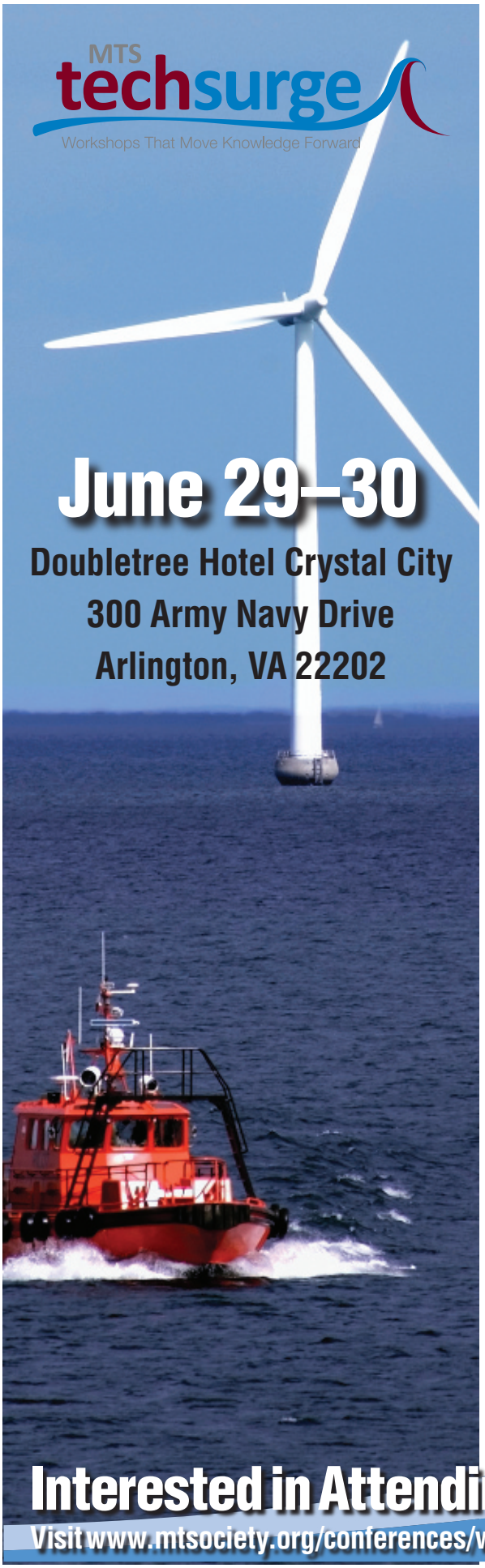

2009 Marine Technology for Offshore Wind Power Workshop

Highlights

- The workshop will open with keynote speakers and an analysis of the current situation in the U.S. as compared to other countries.
- On the first day, the afternoon session will focus on case studies, with experts from a number of European countries as well as the U.S. discussing their experiences.
- Day two of the workshop will have a more technical flavor, with sessions on site selection, structure and foundation design, and power transmission, as well as costs and the difference between installing on land versus offshore.

Speakers (As of May 1)

- Dr. Walter Cruickshank, Acting Director of the Minerals Management Service, and Dr. Richard Spinrad, Assistant Administrator at NOAA, will be among the keynote speakers.
- Tom McNeilan, P.E., Vice President at Fugro Atlantic: Site considerations
- Jaco Korbijn, Commercial Director, Blue H Technologies BV
- Jean-Francisco Wintgens, General Manager of Fugro Engineers in Belgium: Cable trenching and installation, the strengths and limitations of tools in different soil conditions, selecting the most appropriate tool for a specific area
- Jim Pryah, Ph.D., chartered geologist with the British firm CTC Marine Projects: Cutting versus jetting, cable protection, and installation techniques

Exhibitors (As of May 1)

- ABS Consulting
- MMS/Ohmsett
- Hibbard Inshore
- Fugro
- SEA CON®
- Gregg Drilling and Testing, Inc.
- South Bay Cable
- Antares Offshore

Sponsors

- Fugro
- *Sea Technology* Magazine
- Minerals Management Service
- Ocean Renewable Energy Coalition
- MTS Renewable Energy Professional Committee

Program Chairs

- Tom McNeilan, Fugro Atlantic
- Hank Lobe, Marine Safety Systems
- Bob McClure, BioSonics

Interested in Attending... Exhibiting... Sponsoring?

Visit www.mtsociety.org/conferences/windworkshop.aspx or call Chris Barrett at (410) 884-5330

Dynamic Positioning Conference

October 13–14
Houston, Texas
www.dynamic-positioning.com

The highly acclaimed DP Conference will include topics on operations and procedures, simultaneous operations, thrusters, sensors, design and control, power plant management, risk, vessels and training methods. The conference is recognized as the leading international symposium covering developments and technology pertaining to dynamic positioning. Early registration ends September 14.

OCEANS'09 MTS/IEEE Biloxi

Ocean Technology and Our Future:
Global and Local Challenges
October 26–29
Biloxi, Miss.
www.ocean09mtsieeebiloxi.org

The OCEANS'09 Conference promises to be one of the most exciting OCEANS conferences ever. For the first time, the conference is offering a Career Fair—slated for October 26—to all exhibitors and attendees at no cost. New sponsoring opportunities are also available:

- Sponsor-A-Student will help expand the student poster competition.
- High School Outreach gives local seniors a chance to see marine data in action.
- The inaugural Career Fair provides a forum for employees and potential employers to meet.
- Transportation lets you put your company's name on conference buses.

Along with the core conference topics, OCEANS'09 includes four additional topics focused on local interests: Operational Oceanography, Ocean Observing Systems, Coastal Restoration and Hurricane Katrina: Lessons Learned. Early registration ends August 31; online registration closes October 16.

Notes

Notes

Marine Technology Society Membership Application

and MTS Journal Subscription Request

☐ ***Yes, I want to become a member of the Marine Technology Society.***

☐ ***I wish to purchase a subscription to the print version of the MTS Journal. (MTS Journal online is a free member benefit.)***

☐ ***I'm not ready to join at the present time, but I would like to receive news and information from MTS. Please keep my name on your mailing list. (Please fill in member information section and return to MTS.)***

MEMBER INFORMATION *(Please fill in the address where MTS publications and correspondence should be sent.)*

Name: _____ Company (if applicable): _____

Title: _____ Email: _____

Phone: _____ FAX: _____

Address: _____

_____

MEMBERSHIP CATEGORIES

☐ **MEMBER: $75** Any person with active professional interest in the marine field or a closely related field. Includes the online version of the Journal.

☐ **ASSOCIATE: $75** Any person with an interest in the marine field and supporting MTS objectives. Includes the online version of the Journal.

☐ **STUDENT: $25** Must be a full-time undergraduate or graduate student. Includes the online version of the Journal.

☐ **PATRON:** Any person supporting MTS objectives by contributing $100 or more annually. (Contribution above $75 dues is tax deductible.) Includes the online version of the Journal.

☐ **EMERITUS: $40** Any person who is retired from active professional interest in the marine field. Includes the online version of the Journal.

☐ **LIFE: $1000** One-time payment. Includes both the online version of the Journal and the paper copy of the Journal.

☐ **CORPORATE Fortune 500: $2000** Any corporation endorsing the objectives, policies and activities of MTS. May appoint 16 representatives to the Society, who have the same rights and privileges as Members. Includes the online version of the Journal for each representative. The main contact receives a subscription to the paper copy of the Journal.

☐ **CORPORATE Non-Fortune 500: $1000** Any corporation endorsing the objectives, policies and activities of MTS. May appoint 11 representatives to the Society, who have the same rights and privileges as Members. Includes the online version of the Journal for each representative. The main contact receives a subscription to the paper copy of the Journal.

☐ **BUSINESS: $550** Any business firm whose gross annual income is less than $4 million endorsing the objectives, policies and activities of MTS. May appoint six representatives to the Society, who have the same rights and privileges as Members. Includes the online version of the Journal for each representative. The main contact receives a subscription to the paper copy of the Journal.

☐ **INSTITUTION: $550** Any library, government unit or other qualified nonprofit organization endorsing the objectives, policies and activities of MTS. May appoint six representatives to the Society, who have the same rights and privileges as Members. Includes the online version of the Journal for each representative. The main contact receives a subscription to the paper copy of the Journal.

MTS JOURNAL PRINT VERSION SUBSCRIPTION

Domestic Subscription

☐ Member Rate: ..... **$ 27**

☐ Non-Member Rate: **$124**

Foreign Subscription

☐ Member Rate: ..... **$ 50 + $50 S&H**

☐ Non-Member Rate: ..... **$140 + $50 S&H**

NON-MEMBER AND LIBRARY SUBSCRIPTIONS TO *MTS JOURNAL* ONLINE

☐ Online only **$420**

☐ Print and Online (worldwide) **$435**

Please complete other side

EDUCATIONAL INFORMATION

Please fill out the following information about yourself:

Check your highest level of education:

☐ High School Diploma ☐ Associate (2 yr.) Degree ☐ Four Year Degree ☐ Graduate Degree ☐ Doctorate

Check all that apply: ☐ B.S. ☐ B.E. ☐ B.A. ☐ M.S. ☐ M.A. ☐ M.E. ☐ Ph.D. ☐ Sc.D.

Do you have a P.E. license? ☐ YES ☐ NO

BUSINESS/PROFESSIONAL INFORMATION

Name of current employer: _____

Your employer's primary line of business at your location: _____

If you don't work for an employer, please identify your business: _____

If military, rank: _____

Your principal job function/responsibilities:

__Engineeing Management
__Science Management
__Sales
__Marketing
__Administration
__Policy Making, Regulatory
__Public Affairs
__Engineering Design
__Mechanical Engineering
__Software Engineering
__Education/Teaching
__Legal
__Consulting
__Retired
__Other (please specify)
_____

Your job title:

__President/CEO/COO
__Owner/Partner
__VP, Senior Manager
__Project Manager, Engineering
__Project Manager, Other
__Corporate VP, Engineering
__Engineering Director
__Chief/Senior Engineer
__Chief/Senior Scientist
__Project Manager
__Engineer
__Operations VP
__Scientist
__Other (please specify)
_____

Check areas of interest:

__Buoy Technology
__Cables & Connectors
__Deepwater Field Development
__Diving
__Dynamic Postioning
__Manned Underwater Vehicles
__Marine Archaeology
__Marine Education
__Marine Geodetic Information Systems
__Marine Law & Policy
__Marine Materials
__Marine Mineral Resources
__Marine Security
__Moorings
__Ocean Economic Potential
__Ocean Exploration
__Ocean Observing Systems
__Ocean Pollution
__Oceanographic Instrumentaion
__Offshore Structures
__Physical Oceanography & Meteorology
__Remote Sensing
__Remotely Operated Vehicles
__Renewable Energy
__Ropes & Tension Members
__Seafloor Engineering
__Underwater Imaging
__Unmanned Maritime Vehicles
__Other (please specify)
_____

Optional Information:

☐ Male ☐ Female What is your age? ☐ Under 30 ☐ 30-40 ☐ 41-50 ☐ 51-60 ☐ Over 60

MEMBERSHIP AND JOURNAL PAYMENT

Payment Method: ☐ Check Enclosed CK#_____ ☐ Master Card ☐ Visa ☐ Diners Club ☐ Am Ex

Make checks payable to the Marine Technology Society (U.S. funds only)

Card #: _____ Expiration Date: _____

Signature: _____ Date: _____

TOTAL PAYMENT:

Membership: $_____

Journal: $_____

TOTAL: $_____

Four easy ways to join!

Mail: Send application with check or credit card info to:
Marine Technology Society / 5565 Sterrett Place, Suite 108 / Columbia, MD 21044

Fax: Fax application to: 410-884-9060 (credit card payments only)

Online: Apply online at www.mtsociety.org

Phone: Contact us at: 410-884-5330

Marine Technology Society Member Organizations

CORPORATE MEMBERS

Allseas USA, Inc.
Houston, Texas
AMETEK Sea Connect Products, Inc.
Westerly, Rhode Island
C & C Technologies, Inc.
Lafayette, Louisiana
C-MAR America, Inc.
Houston, Texas
Compass Publications, Inc.
Arlington, Virginia
Converteam
Houston, Texas
Cortland Cable Company
Cortland, New York
Deep Marine Technology, Inc.
Houston, Texas
DOF Subsea USA
Houston, Texas
Dynacon, Inc.
Bryan, Texas
E.H. Wachs Company
Houston, Texas
Electrochem Solutions, Inc.
Clarence, New York
Fluor Corp.
Sugar Land, Texas
Fugro Chance, Inc.
Lafayette, Louisiana
Fugro Geoservices, Inc.
Houston, Texas
Fugro-McClelland Marine Geosciences
Houston, Texas
Fugro Pelagos, Inc.
San Diego, California
Geospace Offshore Cables
Houston, Texas
Global Industries Offshore, LLC
Houston, Texas
Hydroid, LLC
Pocasset, Massachusetts
Innerspace Corporation
Covina, California
INTEC Engineering
Houston, Texas
InterMoor, Inc.
Houston, Texas
J P Kenny, Inc.
Houston, Texas
Kongsberg Maritime, Inc.
Houston, Texas
L-3 Communications Dynamic Positioning and Control Systems
Houston, Texas
L-3 Communications Klein Associates, Inc.
Salem, New Hampshire
L-3 MariPro
Goleta, California
Lockheed Martin Sippican
Marion, Massachusetts
Maritime Communication Services
Melbourne, Florida
Mitsui Engineering and Shipbuilding Co. Ltd.
Tokyo, Japan
Mohr Engineering & Testing
Houston, Texas
Ocean Design, Inc.
Daytona Beach, Florida
Oceaneering Advanced Technologies
Hanover, Maryland
Oceaneering International, Inc.
Houston, Texas
Odyssey Marine Exploration
Tampa, Florida
Oil States Industries, Inc.
Arlington, Texas
Pegasus International, Inc.
Houston, Texas
Perry Slingsby Systems, Inc.
Houston, Texas
Phoenix International Holdings, Inc.
Largo, Maryland
Planning Systems, Inc.
Reston, Virginia
S&J Diving, Inc.
Houston, Texas
Saipem America, Inc.
Houston, Texas
SBM-IMODCO, Inc.
Houston, Texas
Schilling Robotics, LLC
Davis, California
SEA CON Brantner and Associates, Inc.
El Cajon, California
SonTek/YSI, Inc.
San Diego, California
South Bay Cable Corp.
Idyllwild, California
Subconn, Inc.
Burwell, Nebraska
Subsea 7 (US), LLC
Houston, Texas
Superior Offshore International
Houston, Texas
Technip
Houston, Texas
Teledyne RD Instruments, Inc.
Poway, California
Tyco Telecommunications (US), Inc.
Morristown, New Jersey

BUSINESS MEMBERS

Aanderaa Data Instruments, Inc.
Attleboro, Massachusetts
Ashtead Technology, Inc.
Houston, Texas
Bennex Subsea, Houston
Houston, Texas
C.A. Richards and Associates, Inc.
Houston, Texas
C-Innovation LLC
Mandeville, Louisiana
Cochrane Technologies, Inc.
Lafayette, Louisiana
Compass Personnel Services, Inc.
Katy, Texas
DeepSea Power and Light
San Diego, California
Deepwater Rental and Sypply
New Iberia, Louisiana
DOER Marine
Alameda, California
DTC International, Inc.
Houston, Texas
Equipment and Technical Services, Inc.
Houston, Texas
Exousia Advanced Materials, Inc.
Sugar Land, Texas
Falmat, Inc.
San Marcos, California
FibreMax
Joure, Netherlands
Fugro Atlantic
Norfolk, Virginia
Fugro Seafloor Surveys, Inc.
Seattle, Washington
Gilman Corporation
Gilman, Connecticut
Horizon Marine, Inc.
Marion, Massachusetts
Hydroacoustics, Inc.
Henrietta, New York
Impulse Enterprise
San Diego, California
Intrepid Global, Inc.
Houston, Texas
IPOZ Systems, Inc.
Katy, Texas
IVS 3D
Portsmouth, New Hampshire
JIFMAR Offshore Services
Marseille, France
Lighthouse R&D Enterprises, Inc.
Houston, Texas
Makai Ocean Engineering, Inc.
Kailua, Hawaii
Marine Desalination Systems, LLC
St. Petersburg, Florida
Matthews-Daniel Company
Houston, Texas
North Pacific Crane Company
Seattle, Washington
Oceanic Imaging Consultants, Inc.
Honolulu, Hawaii
OceanWorks International
Houston, Texas
Physics Materials and Applied Mathematics Research
Tucson, Arizona
Quest Offshore Resources
Sugar Land, Texas
Remote Ocean Systems, Inc.
San Diego, California
RRC Robotica Submarina
Macaé, Brazil
Saab Seaeye
Fareham, Hampshire, United Kingdom
SAIC Maritime Technologies
Bremerton, Washington
SeaBotix
San Diego, California
SeaLandAire Technologies, Inc.
Jackson, Mississippi
SES – Subsea Engineering Solutions, Inc.
Houston, Texas
Sonardyne, Inc.
Houston, Texas
Sound Ocean Systems, Inc.
Redmond, Washington
Stress Subsea, Inc.
Houston, Texas
Subsea Intervention Technologies, Ltd.
Fairways, Trinidad
Technology Systems Corporation
Palm City, Florida
Tension Member Technology
Huntington Beach, California
Videoray, LLC
Phoenixville, Pennsylvania
WET Labs, Inc.
Philomath, Oregon
Williamson & Associates, Inc.
Seattle, Washington

INSTITUTIONAL MEMBERS

CLS America, Inc.
Largo, Maryland
Consortium for Ocean Leadership
Washington, DC
Department of Transportation Library/OST
Washington, DC
Foundation for Underwater Research and Education
Charleston, South Carolina
Fundação Homem do Mar
Rio de Janeiro, Brazil
Harbor Branch Oceanographic Institution, Inc.
Fort Pierce, Florida
International SeaKeepers Society
Fort Lauderdale, Florida
MOERI/KORDI Library
Dagjeon, Korea
Monterey Bay Aquarium Research Institute
Moss Landing, California
Naval Facilities Engineering Service Center
Port Hueneme, California
NOAA/PMEL
Seattle, Washington
Noblis
Falls Church, Virginia
ProMare, Inc.
Houston, Texas
Society of Ieodo Research
Jeju-City, South Korea
University of California Library
Berkeley, California

The Marine Technology Society gratefully acknowledges the critical support of the Corporate, Business, and Institutional members listed.
Member organizations have aided the Society substantially in attaining its objectives since its inception in 1963.

Marine Technology Society
5565 Sterrett Place, Suite 108
Columbia, Maryland 21044

Postage for periodicals
is paid at Columbia, MD,
and additional mailing offices.